



A Basic Technique and Models for Determining Exposure Rates over Uranium-Bearing Soils



EPA-520/6-82-014
August 1982

A BASIC TECHNIQUE AND MODELS
FOR DETERMINING EXPOSURE RATES
OVER URANIUM-BEARING SOILS

George V. Oksza-Chocimowski

August 1982

Office of Radiation Programs-Las Vegas Facility
U.S. Environmental Protection Agency
Las Vegas, Nevada 89114

DISCLAIMER

This report has been reviewed by the Office of Radiation Programs - Las Vegas Facility, U. S. Environmental Protection Agency, and approved for publication. Mention of trade names or commercial products does not constitute endorsement or recommendation for their use.

PREFACE

The Office of Radiation Programs of the U.S. Environmental Protection Agency carries out a national program designed to evaluate the exposure of man to ionizing and non-ionizing radiation, and to promote development of controls necessary to protect the public health and safety and assure environmental quality.

Exposures by direct external gamma irradiation from nuclides in the uranium-238 decay chain, naturally present in the environment - as in commercial grade ore deposits - or in byproducts - as in the tailings piles of uranium mills - represent an element of risk that must be quantitatively assessed to determine the need for remedial action and the setting of necessary controls. This report illustrates the application of basic theoretical methods and models for the prediction of exposure rates at the locations of concern, as an initial step for the required risk assessment. Readers of this report are encouraged to inform the Office of Radiation Programs of any errors or omissions. Comments or requests for further information are invited.

Wayne A. Bliss
Acting Director
Office of Radiation Programs, LVF

ABSTRACT

The application of simple computer-implemented analytical procedures to predict exposure rates over uranium-bearing soil deposits is demonstrated in this report. The method is based, conceptually, on the energy-dependent point-source buildup factor and, operationally, on two consecutive integrations. The dependence of photon fluxes on spatial variables is simplified by an analytical integration over the physical dimensions of the deposit, represented as a slab bearing homogeneously distributed nuclides of the uranium-238 decay chain, at equilibrium, and covered with a source-free overburden slab; both slabs being of variable thickness but of infinite areal extent. The resultant analytical expression describes flux as function of energy-dependent parameters, thickness of the source slab, and depth of overburden, and is equated analytically to exposure rates bearing the same dependence. Elementary computer techniques are then employed to integrate numerically the exposure rates corresponding to the specific energies of uranium-238 decay chain, for chosen thicknesses of the overburden and uranium-bearing slabs. The numerical integration requires the use of buildup factors, attenuation and absorption coefficients expressed as continuous functions of energy by curve-fitting equations included in the report.

As direct application of the method, maximum exposure rates over uranium-bearing deposits are calculated. In addition, the dependence of exposure rates on the thickness of the uranium-bearing slab and depth of overburden is reduced to a simple model. These results, valid for uranium mill tailings piles, are compared to those obtained by other authors, and then applied to determine changes in exposure rates due to radon gas emanation from source materials.

CONTENTS

Preface	iii
Abstract	iv
Figures	vi
Tables	viii
Acknowledgment	ix
1. Introduction	1
2. Analytical Bases and Development	4
3. Implementation	19
4. Results	26
I. Previous Results and Models	26
II. Comparison with Present Results	28
III. Models Based on Present Techniques and Comparison with Previous Models	31
5. Applications	48
References	54
Appendices	
A. Choice of Empirical Function to Represent Gamma-Ray Buildup	56
B. Simplifying Assumptions	61
C. Exposure Rates and Flux Equations	67
D. Decay Scheme and Energy Spectrum	83
E. Choice of Medium Representing Uranium Mill Tailings	91
F. Dose Buildup Coefficients for Taylor's and Berger's Formulas	96
I. Taylor's Coefficients	96
II. Berger's Coefficients	101
G. Ancillary Curve-Fitting Equations	107
H. Computer Implementation	121
I. Sample Calculations for a Monoenergetic Case	127
J. Comments on Curve-Fitting Exposure Rate Models	131
K. Interrrelationship of Exposure Rates	137
L. Radon Distribution Through Overburden	140
M. Effects of Radon Diffusion on Exposure Rates	145

FIGURES

<u>Number</u>	<u>Page</u>
1 Section of overburden and tailings slab	12
2 Depth-dependent relaxation parameter $L(d)$	35
3 Comparison of depth-dependent relaxation parameter $L(d)$ with Schiager (1974) relaxation constant	38
4 Relative decrease in exposure rates with increasing thickness of cover slab, applying depth-dependent relaxation parameter and Schiager (1974) relaxation constant	39
5 Relative increase in exposure rate according to present model, compared to Schiager (1974) model	41
6 Effects of increasing source slab thickness on exposure-rates comparing present results with Schiager's	42
7 Relative decrease in exposure rates with increasing thickness of overburden, for emanation power $E=20$ and various radon diffusion coefficient values	51
8 Effects of radon emanation in reducing maximum exposure rate, for $E=20$ and various values of radon diffusion coefficient D	53
1-C Geometry for flux calculations	68
1-D Uranium-238 Decay Series	84
1-E Magnitude of $[A/(1+\alpha_1) + (1-A)/(1+\alpha_2)]$ for various energies in various media	95
1-F Taylor's Dose Buildup coefficient A , for a point isotropic source in water, as function of energy	98
2-F Taylor's Dose Buildup coefficient α_1 , for a point isotropic source in water, as function of energy	99
3-F Taylor's Dose Buildup coefficient α_2 , for a point isotropic source in water, as function of energy	100
4-F Comparison of 20 MFP and 7 MFP Berger's buildup factors as function of distance, for a 0.255 MeV source	102

Figures (continued)

<u>Number</u>	<u>Page</u>
5-F Effective Buildup Factors for the surface of an infinitely thick source slab, based on Berger's 7 MFP coefficients, as function of energy	106
1-G Mass attenuation coefficients for various materials	109
2-G Mass attenuation coefficient for water, as function of energy	114
3-G Mass attenuation coefficient for air, as function of energy	116
4-G Mass energy-absorption coefficient for air, as function of energy	118
5-G Graphical representation of the Second Order Exponential Integral E_2 , as function of generalized argument	120
1-H Example of computer implementation basic operational scheme	126
1-I Mass-attenuation coefficient and buildup for aluminum, as function of energy	129
1-L Tailings and cover configuration	140
2-L Distribution of free radon in tailings and cover for 9 different values of D , with a cover thickness $d=30$ cm, and $E=0.2$	144
1-M Schematic representation of numerical integration method, applied to a cover $d=100$ cm	145
2-M Relative decrease in exposure rates, as function of increasing overburden slab thickness for emanation power $E=20$ and different values of radon diffusion coefficient	147

TABLES

<u>Number</u>	<u>Page</u>
1 Analytical Expressions of Flux at the Surface of a Tailings Pile, Based on Taylor's Buildup Formula	14
2 Proportional Increase in Exposure Rates, with Respect to Maximum, as Function of Increasing Source Slab Thickness	33
3 Proportional Decrease in Exposure Rates, with Respect to Maximum, as Function of Increasing Cover Slab Thickness	34
4 Comparison of Present Maximum Exposure Rates and Models with Previously Published Models and Values	47
1-A Dose Buildup Factor (B) for a Point Isotropic Source	58
2-A Comparison of Taylor's and Berger's Buildup Factors with Tabulated Values of Buildup for Eight Energies	60
1-D Volumetric Source Strengths $S_V(E)$ for Energies $E \leq 0.5$ MeV	85
2-D Volumetric Source Strengths $S_V(E)$ for Energies $E \geq 0.5$ MeV	87
1-E Buscaglione-Manzini Coefficients for Taylor Dose Buildup Factor Formula	93
1-F Values of B_{WC} , C and D for Energies 0.255 MeV to 1.0 MeV	104
1-G Effects on Flux and Exposure Rates of Using Water and Aluminum Buildup Factors and Attenuation Coefficients	112
1-J Thickness of Overburden Slab Which Must not be Exceeded with the Use of a Constant L	136

ACKNOWLEDGMENT

The author gratefully acknowledges the assistance and advice of several individuals in the preparation of this report. Special recognition is extended to Dr. Harold L. Beck, of the Environmental Measurements Laboratory, New York, of the Department of Energy, for constructive criticism ultimately leading to a better study; to Mr. David E. Bernhardt, of the Office of Radiation Programs, Evaluation Branch - Las Vegas, of the Environmental Protection Agency, for significant contributions in problems of format and presentation; to Mr. Thomas R. Horton, of the Eastern Environmental Radiation Facility (EERF), Environmental Studies Branch, for valuable suggestions concerning needed expansion of the present work; and to Dr. Ross A. Scarano of the Nuclear Regulatory Commission, Uranium Recovery Licensing Branch, Division of Waste Management, for useful comments on applications of the present technique.

Although the scope of the present work and other limitations did not permit pursuing every suggested improvement to a logical conclusion, the author appreciates the interest and recognizes the assistance of the above named individuals, but accepts full responsibility for the contents of this report.

Introduction

External gamma exposure rates over soils containing nuclides of the ^{238}U decay chain (such as uranium mill tailings piles) have been evaluated with models and techniques differing in generality and level of sophistication. The resultant range of estimates reflects the diversity of approaches. Some of the higher predictions are unquestionably due to simple methods incorporating, necessarily, conservative assumptions. More reliable methods, based on thorough analytical treatment and processing of abundant input data, frequently require complex programming and extensive computer use, in excess of resources and time allotted by many facilities to specific projects. It follows that the immediate practical value of such evolved techniques is limited to that of the published final results, which may not be directly applicable to the needs of potential users.

Such limitations and drawbacks were an important factor motivating the present work, extended to serve a threefold purpose, as described below:

- 1) to demonstrate the reliability of a method, based on the "buildup factor" concept, requiring limited programming and computer use while avoiding many of the inaccuracies or uncertainties inherent in simplified models;
- 2) to apply this method in generating simple models relating exposure rates to depths of uranium-bearing soil deposits and cover material;

- 3) to illustrate the usefulness of these simple models under conditions of greater complexity – specifically, by examining the reduction in exposure rates due to radon exhalation from uranium-bearing soil and the effects of radon penetration into the overburden. Additional analysis was required to realize this last objective.

The proposed method, models, their application, results and comparisons with results obtained by other authors are described or presented in the main text of the report. Analytical treatments, assumptions, curve-fitting equations, ancillary tables and graphs are discussed in appendices, referenced in the main text.

This report evolved from an exploration of simple, analytically based techniques whereby results from previous methods could be critically examined. Given the exploratory nature of the original study, the use of substitutions, extrapolations and approximations in applying the method was due to unavailability of other data or convenience rather than the rigorous analysis on which the method is based. Nevertheless, their use may be justified by their contribution to the effectiveness of the technique, demonstrated by results which are in close agreement with previously published models and values, particularly with some that "have been reproduced by a number of other investigators" (Beck, 1981).

In view of the relative simplicity of the method, such close agreement may exceed expectations fostered by reliance on more complex techniques. The

element of fortuity cannot be entirely denied, in that the substitutions, extrapolations and approximations used in implementing the method undoubtedly produced errors that were mutually compensatory to a large extent, as evidenced by the results. To further support the validity of the latter, extensive appendices were included with the report. These provide a detailed description of the analytical bases of the method, the logical foundation of assumptions, substitutions, etc., complete presentation of the data base and treatment (including curve-fitting errors), computer implementation and sample calculations. Additional appendices contain some basic but relevant comments on the models derived from the results, their interrelationship and application.

Analytical Bases and Development

In principle, the assessment of exposure rates from any radioactive source requires identifying the energies of photons reaching the point of concern and calculating the photon flux corresponding to each of these energies. In common practice, the first requirement is reduced to equating the photon energies at the assessment point to the energies of photons emitted by the source. The second requirement entails determining the effects of distance and the attenuation capabilities of a specified medium in reducing the probability that a photon of a given energy, from a source of known configuration, will reach the point of interest. For a point source, such determination ultimately results in

$$\phi(E) = S(E) \frac{e^{-\mu(E)r}}{4\pi r^2} \quad (1)$$

where $\phi(E)$ = flux of photons of energy E at assessment point, photons/cm²sec

$S(E)$ = point-source rate of emission of photons of energy E, or "point-source strength", photons/sec

$4\pi r^2$ = surface of a sphere of radius r, cm²

$\exp[-\mu(E)r]$ = exponential attenuation term, function of distance r, absorbing medium, and photon energy E, dimensionless

$\mu(E)$ = total linear attenuation coefficient of absorbing medium for photons of energy E, cm⁻¹

r = distance between point-source and assessment point, cm

E = energy with which photons are emitted by the point source, MeV

The linear attenuation coefficient $\mu(E)$ represents the probability that a photon of energy E will interact with the medium in any one of several

possible ways per each unit of distance it travels in this medium. Since any detectable interaction of a photon with the medium involves a detectable energy loss and/or change of direction, the use of $\mu(E)$ in (1) implies that any photon emitted with energy E that interacts with the medium will not contribute to the flux of photons of energy E at the point of concern. The exclusion of such "secondary" or "scattered" photons, of energies less than E , facilitates the calculation and definition of a "primary exposure rate", limited to those ("primary") photons that succeed in reaching the point of interest without any prior interaction. The calculation requires the use of $\phi(E)$ from Equation (1) in the following general expression for exposure rates,

$$\dot{X}(E) = F_{\dot{X}} E \left[\frac{\mu_{en}(E)}{\rho} \right]_{\text{air}} \phi(E) \quad (2)$$

where $\dot{X}(E)$ = exposure rate from photons of energy E , in R/s

$F_{\dot{X}}$ = conversion constant

$$= 1.824401368 \times 10^{-8} \text{ g} \cdot \text{R/MeV}$$

E = gamma energy, in MeV

$\phi(E)$ = "flux" of gammas of energy E , in gammas/(cm².s)

$$\left[\frac{\mu_{en}(E)}{\rho} \right]_{\text{air}} = \text{energy dependent mass energy absorption coefficient for air, in cm}^2/\text{g}$$

Photons excluded from the primary flux by an interaction with the medium are not exempt from subsequent absorption and scattering events, and have a finite probability of reaching the point of assessment after successive scatterings. Because of the large number of possible occurrences of every type of interaction, the photons scattered to this point compound a complex aggregate of "secondary fluxes" of virtually every energy below the energy of

emission E. The difficulty of individually calculating each of these fluxes is a serious obstacle to the determination of the corresponding exposure rates [see Equation (2)], a significant concern since the latter contribute substantially to the total exposure rate at the point of interest. To circumvent these difficulties, the total net effect of secondary radiations may be equated to a nominal increase of the primary flux, by a so-called "buildup factor B", based on experimental and theoretical results, so that

$$\phi(E) = S(E) B(E) \frac{e^{-\mu(E)r}}{4\pi r^2} \quad (3)$$

The values tabulated for B depend on the energy of emission, on the source configuration, on the absorbing medium and, to some extent, on the effect being observed. Thus, there are slight differences between energy buildup, energy-absorption buildup, and dose buildup factors for the same energy, medium and configuration. Since dose in air is proportional to exposure, "point-source dose buildup factors," valid for infinite media, are used in the present work. These may be used to illustrate the above description of buildup factors as

$$B(E) = 1 + \frac{\text{secondary dose rate due to point source emitting photons of energy } E}{\text{primary dose rate due to point source emitting photons of energy } E} \quad (4)$$

= energy-dependent point-source dose buildup factor, for unspecified
infinite medium, dimensionless

Applying B(E) in (3) results in a flux $\phi(E)$, nominally of photons retaining their initial energy E, which can be used in (2) to calculate exposure rates including both primary and scattered photons.

Tabulations of buildup factor values at various distances from a source in an infinite medium have been available since 1954, or earlier, for each set of conditions specifying either a point isotopic or monodirectional plane source, one of nine source energies, and one of seven* infinite medium materials. To facilitate analytical treatment and interpolation for untabulated energies, several empirical functions have been fitted to these tables. These include "linear," "quadratic" and "cubic" forms, as well as other polynomial fits containing exponential terms, all of them with fitting coefficients valid for a specific source energy. The fitting coefficients in some of these forms apply only within specified distances from the source, which prompted the selection of a form employing coefficients of greater generality, such as Taylor's Dose Buildup Factor Formula (see Appendix A),

$$B_T(E, \mu r) = A(E)e^{-\alpha_1(E)\mu(E)r} + [1-A]e^{-\alpha_2(E)\mu(E)r} \quad (5)$$

where $B_T(E, \mu r)$ = energy and distance dependent buildup factor, Taylor's Formula, dimensionless

$A(E), \alpha_1(E), \alpha_2(E)$ = Taylor's energy-dependent fitting parameters,
dimensionless

$\mu(E)$ = energy-dependent attenuation coefficient, cm^{-1}

r = distance, cm

*Author's note. Four additional materials are included in Trubey (1966).

Taylor's fitting parameters $A(E)$, $\alpha_1(E)$ and $\alpha_2(E)$ "are not available below 0.5 MeV" (Trubey, 1966), which excludes a range of lower energies comprising roughly 15% of the total energy emitted by the ^{238}U decay chain at radioactive equilibrium. Part of this range may be covered by the use of Berger's Buildup Factor Formula,

$$B_B(E, \mu r) = 1 + C(E)\mu(E)r e^{D(E)\mu(E)r} \quad (6)$$

where $C(E)$, $D(E)$ = energy-dependent fitting parameters, dimensionless

Berger's fitting parameters are available for energies equal to or greater than 0.255 MeV, excluding energies corresponding to only 3% or 4% of the total energy emitted by the decay chain. Buildup at these energies can be tentatively estimated by a specialized application of Berger's formula, as discussed in the appropriate section.

Although Taylor's fitting coefficients apply over a smaller energy range than Berger's parameters, the latter have the disadvantage of being valid only for specified distances from the source of emission. Thus, a set of Berger's parameters is applicable for up to seven "mean free path" lengths ($\mu r = 7$), another for up to 20 MFPs, etc. This restricts the application of Berger's formula to special cases, as will be seen, while Taylor's formula is not subject to such restrictions.

The wide range of applicability of Taylor's fitting parameters makes this formula suitable for analytical treatments involving distributed gamma-ray sources of variable dimensions, a useful generalization of ^{238}U decay chain deposits when studied as a set. For present purposes, such a generalized

repository is represented as a smooth, flat, moisture-free soil slab of uniform, specified (variable) thickness but infinite in area, containing, in uniform distribution and radioactive equilibrium, all the nuclides of the uranium decay chain from ^{238}U to stable lead. This nuclide-bearing soil slab is covered with an infinitely wide slab of source-free overburden, of a uniform, specified (variable) thickness, having the same buildup and attenuation properties as the slab beneath. The bases for these simplifying assumptions are discussed, to some extent, in Appendix B.

The physical model outlined above requires some qualifications affecting the course of subsequent analysis and import of the results, as follows:

- 1) The thicknesses specified for the nuclide-bearing slab or overburden slab need not be limited to finitude. Infinitely thick source slabs without overburden are included in the analysis.
- 2) The radioactive equilibrium of the ^{238}U decay chain nuclides and their uniform distribution in the source slab allow equating the activity per unit volume of any such nuclide to that of the parent. This is assumed to be "1 pCi of ^{238}U per cm^3 " in uranium-bearing soils, or "1 pCi of ^{226}Ra per cm^3 " in uranium mill tailings piles, if the absence of the ^{226}Ra progenitors ^{238}U through ^{230}Th in tailings is taken into account. However, these last mentioned nuclides are of small consequence in exposure rate calculations. To simplify the study, both uranium-bearing soils and (conservatively) tailings piles are assumed to contain activity concentrations of $1 \text{ pCi}/\text{cm}^3$ of every nuclide from ^{238}U to stable lead.

- 3) The repository is nominally "moisture free", for purposes of analysis, since the present method can not determine the buildup and attenuation effects of water independently from the material in which it is entrapped. The consequences of including or increasing soil moisture must be learned indirectly, as results from the attendant increase in soil density. Calculations implementing the analysis assume a soil density of 1.6 g/cm^3 , corresponding to the densities of "dry packed tailings" and "moist packed earth" studied by Schiager (1974) and that of soil containing "10% water" by Beck (1972).
- 4) To facilitate analytical application of Taylor's and Berger's Buildup Factor Formulas, the buildup properties of both the source slab and overburden material are assumed to be sufficiently similar as to be characterized by the same set of energy-dependent fitting parameters A , α_1 , α_2 , etc. This similarity may be expected to extend to other properties of relevance, such as densities and mass-attenuation coefficients, or linear attenuation coefficients; it is so assumed in the calculations implementing the analysis. Nevertheless, the analysis does not require equal linear attenuation coefficients for source slab and overburden, thus they are allowed to differ in the analytical development, as a concession to greater generality.
- 5) The assumption of a source-free overburden does not consider the migratory capabilities of ^{222}Rn gas, which will permeate the overburden slab transforming it into a "secondary" repository of uranium decay chain nuclides, from ^{222}Rn to stable lead. Consequently, the direct results of the analysis and subsequent numerical treatment will apply strictly to uranium-bearing soils (or uranium mill tailings piles) covered with

overburden impervious to radon gas penetration. Nevertheless, the numerical models developed for this specialized case are useful in dealing with radon-permeable overburdens, as demonstrated in another section.

Any single decay of a nuclide in the ^{238}U series may be accompanied by the release of photons of specific energies, characteristic of the decaying nuclide, with probability of emission varying according to photon energy. These probabilities of emission, or "intensities", have been determined for all the characteristic photon energies observed in the decay of each uranium series nuclide, and tabulated as dimensionless decimal fractions or percentages with the implicit units of "number of photons of energy E emitted per decay" of the nuclide of interest. The product of the latter and a known amount of this nuclide (in activity units of "decays per unit time) produces a set of "source strengths" or "emission rates" of "photons of energy E emitted per unit time" by the given quantity of the decaying nuclide, for all the energies E characterizing this decay. Applying this process to each of the ^{238}U decay chain nuclides, uniformly distributed throughout the source slab with equilibrium activities of 1 pCi/cm^3 (or $3.7 \times 10^{-2} \text{ decays/cm}^3$ per second), generates an ensemble of "volumetric source strengths $S_V(E)$ " - bearing units of "photons of energy E emitted per cm^3 per second" - for every photon energy E released in the chain.

The product of any given volumetric source strength $S_V(E)$ and an infinitesimal volume element dV is analogous to a joint source, emitting $S_V(E)dV$ photons of energy E per second, not unlike the joint sources of Equations (1) and (3). To exploit this analogy in the context of the present physical model it is helpful to examine Figure 1.

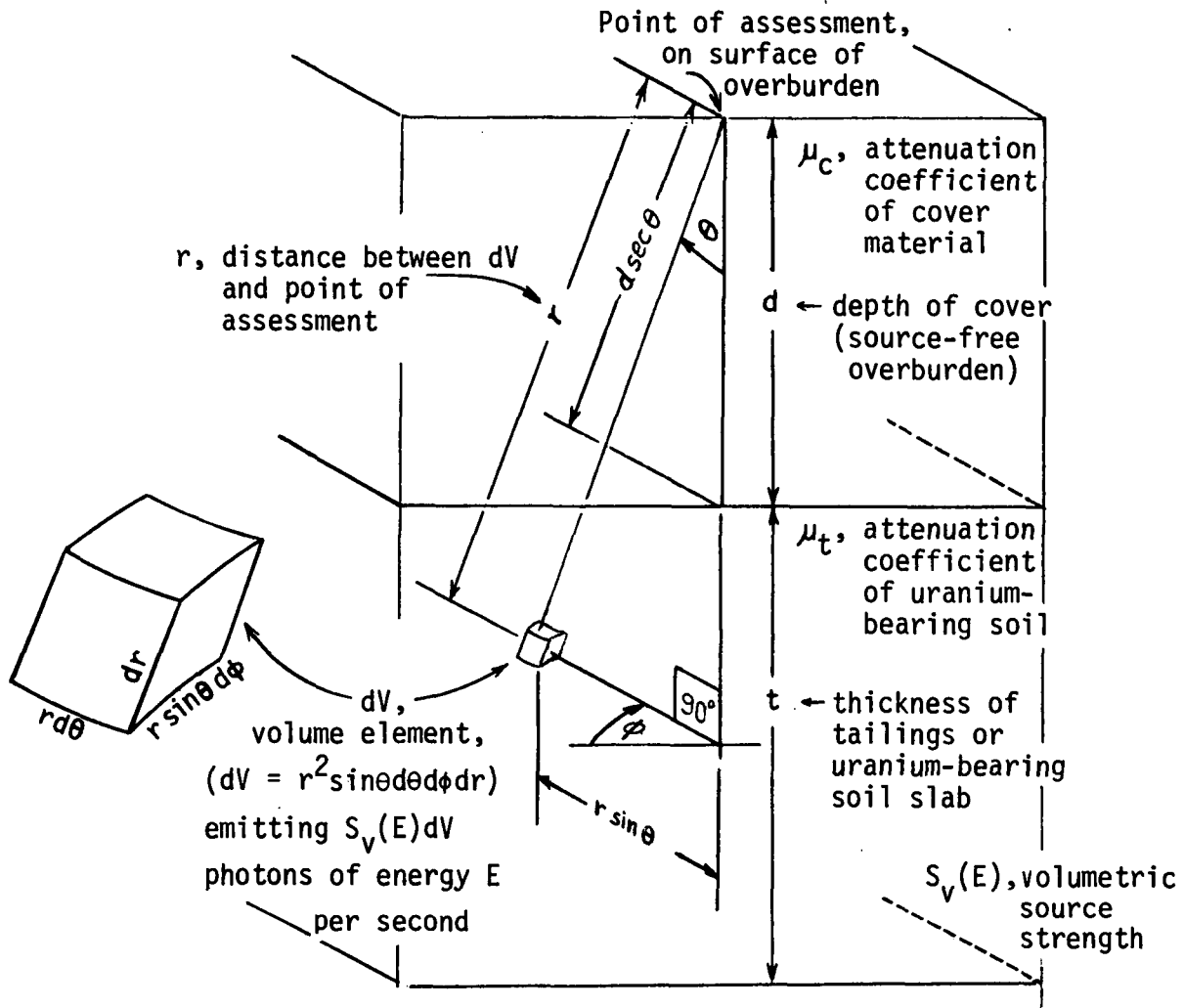


Figure 1. Section of overburden-covered tailings or uranium-bearing source slab with analytically relevant angles, dimensions and material properties.

The photons of energy E originating from a volume dV are subject to spatial and material attenuation and buildup effects of travelling a distance r , from some generalized emission point within a source slab of thickness t , to the point of assessment at the surface of an overburden of depth d , where they contribute an element of flux $d\phi(E)$ such that

$$d\phi(E) = S_v(E)B(E) \frac{e^{-\mu_t(E)(r-d)\sec\theta} - e^{-\mu_c(E)d\sec\theta}}{4\pi r^2} dV \quad (7)$$

where $d\phi(E)$ = differential flux element, photons of energy $E/\text{cm}^2 \cdot \text{s}$

$S_v(E)$ = source strength per unit volume, photons of energy $E/\text{cm}^3 \cdot \text{s}$

$B(E)$ = buildup factor for photons of energy E , dimensionless

= Taylor's buildup factor, Equation (5), for $E \geq 0.5$ MeV

= Berger's buildup factor, Equation (6), for $E < 0.5$ MeV

$\mu_t(E), \mu_c(E)$ = attenuation coefficients for uranium-bearing soil and cover material, for photons of energy E , respectively, cm^{-1}

$dV = r^2 \sin\theta \, d\theta \, d\phi \, dr$, volume element, cm^3

To determine the total flux of photons of (nominally) energy E at the assessment point, Equation (7) must be integrated analytically over the dimensions of the source and cover slabs. Given the alternative formulations of the buildup factor in (7), two different integrations are required, as described in some detail in Appendix C. Both integrations produce analytically valid expressions of the total flux of photons of energy E , at the ground-air interface, as function of energy-dependent properties of source and cover slabs, these thicknesses, and the volumetric source strength $S_v(E)$ in the source slab. However, numerical implementation of these equations points out an inconsistency in the integration involving Berger's buildup factor. In a strict sense, Berger's fitting coefficients C and D are applicable only within specified distances from a point source, whereas the integration is performed between limits including "infinity" (infinite areal extent of source and cover slabs), which implies a contradiction. Accordingly, the summary of integration results in Table 1 emphasizes those

Table 1. Analytical expressions of flux $\phi(E)$ at the surface of an infinitely wide uranium-bearing soil slab or tailings pile of uniform thickness, covered with an overburden of uniform depth, based on Taylor's buildup factor formula and valid for all $E \geq 0.5$ MeV. An equation originating from Berger's form of the buildup factor, for all $E < 0.5$ MeV, has been included for the conditions of maximum flux.

	Tailings Pile or Uranium-Bearing Soil of Finite Thickness "t". $t = \text{independent variable}$	Tailings Pile or Uranium-Bearing Soil of Infinite Thickness. $t = \infty$
Cover Material or Overburden of Finite Thickness "d". $d = \text{independent variable}$	$\phi(E) = \frac{S_V(E)A(E)}{2\mu_t(E)[1+\alpha_1(E)]} \left\langle E_2 \left\{ \mu_c(E)d[1+\alpha_1(E)] \right\} \right. \\ \left. - E_2 \left\{ [\mu_c(E)d + \mu_t(E)t][1+\alpha_1(E)] \right\} \right\rangle \\ + \frac{S_V(E)[1-A(E)]}{2\mu_t(E)[1+\alpha_2(E)]} \left\langle E_2 \left\{ \mu_c(E)d[1+\alpha_2(E)] \right\} \right. \\ \left. - E_2 \left\{ [\mu_c(E)d + \mu_t(E)t][1+\alpha_2(E)] \right\} \right\rangle$ <p>General Case: finite, variable t, d</p>	$\phi(E) = \frac{S_V(E)A(E)}{2\mu_t(E)[1+\alpha_1(E)]} \left\langle E_2 \left\{ \mu_c(E)d[1+\alpha_1(E)] \right\} \right\rangle \\ + \frac{S_V(E)[1-A(E)]}{2\mu_t(E)[1+\alpha_2(E)]} \left\langle E_2 \left\{ \mu_c(E)d[1+\alpha_2(E)] \right\} \right\rangle$ <p>Special Case: infinite t; finite, variable d for studying effects of cover thickness in reducing $\phi(E)$</p>
Absence of Cover or Overburden Material. $d = 0$	$\phi(E) = \frac{S_V(E)A(E)}{2\mu_t(E)[1+\alpha_1(E)]} \left\langle 1 - E_2 \left\{ \mu_t(E)t[1+\alpha_1(E)] \right\} \right\rangle \\ + \frac{S_V(E)[1-A(E)]}{2\mu_t(E)[1+\alpha_2(E)]} \left\langle 1 - E_2 \left\{ \mu_t(E)t[1+\alpha_2(E)] \right\} \right\rangle$ <p>Special Case: finite, variable t ; d = 0 for studying effects of increasing pile thickness on $\phi(E)$</p>	$\phi(E) = \frac{S_V(E)}{2\mu_t(E)} \left[\frac{A(E)}{1+\alpha_1(E)} + \frac{1-A(E)}{1+\alpha_2(E)} \right]$ <p>and</p> $\phi(E) = \frac{S_V(E)}{2\mu_t(E)} \left\{ 1 + \frac{C(E)}{[D(E)-1]^2} \right\} \quad \text{(From Berger's Form of Buildup Factor: for } E < 0.5 \text{ MeV)}$ <p>Maximum Flux, Exposure Rate, Case: $t = \infty, d = 0$</p>

based on Taylor's form of the buildup factor, limiting the application of Berger's form to the case of "maximum flux", as explained below.

For each of the four cases covered in Table 1, a relationship between $\phi(E)$ and exposure rate $\dot{X}(E)$ may be readily obtained using Equation (2). The total exposure rate applicable to a given case would obviously require a summation of exposure rates $\dot{X}(E)$ corresponding to that case, for all energies E emitted in the source slab. Such summation would naturally divide into two partial sums, for energies above (or equal to) 0.5 MeV and below 0.5 MeV, involving the use of Taylor's and Berger's coefficients, respectively. Since the latter produce the inconsistency alluded to above, the effects of varying depth of cover d and thickness of source slab t on the total exposure rate are inferred from the effect of such variations on the partial sum of exposure rates for energies $E \geq 0.5$ MeV. These exposure rates correspond to fluxes determined with Taylor's coefficients (see "special cases" in Table 1), and roughly 85% of the total energy emitted by the ^{238}U decay chain at equilibrium, a factor that supports the inferred relationships. Emphasizing the variable of concern, they may be expressed as

$$\frac{\sum_{\text{all } E > 0.5 \text{ MeV}} \dot{X}(E, d)}{\sum_{\text{all } E > 0.5 \text{ MeV}} \dot{X}(E, 0)} = \frac{\sum_{\text{all } E} \dot{X}(E, d)}{\sum_{\text{all } E} \dot{X}(E, 0)} = \frac{\dot{X}(d)}{\dot{X}(0)} \quad (8)$$

and

$$\frac{\sum_{\text{all } E > 0.5 \text{ MeV}} \dot{X}(E, t)}{\sum_{\text{all } E > 0.5 \text{ MeV}} \dot{X}(E, \infty)} = \frac{\sum_{\text{all } E} \dot{X}(E, t)}{\sum_{\text{all } E} \dot{X}(E, \infty)} = \frac{\dot{X}(t)}{\dot{X}(\infty)} \quad (9)$$

where $\dot{X}(E, d)$ = exposure rate due to photons of energy E , with cover of depth d , assuming infinitely thick source slab (see Table 1).

$\dot{X}(E,t)$ = exposure rate due to photons of energy E , with a source slab of thickness t , assuming absence of cover (see Table 1).

$\dot{X}(E,0) = \dot{X}(E,\infty)$ = maximum exposure rate due to photons of energy E , with a bare source slab of infinite thickness (see Table 1).

$\dot{X}(d)$ = total exposure rate, with cover of depth d , assuming infinitely thick source slab (simplified notation).

$\dot{X}(t)$ = total exposure rate, with a source slab of thickness t , assuming absence of cover (simplified notation).

$\dot{X}(0) = \dot{X}(\infty)$ = maximum total exposure rate, with a bare source slab of infinite thickness (simplified notation)

A corollary assumption implicit in (8) and (9) is that the partial sum of exposures due to all $E < 0.5$ MeV depends on d and t in exactly the same manner as the partial sum of exposures due to all $E \geq 0.5$ MeV. This may be only approximately true. As Beck (1981) points out, "low energy photons will clearly be attenuated and absorbed at a faster rate than higher energy photons [with increasing depth of overburden]," although recognizing that the error (overestimate) is "relatively small since the low energy sources contribute only a small fraction of the exposure" allows retaining Equations (8) and (9) as valid approximations.

With numerical implementation, the ratios in (8) and (9) can express the dependence of total exposure rate on d and t without specifying the magnitude of the maximum total exposure rate $\dot{X}(0) = \dot{X}(\infty)$ - i.e. the case of a bare source slab of infinite thickness. This allows for a separate evaluation of the maximum exposure rate, without jeopardizing the reliability of the above dependence by the inclusion of terms of conceivably lesser accuracy. Such a separate evaluation would consist of a summation of maximum exposure rates

corresponding to all energies emitted in the source slab, both above and below 0.5 MeV. In the present context, this means adding maximum exposure rates obtained using Taylor's coefficients to the somewhat more tentative maximum rates based on Berger's buildup formula, despite integration inconsistencies discussed in a previous paragraph. The relevant flux formulas are presented in Table 1 ("maximum flux, exposure rate, case") with further details given in "Implementation."

The formulas in Table 1 do not include the minor contributions of "skyshine" (see Appendix B). Determination of this component by the buildup factor method would require buildup coefficients for "air", unavailable in the consulted references. On the premise that the "skyshine" effect is minor for bare source slabs, and totally negligible for covered slabs, exposure rates obtained from Table 1 and Equation (2) are valid for the air-ground interface. A simple modifying factor was sought to convert these to the corresponding exposure rates at one meter above ground, for a closer comparison with previously published values. Such a conversion should, ideally, account for the energy-dependent buildup and attenuation capabilities of the intervening meter of air. However, the unavailability (or nonexistence) of buildup factor coefficients for "air" leads to a simpler approach, limited to attenuation effects.

The modifying factor is expressed as the ratio of exposure rate at one meter above ground, including air attenuation effects, to the corresponding exposure rate at ground level, for photons of a given energy E . Since the correction is intended primarily for the case of maximum exposure rate, the source slab is assumed to be infinitely thick, with an air "cover" of generalized height h (1 meter, in this case). The assumption of infinite

thickness also simplifies analysis while remaining consistent with situations encountered in practice, since exposure rates from an "infinitely" thick slab compare closely to those from any slab over 1 to 2 feet in thickness, as shown in "Results." The analysis involves the use of yet another version of the buildup factor, the "linear form",

$$B_L(E, \mu r) = 1 + \alpha(E)\mu(E)r \quad (10)$$

Leaving pertinent details to Appendix C, the analytical process results in the modifying factor

$$F_M = E_2[\mu_{\text{air}}(E)h] \quad (11)$$

The product of (11) and any of the flux formulas in Table 1 represents the corresponding flux at a height h above ground level. Setting $h = 100$ cm and applying the results in (2) produces exposure rates corrected for air attenuation at one meter above ground, facilitating comparison to previous results. The exclusion of buildup effects in (11) implies a slight underestimation of these exposure rates, just as neglect of "skyshine" effects produces a similarly small underestimation of exposure rates at ground level. However, these two effects are not cumulative, and may be balanced, to some extent, by the overestimate in low-energy exposure rates described in Appendix G.

Implementation

Determination of total exposure rates $\dot{X}(E)$, at ground level and at one meter above the surface, requires establishing the values of S_v , μ_t , μ_c , μ_{air} , $(\mu_{en}/\rho)_{air}$, A , α_1 , α_2 , C and D for every energy E borne by photons emitted in the source slab. Some of these parameters, in conjunction with the cover and source slab thicknesses d and t , produce the argument of the second order integral E_2 , which must also be quantitatively determined [see Table 1 and Equations (2) and (11)]. All but one of these parameters may be expressed as piecewise continuous functions of energy or of the argument, in the case of E_2 , by means of curve-fitting equations. The only exception is the volumetric source strength S_v , which is not a continuous function of energy, and entails a tabulation.

The tabulation consists of "source terms" $S_v(E)$, in units of "photons of energy E per cm^3 per second," corresponding to all the possible photon energies E accompanying decay of source slab nuclides. Quantitatively, these entries represent the products of intensities, in "photons of energy E emitted per decay," and the rate of decay equivalent to an assumed equilibrium activity of 1 pCi/cm^3 (or $3.7 \times 10^{-2} \text{ decays/cm}^3$ per second) of each nuclide in the uranium series from ^{238}U to ^{206}Pb . Omitted from consideration are ^{218}Po , ^{210}Bi and the branch decay nuclides ^{218}At , ^{206}Tl and ^{210}Tl , since they are not photon emitters or have an extremely low probability of emitting gammas (see decay scheme in Appendix D).

The need to rely on tabulated values necessitates the use of numerical integration techniques in obtaining a total exposure rate $\dot{X}(E)$. For ease of implementation, the 282 volumetric source strengths $S_v(E)$ calculated with

decay data from Kocher (1977) are distributed between two tables, in Appendix D. One of these, with 105 $S_V(E)$ values for energies $E < 0.5$ MeV, is meant for applications of Berger's buildup formula (see Table 1). The remaining 177 entries, for $E \geq 0.5$ MeV, serve as input to the various expressions in Table 1 derived with Taylor's buildup coefficients.

Values of Taylor's buildup parameters A , α_1 , and α_2 for energies 0.5 MeV to 3.0 MeV are listed in Appendix E, for 11 materials, none of which is "soil" or "uranium mill tailings." The unavailable coefficients must be replaced with those corresponding to one of the listed materials, if the flux equations in Table 1 are to be numerically implemented. The selection of a material with buildup properties allegedly similar to those of soil may be made less arbitrary by setting the criteria discussed below.

One of the criteria of a realistic choice is that it be made conservatively, in that the set of buildup coefficients selected should produce a greater "buildup" of secondary radiation than those resulting from other possible choices. The comparison of "buildup" effects is facilitated by the equation for "maximum flux" in Table 1, reproduced below.

$$\phi(E) = \frac{S_V(E)}{2\mu_t(E)} \left[\frac{A(E)}{1+\alpha_1(E)} + \frac{1-A(E)}{1+\alpha_2(E)} \right] \quad (12)$$

The factor outside the brackets, $S_V(E)/2\mu_t(E)$, represents the "uncollided" or "primary" flux at the surface of a bare, infinitely thick tailings slab. The total buildup produced by a given choice of buildup coefficients $A(E)$, $\alpha_1(E)$ and $\alpha_2(E)$ is expressed by the terms within brackets, and called $[B]$ for ease of reference,

$$[B](E) = \left[\frac{A(E)}{1+\alpha_1(E)} + \frac{1-A(E)}{1+\alpha_2(E)} \right] \quad (13)$$

Values attained by $[B](E)$ in the energy range $0.5 \text{ MeV} \leq E \leq 3.0 \text{ MeV}$, for each of the materials under consideration, are compared graphically in Appendix E. The comparison establishes that Taylor's buildup parameters for either "water" or "ordinary concrete" generate the highest values of buildup $[B](E)$ in the range of energies examined. This necessitates additional criteria to effect a choice.

The decisive selection criterion originates from the need to extend analysis to energies below 0.5 MeV, lower limit of applicability for Taylor's buildup coefficients. Berger's coefficients for "water" are available for energies down to 0.255 MeV, while those for "ordinary concrete" and other materials do not exist for energies under 0.5 MeV (Trubey, 1966). By elimination, the buildup properties of "soil" are maximized by using "water" buildup coefficients.

On the basis of the above selection, Taylor's buildup coefficients $A(E)$, $\alpha_1(E)$ and $\alpha_2(E)$ for water (i.e. "soil") are represented in Appendix F by the corresponding number of energy-dependent curve-fitting equations. A different method is applied to Berger's coefficients, since these are used only for conditions of maximum flux and exposure rate. Referring to the appropriate equation in Table 1, these conditions can be seen to result in a "buildup term" $\left\{ 1+C(E)/[D(E)-1]^2 \right\}$ totally independent of spatial parameters d and t . This allows expressing the entire "buildup term," in a compound manner, as a single energy-dependent variable, and representing it accordingly by a curve-fitting equation.

The dependence of this compound "buildup term" on $C(E)$ and $D(E)$ allows it to be represented in different ways, corresponding to the manner in which the energy-dependence of C and D is expressed. The latter varies according to what range of distances between point source and detector requires application of Berger's buildup factor formula, with 7 MFP*, 10 MFP, 15 MFP and 20 MFP fits reported by Trubey (1966). A discussion in Appendix F suggests that Berger's coefficients C and D based on a 7 MFP fit are appropriate for 0.255 MeV sources in an infinitely thick soil slab having "water" buildup properties. For 0.255 MeV gammas, 7 MFP in water are approximately 55 cm, which matches closely the slab thickness equivalent to an "infinite" slab when exposure rates are calculated with Taylor's coefficients, as will be seen in "Results".

Accordingly, the bracketted "buildup term" $\left\{ 1 + C(E)/[D(E)-1]^2 \right\}$ is represented by a curve-fitting equation using $C(E)$ and $D(E)$ values based on a 7 MFP fit. This selection provides the added advantage of greater accuracy, as discussed in Appendix F, and a correspondingly more solid base for extrapolations. Since the parameters $C(E)$ and $D(E)$ are not available for energies below 0.255 MeV, some judicious extrapolation is required to cover the remainder of the photon energies emitted in uranium-bearing soils.

In lieu of extrapolation, an energy-dependent "correction term" is added, for energies below 0.255 MeV, to the curve-fitting equation describing the "buildup term" as function of energy. The net effects of the correction include a buildup of "1.0" at $E = 0.01$ MeV and a maximum buildup occurring at $E = 0.12$ MeV, meeting constraints set in Appendix F. The energy of maximum

* MFP - mean-free-path lengths, as multiples of $\mu(E)r = 1$

buildup reflects mathematical convenience, without benefit of new or special insights into buildup in water (or soil) at small energies. Nevertheless, a rough analysis by Evans (1972) suggests that the assumption of maximum buildup at 0.12 MeV is not in great error.*

Conservative maximization of the buildup properties of soil was an important factor in selecting water as a soil surrogate. The effect of this selection on flux may be gaged by examining Equation (12). Assuming the attenuation coefficient $\mu_t(E)$ for soil to be known, and to be equally valid and applicable to all possible soil surrogates, maximum buildup at a given energy would inevitably lead to maximum flux (see Appendix E). Furthermore, if this were true for all the energies of concern, a maximum total exposure rate would be equally certain.

A reasonable estimate of $\mu_t(E)$ as function of energy may be obtained from a graph in Appendix G, showing the energy-dependent behavior of mass-attenuation coefficients μ/ρ of typical soil components, including water. For energies $E > 0.23$ MeV, the μ/ρ coefficients of these materials lie within a narrow band of values, with a maximum difference of about 15% (between H_2O and Fe). Consequently, the product of any such coefficient times the density of soil, assumed to be 1.6 gm/cm^3 , will represent $\mu_t(E)$ with a maximum possible

* Evans' estimate of buildup, for point sources in an infinite medium, as function of Compton scattering, total attenuation and total absorption linear coefficients, respectively σ_s , μ_0 and μ_a , is

$$B \approx 1 + \frac{\sigma_s}{\mu_a} (\mu_0 r) \quad [\text{"The Atomic Nucleus", Chapter 25, Eqn. (4.18)}]$$

The energy-dependence of σ_s , μ_0 and μ_a implies a maximum B in the range $0.06 \text{ MeV} < E < 0.09 \text{ MeV}$, in water, and in the range $0.09 \text{ MeV} < E < 0.15 \text{ MeV}$ in aluminum (indicated as an alternative replacement for "soil" by Beck, 1981).

error of 15%. Taking into account that Si and O constitute 75% of soil, by weight (Hammond, 1966), reduces this maximum error to the probable range of 10% - 12%.

However, buildup and attenuation are not independent effects (see Evans's approximation, footnote of preceding page) and thus the choice of μ/ρ coefficient may not be entirely arbitrary. Since water was used to represent the buildup properties of soil, the corresponding choice of $(\mu/\rho)_{H_2O}$ for the mass-attenuation coefficient of soil would maintain consistency. Some consequences of this consistency are viewed in Appendix G, with emphasis on resultant compensating errors. The rest of this appendix is allocated to curve-fitting equations for $(\mu/\rho)_{H_2O}$, $(\mu/\rho)_{air}$ and $(\mu_{en}/\rho)_{air}$, as functions of energy, and for the 2nd order exponential function $E_2(x)$ as function of the argument.

In both Appendix F and Appendix G, the accuracy of the various curve-fitting equations is emphasized by reference to maximum errors-of-fit (at any point) ranging from 0.5% to $\pm 1.74\%$. The only exception is the 3% error estimated at $E = 2.45$ MeV in the curve fit for $\alpha_1(E)$, a parameter of small magnitude always added to "1.0", which effectively reduces this maximum error to approximately 0.1% (see Table 1). Consequently, curve-fitting inadequacies must be eliminated as a potential source of major error - the above piecewise-continuous functions of energy appear to be viable alternatives to interpolating subroutines commonly used in computer implementation.

The present scheme of computer implementation, designed to obtain total exposure rates based on Table 1, Equation (2), tables and energy-dependent parameters in the various appendices, etc., is outlined in Appendix H. An

application of this scheme to the case of a monoenergetic emitter (^{40}K) uniformly distributed throughout a bare, infinitely thick source slab is presented in Appendix I, as illustration.

Results

The theoretical and empirical foundations of the buildup factor concept have been extensively discussed in the leading section of this report, to provide the necessary solid basis for subsequent analytical development. The resultant mathematical formulations in Table 1, Equations (2), (11), etc. are, in their context, generally valid and represent an equally reliable operational base for quantitative implementation of the method. However, the translation from generality to specificity required in the implemental process incorporates approximations, simplifications and extrapolations of unverified effect on accuracy of results. Above all, the unavailability of buildup and attenuation parameters for soil and their substitution with the corresponding coefficients for water indicates that the method, however analytically sound, produces results that must be regarded as only tentatively valid. To test their validity and, by implication, that of the techniques employed, these results may be usefully compared with the results and models of previous investigators, such as Beck (1972) and Schiager (1974).

I. Previous Results and Models

Beck (1972) employs a polynomial series approximation to the Boltzmann transport equation to determine exposure rates due to ^{238}U , ^{232}Th and ^{40}K decay chain gamma emitters, distributed uniformly in the ground with infinite half-space geometry. Two of his results are particularly relevant to present purposes. Using the simplified notation of Equations (8), (9) and (47-C), they are:

exposure rate at 1 meter above the surface of a bare, infinitely thick source slab containing a uniform distribution of ^{40}K , source of 1.464 MeV gammas,

$$\dot{X}_{1m}(\infty) = 0.179 \text{ } \mu\text{R/h per pCi/g} \quad (14)$$

total exposure rate at 1 meter above the surface of a bare, infinitely thick source slab containing, in uniform distribution and radioactive equilibrium, all the nuclides of the ^{238}U decay chain through ^{210}Po ,

$$\dot{X}_{1m}(\infty) = 1.82 \text{ } \mu\text{R/h per pCi/g} \quad (15)$$

Schiager (1974) draws from experimental data available to him to propose a buildup factor for calculations involving tailings piles which, in present notation, is

$$B = e^{[\mu t/(1 + \mu t)]} \quad (16)$$

where $\mu = 0.11 \text{ cm}^{-1}$, attenuation coefficient for "dry packed tailings" or "moist packed earth" of density 1.6 g/cm^3

With other correction factors, Schiager's model of total exposure rate as function of a bare tailings slab thickness t may be expressed, in the simplified notation of Equation (9), as

$$\dot{X}(t) = 0.92[1 - E_2(\mu t)]e^{[\mu t/(1 + \mu t)]} \mu\text{R/h per pCi/g} \quad (17)$$

It follows from the above that, for bare, "infinitely" thick tailings, the total exposure rate is

$$\begin{aligned}\dot{X}(\infty) &= 0.92 \text{ e } \mu\text{R/h per pCi/g} \\ &= 2.5 \text{ } \mu\text{R/h per pCi/g}\end{aligned}\tag{18}$$

In addition, Schiager (1974) includes a graph of decreasing exposure rate as function of increasing thickness of overburden. Using the simplified notation of Equation (8), this is interpreted as

$$\frac{\dot{X}(d)}{\dot{X}(0)} = e^{-d/L}\tag{19}$$

where L = soil relaxation length with respect to exposure rate, cm
 ≈ 14 cm, in Schiager's graph (1974)

Schiager's equations are intended for tailings, thus primarily for ^{226}Ra and daughters rather than for the more inclusive ^{238}U decay chain. However, the ^{226}Ra decay chain comprises roughly 98% of the total energy emitted by the ^{238}U chain (see Appendix D). Neglecting this minor difference, Schiager's results may be compared to those of the present report.

II. Comparison With Present Results

The first comparison is useful in testing the accuracy of the approximation for $\mu_{\text{soil}}(E)$ in Appendix G, namely

$$\mu_{\text{soil}}(E) = \left[\frac{\mu(E)}{\rho} \right]_{\text{H}_2\text{O}} \times \rho_{\text{soil}}\tag{20}$$

where $\rho_{\text{soil}} = 1.6 \text{ g/cm}^3$

To that effect, Beck's result for the monoenergetic 1.464 MeV gammas from ^{40}K , in Equation (14), is contrasted to that produced by the present simpler method, detailed in Appendix I,

$$\dot{X}_{1m}(\infty) = 0.172 \text{ } \mu\text{R/h per pCi/g} \quad (21)$$

The present result is less than 4% smaller than Beck's corresponding value in Equation (14), suggesting that use of water buildup parameters with the approximation in (20) and Appendix G is not unreasonable for energies above 0.25 MeV. By implication, the use of (20) for energies below 0.25 MeV should produce conservative results (see pertinent discussion in Appendix G).

Another valuable comparison involves maximum total exposure rates at one meter above the air-ground interface of a tailings pile or uranium-bearing soil, containing all the uranium series nuclides from ^{238}U (inclusive) through ^{210}Po in radioactive equilibrium and uniform distribution. Calculation 2 in Appendix H represents the computer-implemented application of the present method, generating

$$\dot{X}_{1m}(\infty) = 1.96 \text{ } \mu\text{R/hr per pCi/g} \quad (22a)$$

This value is 7.7% higher than Beck's in (15). However, the entire energy spectrum for the ^{238}U decay chain was employed in arriving at the result in (22a), whereas Beck explicitly excluded x-rays and low intensity gammas from his calculations. Eliminating the contributions of the same to (22a) permits a more valid comparison:

$$\dot{X}_{1m}(\infty) = 1.89 \text{ } \mu\text{R/hr per pCi/g} \quad (22b)$$

The reduced exposure rate is less than 4% higher than Beck's in (15). Recalling the result in (21), it can be tentatively concluded that the present method estimates exposure rates within $\pm 4\%$ of Beck's results, when adjusted for proper comparison.

The corresponding maximum total exposure rate at ground surface, including all energies in the ^{238}U decay chain, is

$$\dot{X}(\infty) = 2.06 \text{ } \mu\text{R/hr per pCi/g} \quad (23)$$

This result is 5% higher than the exposure rate at one meter above ground, Equation (22a), whereas Beck (1972) mentions a corresponding difference of only 2%.

Schiager (1974) evidently ignores these minor differences, describing his results as "exposure rate over the slab", applicable to "a point near the surface." His maximum exposure rate of "2.5 $\mu\text{R/h}$ per pCi/g" is 21% greater than the ground surface maximum in (23) and 28% greater than the maximum at one meter above ground, in (22a). A comparison of Schiager's maximum to those produced by reduced spectra, i.e., excluding x-rays and low intensity gammas, leads to still greater differences, as may be expected. Thus, Schiager's maximum is 32% greater than the corresponding value in (22b) and 37% greater than Beck's maximum in (15), both for 1 meter above ground.

Based on the above discussion, the most suitable application for Schiager's model is in describing exposure rates at ground level. Nevertheless, his maximum exposure rate appears exceedingly conservative when compared to the various maxima obtained by Beck and the present method. The latter results

may be alleged to be mutually supportive, to an extent limited by the substitutions, approximations and other inadequacies of the present method.

By contrast, Beck underestimates the maximum exposure rate, by excluding x-rays and gammas with intensities less than 0.1% (1972). This eliminates over 200 entries from the tables in Appendix D, pertaining to x-rays, weak gammas represented by their summed intensities and average energy, and gammas of effectively low intensity due to alternate decay modes with low branching ratios (^{234}Pa)*. Although individually insignificant, their summed products of energy times intensity represent a potential 4.6% increment to the total energy emitted in Beck's source spectrum. Being fairly representative of the spectrum as a whole, with energies ranging from 0.01 MeV to 1.93 MeV, these omitted photons may proportionately increase Beck's maximum exposure rate of "1.82 $\mu\text{R/h}$ per pCi/g" to as much as "1.9 $\mu\text{R/h}$ per pCi/g."

III. Models Based on Present Techniques and Comparison with Previous Models

The discrepant estimates of maximum exposure rate in the preceding section indicate the existence of uncertainties in the bases and processes of such estimation. These uncertainties contributed to the rejection of models explicitly postulating numerical values of maximum exposure rate, in favor of expressions describing the dependence of ratios $\dot{X}(d)/\dot{X}(0)$ and $\dot{X}(t)/\dot{X}(\infty)$ on varying d and t . Such "relative effect" models have the advantage of substantially reducing potential error, through mutual cancellation of terms, while avoiding commitment to a maximum value.

* The tables in Appendix D do not differentiate between x-rays, weak gammas and gammas of intensity greater than 0.1%. To verify the assertion motivating this footnote, reference to Kocher (1977) is suggested.

Accordingly, Calculations 3) and 4) in Appendix H were repeated with several t and d values, generating $\dot{X}(t)$ and $\dot{X}(d)$ ground surface exposure rates which were then normalized with respect to $\dot{X}(\infty) = \dot{X}(0) = 1.765 \text{ } \mu\text{R/h per pCi/g}$, maximum exposure rate, at ground surface, due to gammas of energies above 0.5 MeV. The resultant sets of ratios $\dot{X}(t)/\dot{X}(\infty)$ and $\dot{X}(d)/\dot{X}(0)$, displayed in Tables 2 and 3, are expected to apply at ground surface and at one meter above ground level, for exposure rates due to the entire ^{238}U energy spectrum, i.e. including the 15 of total energy emitted in the range $E < 0.5 \text{ MeV}$.

The results in Table 3 [from Calculation 4)] are particularly useful in the development of mathematical models. The depth-dependence of the ratio $\dot{X}(d)/\dot{X}(0)$ has been often expressed as a decreasing exponential function with an argument " $-d/L$ ", where d is the depth of cover and L is the "relaxation length" [see Equation (19)]. This relaxation length represents the thickness of cover required to reduce the exposure rate by a factor of "e", and is assumed to be constant for a given material, e.g. Schiager estimates it to be $\approx 14 \text{ cm}$, for soil, in (19). The ratios $\dot{X}(d)/\dot{X}(0)$ in Table 3 allow testing the accuracy of this assumption by rearranging (19) to produce

$$L \text{ or } L(d) = \frac{-d}{\ln \frac{\dot{X}(d)}{\dot{X}(0)}} \text{ [from Table 3]} \quad (24)$$

The results of (24) are included in Table 3. They indicate that L is by no means a constant, but a well defined function of d. Furthermore, when graphed (Figure 2) they suggest that the increase in L(d) as d increases is not a transient phenomenon for the range $1 \text{ cm} \leq 100 \text{ cm}$, but that the trend will continue for higher d. It is clear, however, that L(d) is a slowly-varying function, particularly as d increases - thus statistical fluctuations

Table 2. Proportional Increase in Exposure Rates*, with Respect to Maximum, as Function of Increasing Thickness of the Uranium Bearing Slab

Thickness t of Uranium-Bearing Slab, cm	Exposure Rate $\dot{X}(t)$ * Due to Slab of thickness t, $\mu\text{R/h}$ per pCi/g	Ratio of Exposure rate $\dot{X}(t)$ to Maximum Exposure Rate $\dot{X}(\infty)$: $\dot{X}(t)/\dot{X}(\infty)$, dimensionless
1	0.31176	0.17665
2	0.51318	0.29077
3	0.66856	0.37881
4	0.79662	0.45137
5	0.90348	0.51192
6	0.99993	0.56657
7	1.0848	0.61464
8	1.1560	0.65500
9	1.2192	0.69080
10	1.2754	0.72264
15	1.4765	0.83660
20	1.5914	0.90170
30	1.6993	0.96283
40	1.7391	0.98536
50	1.7544	0.99406
60	1.7601	0.99753
70	1.7630	0.99896
80	1.7641	0.99955
90	1.7645	0.9998
100	1.7647	0.99991
∞	1.7649	1.0

* Tabulated exposure rates $\dot{X}(t)$ [including $\dot{X}(\infty) = 1.7649 \mu\text{R/h}$ per pCi/g] represent summations of exposure rates due to all gammas of energy greater than 0.5 MeV, using Taylor's buildup factor parameters. Since energies $E > 0.5$ MeV comprise over 85% of the total energy emitted by the ^{238}U decay chain at equilibrium, the resulting ratios are expected to apply to exposure rates due to the entire ^{238}U energy spectrum [with $\dot{X}(\infty) = 2.06 \mu\text{R/h}$ per pCi/g, per example]

Table 3. Proportional Decrease in Exposure Rates¹⁾, With Respect to Maximum, as Function of Increasing Thickness of the Overburden Slab, d

Thickness d ²⁾ of Overburden Slab, cm	Exposure Rate ¹⁾ $\dot{X}(d)$, With Cover Slab of Thick- ness d, $\mu\text{R/h/pCi/g}$	Ratio of Exposure Rate $\dot{X}(d)$ to Maxi- mum Exposure Rate $\dot{X}(0)$, or $\dot{X}(d)/\dot{X}(0)$, dimensionless	Depth-dependent Relaxation Length $L(d)$, cm
0	1.7649	1.0	-
1	1.4531	0.8234	5.145
2	1.2517	0.7092	5.832
3	2.0963	0.6212	6.301
4	0.9683	0.5486	6.663
5	0.8614	0.4881	6.971
6	0.7650	0.4334	7.177
7	0.6801	0.3854	7.341
8	0.6089	0.3450	7.517
9	0.5457	0.3092	7.668
10	0.4895	0.2774	7.797
15	0.2884	0.1634	8.280
20	0.1735	0.0983	8.622
30	6.559×10^{-2}	3.717×10^{-2}	9.112
40	2.583×10^{-2}	1.464×10^{-2}	9.469
50	1.048×10^{-2}	5.937×10^{-3}	9.753
60	4.348×10^{-3}	2.464×10^{-3}	9.990
70	1.837×10^{-3}	1.041×10^{-3}	10.193
80	7.881×10^{-4}	4.465×10^{-4}	10.371
90	3.422×10^{-4}	1.939×10^{-4}	10.529
100	1.502×10^{-4}	8.510×10^{-5}	10.671

¹⁾Tabulated exposure rates $\dot{X}(d)$ [including $\dot{X}(0) = 1.7649 \mu\text{R/h per pCi/g}$] represent summations of exposure rates due to all gammas of energy greater than 0.5 MeV, using Taylor's buildup factor parameters. Since energies $E > 0.5$ MeV comprise over 85% of the total energy emitted by the ^{238}U decay chain at equilibrium, the resulting ratios are expected to apply to exposure rates due to the entire ^{238}U energy spectrum [with $\dot{X}(0) = 2.06 \mu\text{R/h per pCi/g}$, as example]

²⁾Limited to $d \leq 100$ cm because of exponentially increasing computer "roundoff" error.

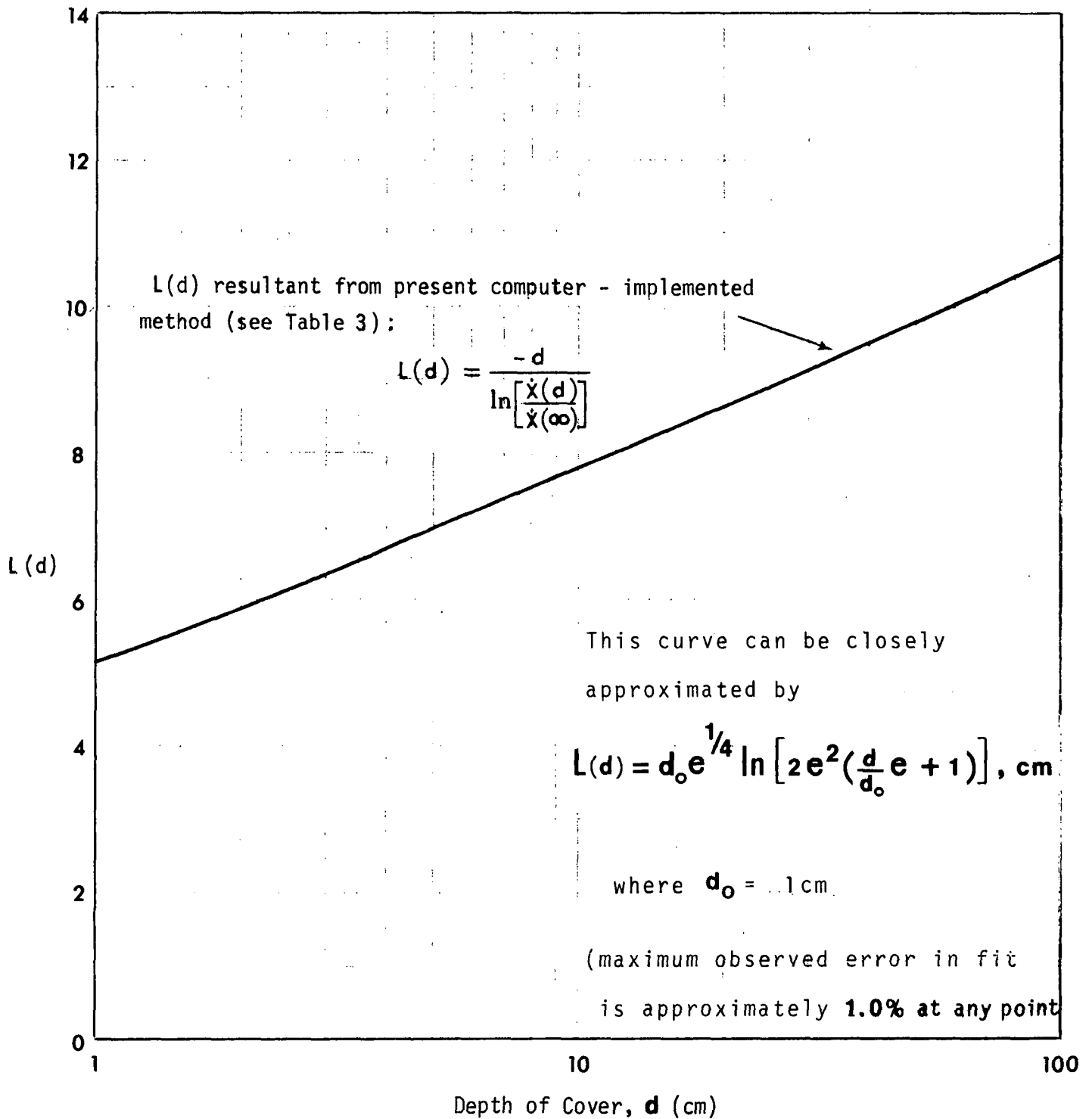


Figure 2 . Depth-dependent relaxation parameter $L(d)$, as obtained by the present computer implemented model. Accompanying the graph is a curve-fitting equation by the present author, which replicates the graphed results with a maximum observed error of 1.0% , at any point.

and equipment inadequacies may frustrate experimental verification of the functional behavior under many conditions. The present author represents $L(d)$ as

$$L(d) = d_0 e^{1/4} \ln \left[2e^2 \left(\frac{d}{d_0} e + 1 \right) \right], \text{ in cm} \quad (25)$$

where $L(d)$ = depth-dependent relaxation length with respect to exposure rate, cm

d = depth of cover, in cm

$d_0 = 1$ cm

The resemblance of (25) to a theoretically derived function requires special emphasis of the fact that it is merely a convenient fit of computer output data. In the process of obtaining this "pseudo-analytical formula," fitting coefficients corresponding to powers of the natural base "e" were found to produce optimum results - replicating the values $L(d)$ in Table 3 with a maximum curve-fitting error, at any point, of 1.0%*. This discouraged the use of simpler, but less accurate formulations of the type $L(d) = a + b \ln(d/d_0)$, as discussed in Appendix J.

Replacing L in (19) with the depth-dependent $L(d)$ in (25) produces

$$\frac{\dot{X}(d)}{\dot{X}(0)} = e^{-\left\{ \frac{d/d_0}{e^{1/4} \ln \left[2e^2 \left(\frac{d}{d_0} e + 1 \right) \right]} \right\}} \quad (26)$$

* The import of the small curve-fitting errors mentioned throughout this section is discussed in the closing paragraphs of same.

This expression matches the corresponding $\dot{X}(d)/\dot{X}(0)$ values in Table 3 with a maximum observed curve-fitting error of about 1.1%, at any point.

Graphical comparisons of Equations (25) and (26) with the models of Equation (19) may be found in Figures 3 and 4. Both these figures demonstrate the conservatism of L and $\dot{X}(d)/\dot{X}(0)$ from Schiager (1974) in contrast to those of the present method.

The ratios $\dot{X}(d)/\dot{X}(0)$ in Table 3 may be theoretically related to the ratios $\dot{X}(t)/\dot{X}(\infty)$ in Table 2 by a relationship derived in Appendix K, for the special cases $t = d$, which is

$$\frac{\dot{X}(t)}{\dot{X}(\infty)} = 1 - \frac{\dot{X}(d)}{\dot{X}(0)}, \text{ for } t = d \quad (27)$$

Applying Equation (26) to the above expression summarizes the ratios $\dot{X}(t)/\dot{X}(\infty)$ as function of source slab thickness t ,

$$\frac{\dot{X}(t)}{\dot{X}(\infty)} = 1 - e^{-\left\{ \frac{t/t_0}{e^{1/4} \ln[2e^2(\frac{t}{t_0}e + 1)]} \right\}} \quad (28)$$

To test the validity of (28) it is necessary to compare the values $\dot{X}(t)/\dot{X}(\infty)$ obtained by this equation to the values in Table 2, which were obtained independently [Calculation 3)] from those of Table 3. This comparison yields a maximum curve-fitting error of less than 1%, at any point (maximum error: 0.7%, at $t = 5$ cm).

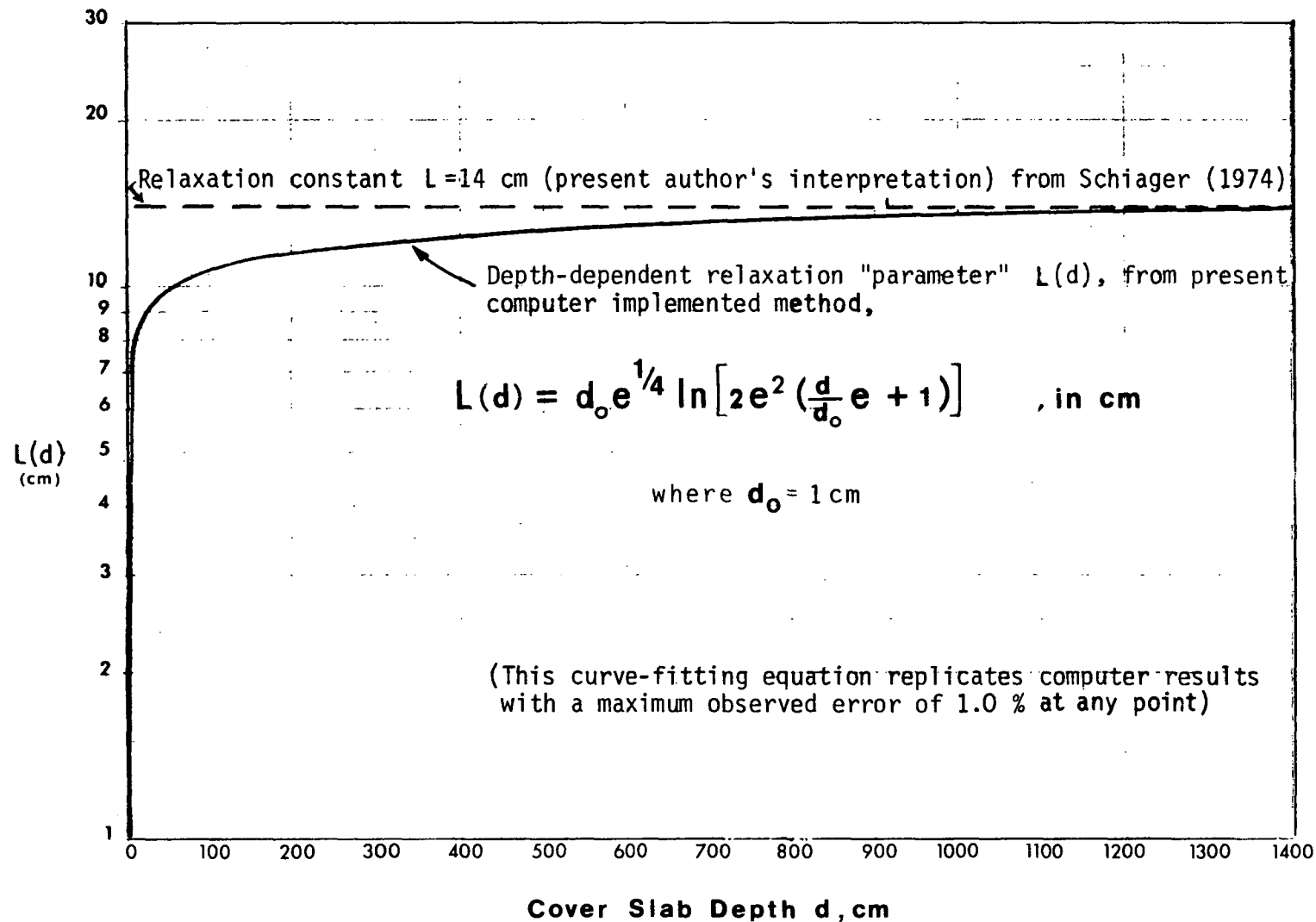


Figure 3 . Comparison of proposed depth-dependent relaxation "parameter" $L(d)$, from results obtained with the present computer implemented model, with the relaxation constant from Figure 4 in Schiager (1974), attributed to Throckmorton(1973), as interpreted by the present author.

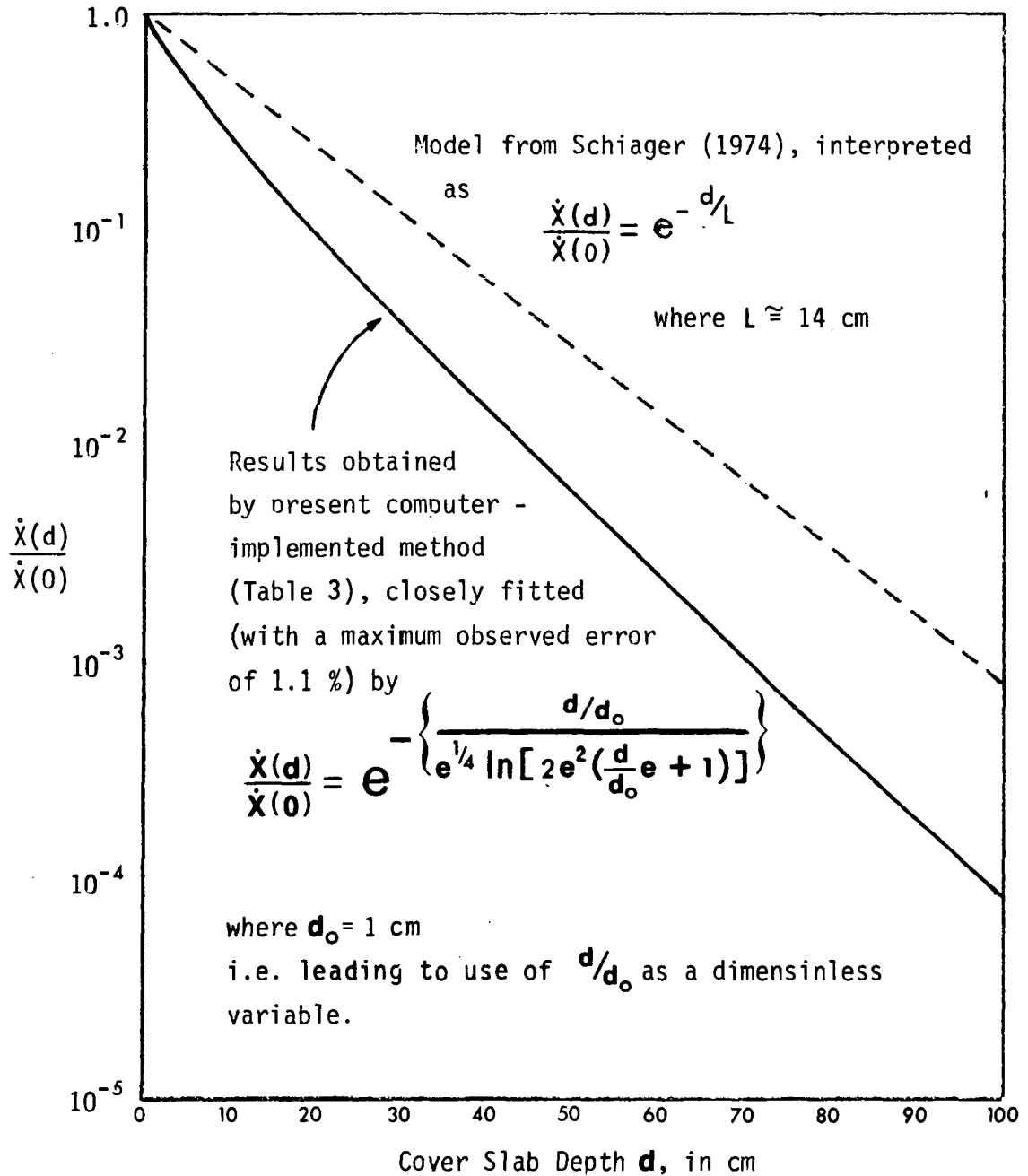


Figure 4 . Relative decrease in exposure rate, with respect to maximum exposure rate possible, as function of increasing thickness of the overburden slab, as obtained by the present proposed computer-implemented method (Table 3), fitted by applying the proposed model of the depth-dependent relaxation length L , and compared to a model from Schiager (1974).

The results in Table 2 or from Equation (28) can be compared with those of Schiager (1974), obtained for tailings. A formalized expression of Schiager's ratios $\dot{X}(t)/\dot{X}(\infty)$ may be produced by dividing Equation (17) by Equation (18), both from Schiager's model,

$$\frac{\dot{X}(t)}{\dot{X}(\infty)} = [1 - E_2(\mu t)] e^{-1/(1+\mu t)} \quad (29)$$

where μ = Schiager's linear attenuation coefficient in dry tailings
 $= 0.11 \text{ cm}^{-1}$

Graphs of $\dot{X}(t)/\dot{X}(\infty)$ and $\dot{X}(t)$ from (29) are presented in Figures 5 and 6, respectively, along with the corresponding graphed values from Table 2 and Equation (28) for the present model. The latter strongly support Schiager's statement that "For any situation involving tailings depths of more than 1 or 2 feet...the external exposure rate over the tailings can be calculated as follows:

$$\dot{X}(\mu R/h) = 0.92eC_{Ra}(\text{pCi/g}) = 2.5 C_{Ra}(\text{pCi/g})''$$

where C_{Ra} = Radium concentration, pCi/g (in Schiager's notation)

In other words, maximum exposure rates [see Equation (18)] should be closely approximated with source slab thicknesses of 1 or 2 feet. In meeting this criterion, the present model is superior to Schiager's, as may be verified by comparing ratios $\dot{X}(t)/\dot{X}(\infty)$ from Equations (28) and (29), graphed in Figure 5. The present model predicts 97% of maximum exposure rate at $t = 30.5 \text{ cm}$ (1 foot) and 99.8% at $t = 61 \text{ cm}$ (2 feet), whereas Schiager's corresponding values are not quite 4/5 and 9/10, respectively. To attain 97% of maximum exposure

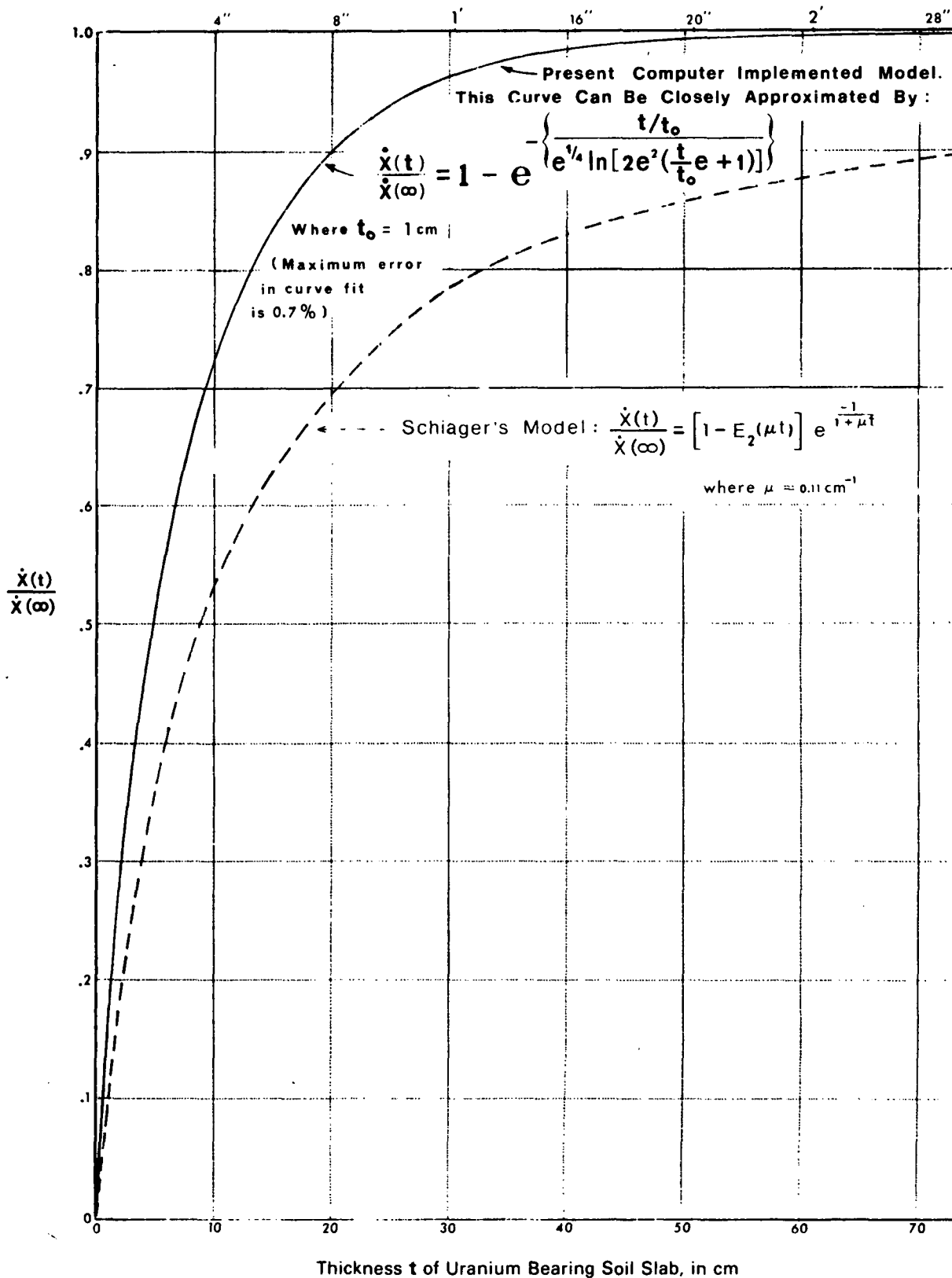


Figure 5. Relative increase in exposure rate, with respect to maximum exposure rate possible, as function increasing thickness of the uranium-bearing soil slab, as obtained by the present computer-implemented method (Table 2), approximated by a curve-fitting equation with a maximum observed error in fit of 0.7 %, and compared to Schiager's model (1974).

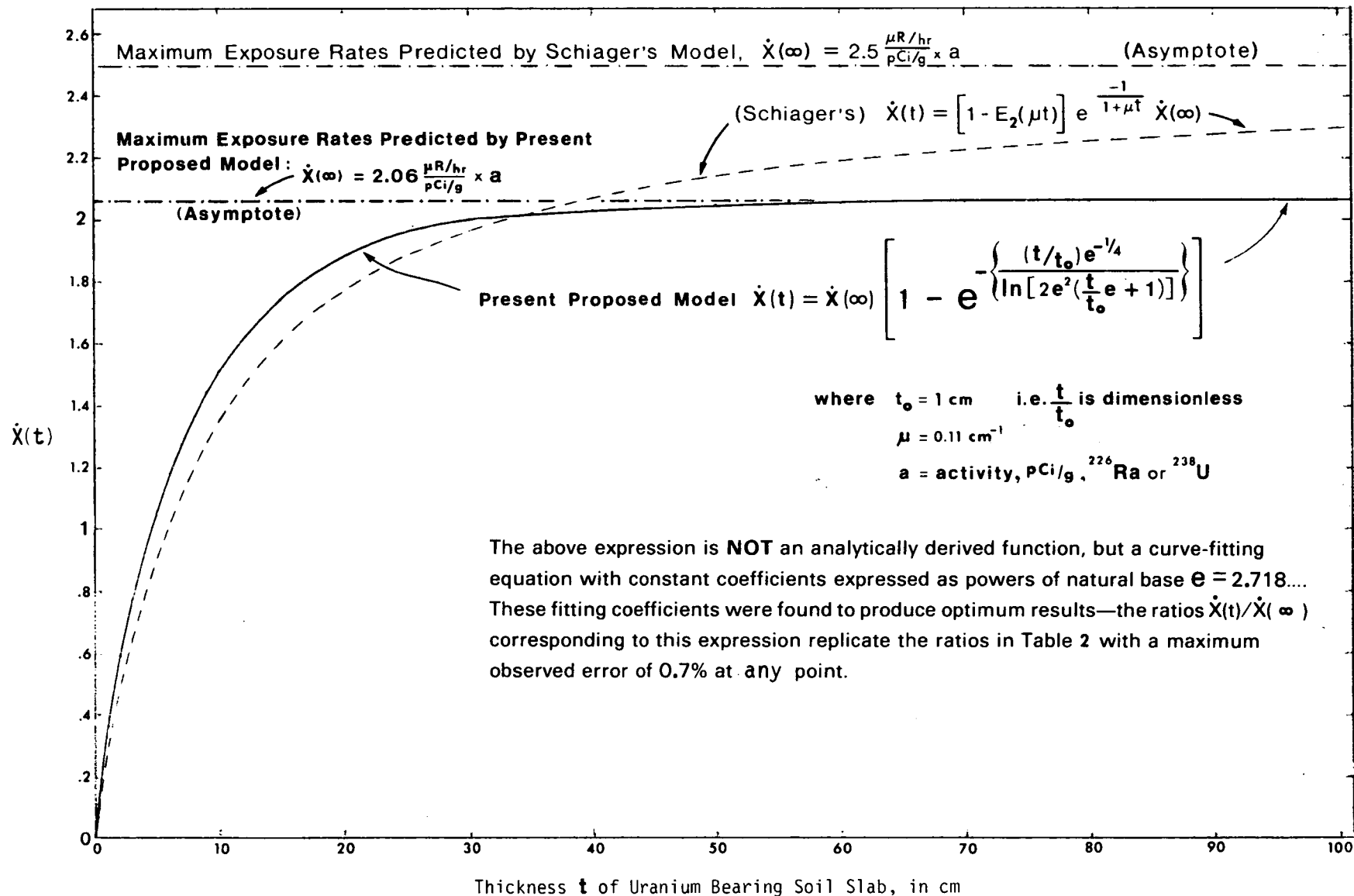


Figure 6. Effects of increasing thickness of a bare uranium bearing soil (or Tailings) slab on the exposure rate at the surface, based on ratios (Table 2) and maximum exposure rate calculated by the present computer-implemented method, and compared to Schiager (1974) results.

rate, Schiager's model requires $t \approx 280$ cm (9 feet), and as much as $t \approx 3700$ cm (120 feet) to reach 99.8%.

The two models show closer agreement when comparing exposure rates (Figure 6), rather than the above $\dot{X}(t)/\dot{X}(\infty)$ ratios. However, this relative agreement is limited to small source slab thicknesses $t \leq 40$ cm, and merely reflects the difference in maximum exposure rates $\dot{X}(\infty)$ - Schiager's maximum of "2.5 $\mu\text{R/h}$ per pCi/g" is substantially higher than Beck's or the present model's maxima.

In summation, the present model expresses the dependence of exposure rate on source slab thickness t in a manner consistent with Schiager's observations, as quoted, has a reliable analytical foundation, and the support of a method of implementation that produced maximum exposure rates within $\pm 4\%$ of Beck's results. One additional advantage of this model is the analytically demonstrable relationship to the dependence of exposure rates on overburden depth d [see Equations (26), (27) and (28)], which leads to an internally consistent comprehensive model of exposure rate as function of d and t ,

$$\dot{X}(d,t) = \dot{X}_{\max} e^{-\left\{ \frac{d/d_0}{e^{1/4} \ln[2e^2(\frac{d}{d_0} + 1)]} \right\}} \left[1 - e^{-\left\{ \frac{t/t_0}{e^{1/4} \ln[2e^2(\frac{t}{t_0} + 1)]} \right\}} \right] \quad (30)$$

where $\dot{X}(t,d)$ = exposure rate, in $\mu\text{R/h}$ per pCi/g, as function of

t = thickness of uranium-bearing soil slab, in cm, and

$t_0 = 1$ cm

d = thickness of source-free cover material slab, in cm

$d_0 = 1$ cm

$\dot{X}_{\max} = \dot{X}(\infty) = \dot{X}(0)$ = maximum possible exposure rate, with $t = \infty$ and $d = 0$

This comprehensive model consists, primarily, of the product of curve-fitting equations (26) and (28), describing the magnitude of ratios $\dot{X}(d)/\dot{X}(0)$ and $\dot{X}(t)/\dot{X}(\infty)$ as functions of their respective arguments. It may be recalled that the choice of ratios to represent exposure rate dependence on d and t was intended to reduce potential errors, while avoiding commitment to explicit values of maximum exposure rate $\dot{X}(0) = \dot{X}(\infty)$. The resultant flexibility of (26) and (28) allowed the formulation of the comprehensive model in (30) (see Appendix J), while qualifying it to incorporate, within reason, different values of maximum exposure rate \dot{X}_{\max} . This is a distinct advantage of the proposed model(s), since uncertainties in buildup and attenuation properties of soil indicate that the present author's maximum exposure rates in (22a) and (23) require further substantiation.

In that context, the $\pm 4\%$ difference* between Beck's results (1972) and those of the present study, although indicative of general agreement, nevertheless represents a residual conflict that cannot be readily resolved. The inadequacies of the present method do not allow proposing the resultant maxima in preference to Beck's. On the other hand, Beck's exclusion of x-rays and low-intensity gammas leads to an underestimation of maximum exposure rate, by up to 4.6% in terms of Beck's results. Consequently, assigning a specific value to maximum exposure rate may be premature, a range of values being more representative of persisting uncertainties. Prudence dictates that the limits of such range be realistic but conservative. Two sets of limits are required for the cases of current interest.

* Excluding the contribution of x-rays and low intensity gammas from the present results.

For the case of maximum exposure rate at one meter above ground, the present estimate in (22a) provides an upper limit. The lower limit of the range was generated by conservatively increasing Beck's result in (15) by 4.6% . Thus, at one meter above ground,

$$1.90 \text{ } \mu\text{R/h per pCi/g} \leq \dot{X}_{\text{max}} \leq 1.96 \text{ } \mu\text{R/h per pCi/g} \quad (31)$$

For maximum exposure rate at ground surface, the upper limit was obtained from (23), i.e. an increase of 5% over the corresponding value in (31). Since Beck estimated a difference of only 2% between exposure rates at ground level and at one meter above ground, the lower limit in (31) was increased proportionately, for consistency with his study. Thus, for ground surface exposure rates,

$$1.94 \text{ } \mu\text{R/h per pCi/g} \leq \dot{X}_{\text{max}} \leq 2.06 \text{ } \mu\text{R/h per pCi/g} \quad (32)$$

The value ranges (31) and (32) imply potential maximum errors of 3% and 6% , respectively, which may be assumed to represent the net effect of different soil-surrogate materials, approximations, etc., in the two studies, but excluding the effect of different spectra. These maximum potential errors delimit the liability of using maxima from (31) or (32)* in the comprehensive model of Equation (30). Including the combined curve-fitting errors of (26) and (28), a total of 1.8% , this model should express exposure rate as function of d and t with a maximum possible error of less than 8% , for any set of d and t values not exceeding 100 cm, severally.

* Implicit in the process of setting ranges (31) and (32) is the constraint that a maximum exposure rate at ground surface, chosen from (32), should be 2% to 5% greater than the corresponding maximum exposure rate at one meter above ground level, from (31).

As pointed out in Figures 2 through 6, the models in (25), (26), (28) and, by extension, the comprehensive model in (30), are based on results obtained by computerized techniques. These are virtually indispensable for the efficient performance of repetitive mathematical tasks, but introduce small inaccuracies in the process of "rounding off" results to a prescribed number of digits. The effect of such "computer round off errors" grows progressively larger with increasing d and t , ultimately compromising the validity of all results corresponding to d and t greater than 100 cm. Such effect is immaterial in modeling $\dot{X}(t)/\dot{X}(\infty)$, but very significant in studying the efficacy of cover thickness d in reducing exposure, as described by $\dot{X}(d)/\dot{X}(0)$. Since "small" round off errors in $\dot{X}(d)$ may represent differences of orders of magnitude, the modeling of $\dot{X}(d)/\dot{X}(0)$ was not extended beyond results verifiable by Equation (27) and comparison of Tables 2 and 3, values corresponding to larger d being left to extrapolation.

In the latter context, the graph of $L(d)$ in Figure 2 suggests that any expression providing an accurate fit to the values graphed should be applicable, with reasonable expectations of accuracy, to a range of cover depths d extending beyond 100 cm. Since Equation (25) meets such requirement with a maximum error of 1% , at any point, corresponding expectations of generality accrue to this equation and the adjunct Equation (26), representing $\dot{X}(d)/\dot{X}(0)$. Such presumed generality does not negate the possibility of increased error for values of d greatly in excess of 100 cm; it merely restates that errors of such magnitude as to invalidate Equation (26) – and thus (28) and (30) – cannot be anticipated on the basis of the graph in Figure 2 and the key equation (25). In that vein, the aforementioned equations are included in the comparison of general models summarized by Table 4.

TABLE 4 . Comparison of Maximum Exposure Rates and Models Based on Present Technique With Previously Published Models and Values.

	Schiager's Models	Curve-Fitting Models, From Values Obtained by Present Technique	
Exposure rate tailings slab thickness t (cm) and overburden depth d (cm) - comprehensive model- ²³⁸ U chain.	As collated from Schiager (1974) $\dot{X}(d,t) = 0.92 [1 - E_2(\mu t)] e^{[\mu t/(1 + \mu t)]} e^{-d/L}$	$\dot{X}(d,t) = \dot{X}_{\max} e^{-\left\{ \frac{d/d_0}{e^{1/4} \ln [2e^2 (\frac{d}{d_0} e + 1)]} \right\}} \left[1 - e^{-\left\{ \frac{t/t_0}{e^{1/4} \ln [2e^2 (\frac{t}{t_0} e + 1)]} \right\}} \right]$	
Ratio of exposure rate due to bare tailings slab t cm thick to exposure rate due to infi- nitely thick slab - ²³⁸ U chain.	As adapted from Schiager (1974) $\frac{\dot{X}(t)}{\dot{X}(\infty)} = [1 - E_2(\mu t)] e^{-1/(1 + \mu t)}$	$\frac{\dot{X}(t)}{\dot{X}(\infty)} = 1 - e^{-\left\{ \frac{t/t_0}{e^{1/4} \ln [2e^2 (\frac{t}{t_0} e + 1)]} \right\}}$ t = tailings slab thickness, in cm d = overburden depth, in cm t ₀ = d ₀ = 1 cm $\dot{X}_{\max} = \dot{X}(\infty) = \dot{X}(0)$ = maximum exposure rate, obtained with t = ∞ and d = 0.	
Ratio of exposure rate due to slab covered with overburden d cm thick to exposure rate due to bare slab - ²³⁸ U chain.	As implied by Figure 4 in Schiager (1974) $\frac{\dot{X}(d)}{\dot{X}(0)} = e^{-d/L}$	$\frac{\dot{X}(d)}{\dot{X}(0)} = e^{-\left\{ \frac{d/d_0}{e^{1/4} \ln [2e^2 (\frac{d}{d_0} e + 1)]} \right\}}$	
Relaxation length, in cm, with respect to exposure rate- ²³⁸ U chain.	From Figure 4 in Schiager (1974) L = 14 cm	$L(d) = d_0 e^{1/4} \ln [2e^2 (\frac{d}{d_0} e + 1)]$ Overburden is assumed to be impervious to radon gas, in these models.	
	Schiager (1974)	Beck (1972)	Values Obtained by Present Technique
Maximum exposure rate at ground surface - ²³⁸ U chain.	$\dot{X}_{\max} = 0.92 \cdot e \text{ } \mu\text{R/h per pCi/g}$ $= 2.5 \text{ } \mu\text{R/h per pCi/g}$		$\dot{X}_{\max} = 2.06 \text{ } \mu\text{R/h per pCi/g}$
Maximum exposure rate at 1 m above ground surface- ²³⁸ U chain.			$\dot{X}_{\max} = 1.96 \text{ } \mu\text{R/h per pCi/g}$
Same as above, excluding weak gammas and X-rays - ²³⁸ U chain.		$\dot{X}_{\max} = 1.82 \text{ } \mu\text{R/h per pCi/g}$	$\dot{X}_{\max} = 1.89 \text{ } \mu\text{R/h per pCi/g}$
Exposure rate over bare, infi- nitely thick deposit of ⁴⁰ K, at 1 m above surface.		$\dot{X}_{\max} = 0.179 \text{ } \mu\text{R/h per pCi/g}$	$\dot{X}_{\max} = 0.172 \text{ } \mu\text{R/h per pCi/g}$

Applications

One of the primary purposes of this report is to demonstrate the application of simple mathematical models, developed in the originating study, to conditions of somewhat greater complexity than those envisioned in the course of such development. It should be recalled that the analysis and implementation ultimately yielding Equations (25), (26), (28) and the comprehensive model in (30) were made possible by a number of simplifying assumptions (Appendix B), which admit of conditions that are, generally, improbable but conceptually not impossible. The relevant exception to this generality is the assumption that radon will not emanate from the tailings or uranium-bearing soil, implying a lack of motivity conceptually improbable and generally impossible for a noble gas in a porous medium.

To illustrate one of the consequences of this faulty assumption, it suffices to apply Equation (30) to the case of a bare tailings slab. Since the \dot{X}_{\max} value in (30) was obtained assuming that ^{222}Rn does not diffuse out of the source material, it follows that (30) will overestimate exposure rate.

The reverse is true when Equations (25), (26), and (30) are applied to determine the shielding effects of cover. Unless the overburden is impermeable to ^{222}Rn , the exposure rates from a tailings pile covered with overburden of thickness d will be substantially underestimated - by orders of magnitude if $d > 100$ cm. This is due to the fact that radon gas may be generally expected to diffuse into the cover material, generating a source of gamma rays with considerably less shielding than the thickness of the overburden would indicate. Fortunately, models developed in the preceding

sections may be used to provide a more realistic estimate of exposure rates due to a covered pile.

The first step in such determination is establishing the distribution of ^{222}Rn in the tailings and cover material. This will depend on the thickness of cover d , the radon emanation power E , and the diffusion coefficient of "free" radon in soil, D . Applying Fick's law to the general diffusion equation, with the boundary conditions and treatment of Appendix L, results in the following two equations:

$$\begin{array}{ll} \text{in overburden} & C_{c\text{TOTAL}}(z) = Ee^{-\alpha d} \sinh[\alpha(d-z)] \\ \text{(for } z \geq 0) & \end{array} \quad (33)$$

$$\begin{array}{ll} \text{in tailings} & C_{t\text{TOTAL}}(z) = 1 - Ee^{\alpha(z-d)} \cosh(\alpha d) \\ \text{(for } z \leq 0) & \end{array} \quad (34)$$

where $C_{c\text{TOTAL}}(z)$ = ^{222}Rn concentration in overburden, in pCi/g of free radon, per pCi/g of ^{226}Ra in tailings, as function of distance z above tailings-cover interface.

$C_{t\text{TOTAL}}(z)$ = ^{222}Rn concentration in tailings, in pCi/g of both free and bound radon, per pCi/g of ^{226}Ra in tailings, as function of distance z below tailings-cover interface.

z = generalized distance, normal to tailings-cover interface

where $z > 0$, above tailings-cover interface,

$z = 0$, at tailings-cover interface,

$z < 0$, below tailings-cover interface

E = emanation power, fraction of ^{222}Rn free to diffuse out of soil grains, dimensionless

$$\alpha = \sqrt{\lambda_{222\text{Rn}}/D} \quad , \text{ where } \lambda_{222\text{Rn}} = \text{decay constant of } ^{222}\text{Rn}, \\ = 2.1 \times 10^{-6} \text{ s}^{-1}$$

D = diffusion coefficient of
 ^{222}Rn , in cm^2/s

d = depth of cover, cm

With the assumption that ^{222}Rn is in radioactive equilibrium with all daughter nuclides throughout the overburden and tailings, the distributions given in (33) and (34) permit establishing exposure rates above the cover, by the use of numerical integration techniques applying the comprehensive model of Equation (30).

The techniques employed take advantage of the fact that the concentration of nuclides increases with decreasing z , and of the linear relationship between concentration and exposure rate, e.g. a concentration of 0.1 pCi/g will lead to an exposure rate one-tenth of that in (30). By representing the concentrations in (33) and (34) as a set of discrete increments ΔC corresponding to distance increments Δz , an ensemble of infinitely thick slabs with different nuclide concentrations ΔC is generated. All but one of these slabs are represented as having source-free overburdens of thicknesses equal to multiples of Δz , according to the number of Δz increments required to reach the depth corresponding to a specific ΔC . This allows direct application of Equation (30) to each of these slabs to calculate an element of exposure rate $\Delta \dot{X}$ (Appendix M).

The sum of all such elements $\Delta \dot{X}$ results in a total exposure rate \dot{X} corresponding to a set of conditions comprising a given thickness of cover d , a diffusion coefficient D , and an emanation power E . Setting $E = 0.2$, a set

of graphs for different D was obtained, describing the effect of increasing d in terms of $\dot{X}(d)/\dot{X}(0)$, in Figure 7.

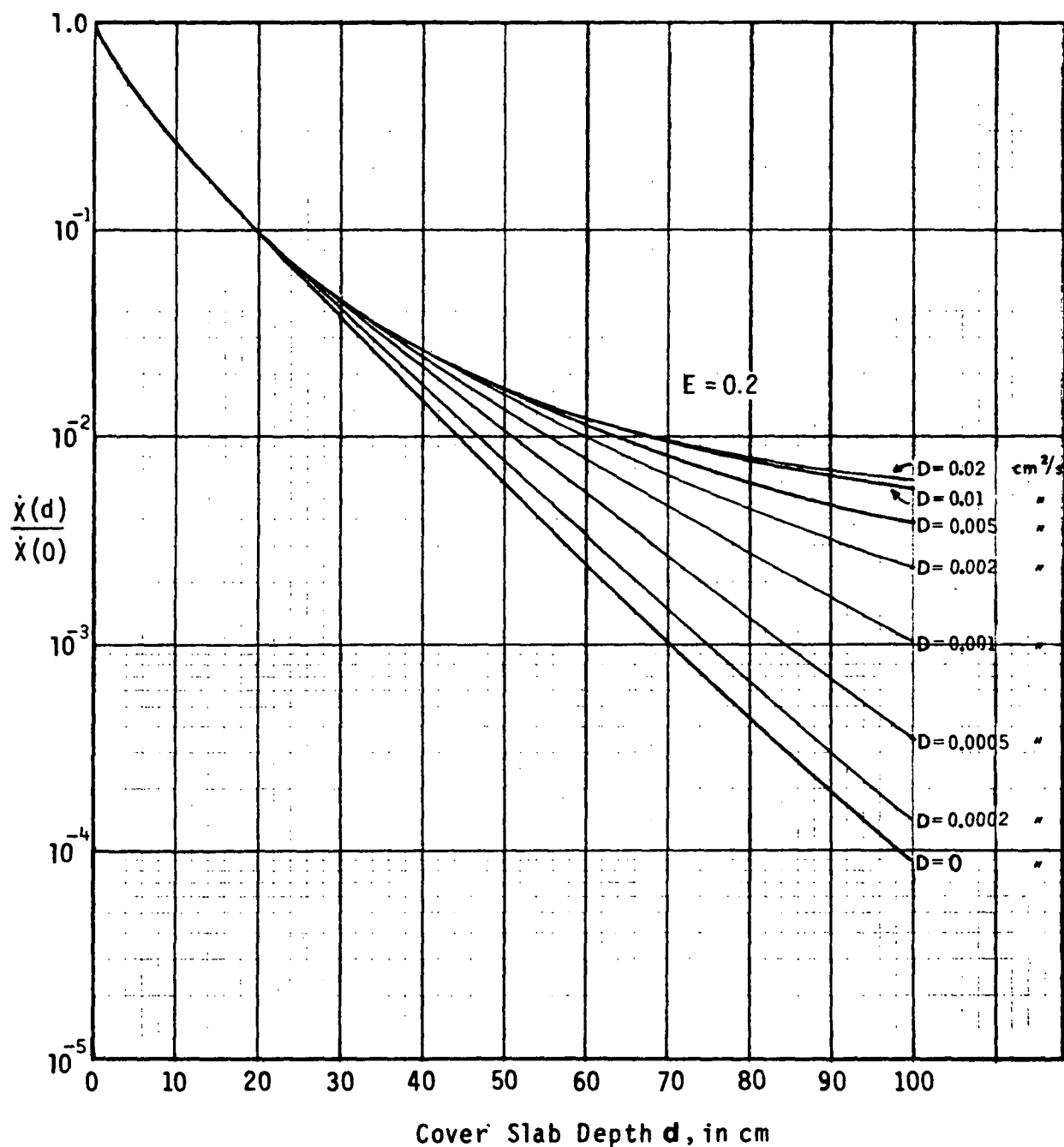


Figure 7 . Relative decrease in exposure rates, with respect to maximum exposure rate possible, as function of increasing thickness d of the overburden slab, for emanation power $E = 20\%$ and different value of radon diffusion coefficient in soil, D , in the range $0.02 \text{ cm}^2/\text{s} \geq D \geq 0.0002 \text{ cm}^2/\text{s}$.

In the case of a bare, infinitely thick tailings slab, the distribution of radon is governed by Equation (34) with $d = 0$, which produces

$$C_{t_{\text{TOTAL}}}(z) = 1 - Ee^{\alpha z}, \text{ for } z \leq 0 \quad (35)$$

Applying to (35) the technique outlined in Appendix M, the effect of radon emanation in reducing maximum exposure rates can be estimated. For the specific case of $E = 0.2$ and $0.0001 \text{ cm}^2/\text{s} \leq D \leq 0.05 \text{ cm}^2/\text{s}$, the process yields results that may be approximated by the curve-fitting Equation (36) and Figure 8.

$$\frac{\dot{X}_{\max_{E=0.2}}^{(D)}}{\dot{X}_{\max_{E=0}}} = 0.75 \left(\frac{D}{D_0} \right)^{-0.21} \quad (36)$$

where $\dot{X}_{\max_{E=0.2}}$ = exposure rate (maximum) over a bare, infinitely thick tailings pile with an emanation power $E = 0.2$, as function of diffusion coefficient D , in $\mu\text{R/h}$ per pCi/g (of ^{226}Ra)

$\dot{X}_{\max_{E=0}}$ = exposure rate (maximum) over a bare, infinitely thick tailings pile without radon emanation, in $\mu\text{R/h}$ per pCi/g .

= \dot{X}_{\max} in Equation (30)

D = radon diffusion coefficient, cm^2/s

D_0 = reference constant

= $1 \text{ cm}^2/\text{s}$

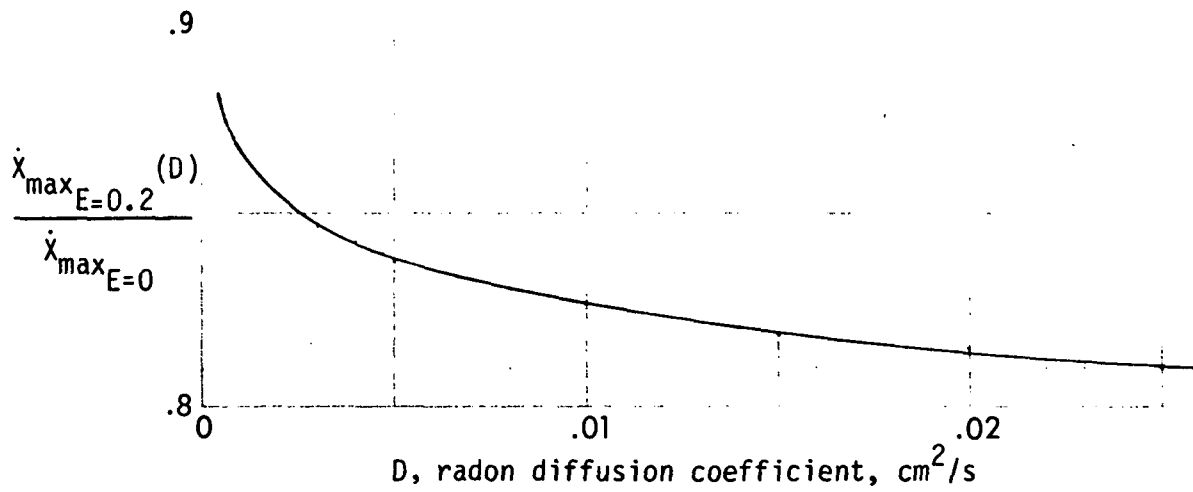


Figure 8. Exposure rate over a bare, infinitely thick tailings pile reduced by radon emanation effects, as function of diffusion coefficient D , for $0.0001 \text{ cm}^2/\text{s} \leq D \leq 0.05 \text{ cm}^2/\text{s}$, and $E = 0.2$.

REFERENCES

- Beck, 1972 Harold L. Beck, "The Physics of Environmental Radiation Fields", The Natural Radiation Environment II, Adams, T. A. S., Lowder, W. M., and Gesell, T., Eds. Report CONF-720805 (U.S. E.R.D.A., Washington)
- Beck, 1981 Personal Communication from H. L. Beck, D.O.E., Environmental Measurements Laboratory, to D. E. Bernhardt, O.R.P.-L.V.F., U.S.E.P.A., May 27, 1981
- Evans, 1972 Robley D. Evans, "The Atomic Nucleus," McGraw-Hill Book Company. Copyright 1955. Fourteenth printing May 26, 1972.
- Ford, Bacon & Davis, 1977 Phase II-Title I, Engineering Assessment of Inactive Uranium Mill Tailings, for U.S. Energy Research and Development Administration (Grand Junction, Colorado) Contract No. E(05-1)-1658, Salt Lake City, Utah, 1977
- G.E.I.S. Uranium Milling, 1979 Generic Environmental Impact Statement on Uranium Milling, NUREG-0511, Volume I, Project M-25, U.S. Nuclear Regulatory Commission, Office of Nuclear Material Safety and Safeguards, April 1979
- Glasstone and Sesonske, 1967 Samuel Glasstone and Alexander Sesonske Nuclear Reactor Engineering, Van Nostrand Reinhold Company, 1967
- Hammond, 1966 C. R. Hammond, "The Elements" Chemical Rubber Co. Handbook of Chemistry and Physics, 47th. Edition, 1966-1967
- Handbook of Mathematical Functions National Bureau of Standards, Applied Mathematical Series, 55, U.S. Department of Commerce, June 1964
- ISIS, 1975 Hugh T. McFadden, "Interactive Statistical Instructional System User's Guide" Computing Center, Lehigh University, June 1975
- Kocher, 1977 D. C. Kocher, "Nuclear Decay Data for Radionuclides Occurring in Routine Releases From Nuclear Fuel Cycle Facilities" ORNL/NUREG/TM-102, Oak Ridge National Laboratory, Oak Ridge, Tennessee, August 1977

Morgan and Turner, 1967 K. Z. Morgan and T. E. Turner, editors Principles of Radiation Protection John Wiley and Sons, Inc., 1967

Radiological Health Handbook Bureau of Radiological Health and Training Institute, Environmental Control Administration. U.S. Department of Health, Education, and Welfare, Public Health Service, Rockville, Maryland, January 1970

Schiager, 1974 Keith T. Schiager, "Analysis of Radiation Exposures on or Near Uranium Mill Tailings Piles", Radiation Data and Reports, Volume 15, No. 7, RDDRA 4 15 (7) 375-476 (1974), U.S. Environmental Protection Agency, Office of Radiation Programs, July 1974

Trubey, 1966 D. K. Trubey, "A Survey of Empirical Functions Used to Fit Gamma-Ray Buildup Factors", ORNL-RSIC-10 Oak Ridge National Laboratory, Radiation Shielding Information Center, February 1966

Appendix A

Choice of Empirical Function to Represent Gamma-Ray Buildup

Determination of external exposure rates from any radioactive source generally requires a calculation of photon fluxes at the points of interest. The latter procedure accounts for the interactions of electromagnetic radiation with the materials it encounters between the point of emission and the receptor. The effects of such interaction can be described in terms of the two related concepts of "attenuation" and "buildup".

By ascribing to each photon an "identity" characterized by energy and direction, the process of "attenuation" can be defined essentially as one of "identity loss", in which scattering and absorption interactions with matter alter the direction and reduce the energy of the original or "primary" radiation. For a well collimated beam, attenuation of primary photons approximates a net loss of photons, since scattering would effectively remove them from the narrow beam. The photon intensity drops exponentially with distance, and is fairly easy to calculate, for such conditions. However, for the more common "poor geometry" or "broad beam" situations, such calculation would result in a sizable underestimation of photon flux at the point of concern.

Calculation of gamma-ray exposure rates from sources distributed in absorbing media must include the effects of "secondary" radiation, consisting mostly of Compton-scattered photons with the addition of annihilation radiation from pair-production, and of X-rays resulting from photoelectric

interactions and bremsstrahlung. Determination of this extra contribution, or "buildup", requires the solution of the Boltzmann transport equation for photons, an extremely involved calculation that has been carried out by several different techniques, with varying success. The most publicized of these techniques, the "method of moments", has ultimately produced "buildup factors" for point isotropic sources of up to nine energies between 0.255 and 10.0 MeV, embedded in infinite media consisting of water or one of six elements with Z ranging from 13 to 92.

Paraphrasing Trubey (1966), a "buildup factor" may be defined as "the ratio of any quantity of interest, characteristic of the total gamma-ray flux, at a chosen point in a given medium, to the same quantity characteristic of the unscattered flux at that same point". Thus, there exist energy-flux buildup, energy-absorption buildup, and dose (or dose rate) buildup factors (Glasstone and Sesonske, 1967). The differences between the various buildup factors are often neglected, but may be significant in critical calculations.

In addition to source energy and medium composition buildup factors are also dependent on spatial coordinates, as implied by the definition and the columnar arrangement of Table 1-A. Since the latter pertains to isotropic point sources in infinite media, such dependence is sufficiently expressed by tabulated values corresponding to one single spatial variable "r", distance from the point source. All other geometries would require an integration over the dimensions of the source, with the spatially-dependent buildup factor included in the integrand. This clearly necessitates expressing the buildup factor as an explicit function of spatial coordinates.

Table 1-A Dose Buildup Factor (B) for a Point Isotropic Source								
Material	MeV	μr^*						
		1	2	4	7	10	15	20
Water	0.255	3.09	7.14	23.0	72.9	166	456	982
	0.5	2.52	5.14	14.3	38.8	77.6	178	334
	1.0 ^a	2.13	3.71	7.68	16.2	27.1	50.4	82.2
	2.0	1.83	2.77	4.88	8.46	12.4	19.5	27.7
	3.0	1.69	2.42	3.91	6.23	8.63	12.8	17.0
	4.0	1.58	2.17	3.34	5.13	6.94	9.97	12.9
	6.0	1.46	1.91	2.76	3.99	5.18	7.09	8.85
	8.0	1.38	1.74	2.40	3.34	4.25	5.66	6.95
	10.0	1.33	1.63	2.19	2.97	3.72	4.90	5.98
Aluminum	0.5	2.37	4.24	9.47	21.5	38.9	80.8	141
	1.0	2.02	3.31	6.57	13.1	21.2	37.9	58.5
	2.0	1.75	2.61	4.62	8.05	11.9	18.7	26.3
	3.0	1.64	2.32	3.78	6.14	8.65	13.0	17.7
	4.0	1.53	2.08	3.22	5.01	6.88	10.1	13.4
	6.0	1.42	1.85	2.70	4.06	5.49	7.97	10.4
	8.0	1.34	1.68	2.37	3.45	4.58	6.56	8.52
	10.0	1.28	1.55	2.12	3.01	3.96	5.63	7.32
Iron	0.5	1.98	3.09	5.98	11.7	19.2	35.4	55.6
	1.0	1.87	2.89	5.39	10.2	16.2	28.3	42.7
	2.0	1.76	2.43	4.13	7.25	10.9	17.6	25.1
	3.0	1.55	2.15	3.51	5.85	8.51	13.5	19.1
	4.0	1.45	1.94	3.03	4.91	7.11	11.2	16.0
	6.0	1.34	1.72	2.58	4.14	6.02	9.89	14.7
	8.0	1.27	1.56	2.23	3.49	5.07	8.50	13.0
	10.0	1.20	1.42	1.95	2.99	4.35	7.54	12.4
Tin	0.5	1.56	2.03	3.09	4.57	6.04	8.64	--
	1.0	1.64	2.30	3.74	6.17	8.85	13.7	18.8
	2.0	1.57	2.17	3.53	5.87	8.53	13.6	19.3
	3.0	1.46	1.96	3.13	5.28	7.91	13.3	20.1
	4.0	1.38	1.81	2.82	4.82	7.41	13.2	21.2
	6.0	1.26	1.57	2.37	4.17	6.94	14.8	29.1
	8.0	1.19	1.42	2.05	3.57	6.19	15.1	34.0
	10.0	1.14	1.31	1.79	2.99	5.21	12.5	33.4
Tungsten	0.5	1.28	1.50	1.84	2.24	2.61	3.12	--
	1.0	1.44	1.83	2.57	3.62	4.64	6.25	(7.35)
	2.0	1.42	1.85	2.72	4.09	5.27	8.07	(10.6)
	3.0	1.36	1.74	2.59	4.00	5.92	9.66	14.1
	4.0	1.29	1.62	2.41	4.03	6.27	12.0	20.9
	6.0	1.20	1.43	2.07	3.60	6.29	15.7	36.3
	8.0	1.14	1.32	1.81	3.05	5.40	15.2	41.9
	10.0	1.11	1.25	1.64	2.62	4.65	14.0	39.3
Lead	0.5	1.24	1.42	1.69	2.00	2.27	2.65	(2.73)
	1.0	1.37	1.69	2.26	3.02	3.74	4.81	5.86
	2.0	1.39	1.76	2.51	3.66	4.84	6.87	9.00
	3.0	1.34	1.68	2.43	2.75	5.30	8.44	12.3
	4.0	1.27	1.56	2.25	3.61	5.44	9.80	16.3
	5.1097	1.21	1.46	2.08	3.44	5.55	11.7	23.6
	6.0	1.13	1.40	1.97	3.34	5.69	13.8	32.7
	8.0	1.14	1.30	1.74	2.89	5.07	14.1	44.6
	10.0	1.11	1.23	1.58	2.52	4.34	12.5	39.2
Uranium	0.5	1.17	1.30	1.48	1.67	1.85	2.03	--
	1.0	1.31	1.56	1.98	2.50	2.97	3.67	--
	2.0	1.33	1.64	2.23	3.09	3.95	5.36	(6.46)
	3.0	1.29	1.58	2.21	3.27	4.51	6.97	9.88
	4.0	1.24	1.50	2.09	3.21	4.66	8.01	12.7
	6.0	1.16	1.36	1.85	2.96	4.80	10.8	23.0
	8.0	1.12	1.27	1.66	2.61	4.36	11.2	28.0
	10.0	1.09	1.20	1.51	2.26	3.73	10.5	28.5

* μr = mass absorption coefficient (μ/p) X distance (cm) X shield density (g/cm^3)

From the Radiological Health Handbook (1970)

There exist many expressions, or "forms", of the buildup factor as function of source energy (E) and distance from the source (r). Three of the best known are the "linear", "quadratic", and "cubic" forms of the buildup factor, polynomials of the 1st, 2nd, and 3rd degree in r, respectively, with energy-dependent coefficients. Two other polynomial forms, "Berger's" and "Taylor's", include exponential terms with products of distance and energy-dependent parameters both as coefficients preceding the exponential functions and/or as function arguments. All but one of the five forms have one common characteristic: that the energy-dependent fitting parameters are valid up to a certain distance from the point source, and have to be replaced with others once that distance is significantly exceeded. The attendant discontinuities plus the fact that each succeeding set of parameters renders a given form increasingly less accurate suggest the need for other choices for a general treatment.

The sole exception to the above mentioned drawbacks is provided by Taylor's Form of the buildup factor, which can be written

$$B_T(E, \mu r) = A(E)e^{-\alpha_1(E)\mu(E)r} + [1-A]e^{-\alpha_2(E)\mu(E)r} \quad (1-A)$$

where $B_T(E, \mu r)$ = energy and distance dependent buildup factor, dimensionless

$A(E), \alpha_1(E), \alpha_2(E)$ = energy-dependent fitting parameters, dimensionless

$\mu(E)$ = energy-dependent attenuation coefficient, cm^{-1}

r = distance, cm

The energy-dependent parameters A , α_1 , and α_2 are expected to retain their validity -to a great extent- at most distances from the source, producing buildup factors (thus, exposure formulas) of consistent accuracy. Table 2-A

illustrates this consistency as contrasted to that of Berger's Form, which is sometimes used as a standard of comparison (Trubey, 1966). There is little variation between the mean percentage deviations of Taylor's Dose Formula at 7 MFP (mean free paths) and the corresponding values at 20 MFP, where 1 MFP = μr . This is particularly true of water and the six pure elements originally examined by the "method of moments" (see Table 1-A) and considerably less so for the various types of concrete, which are mixtures.

Table 2-A Comparison of Average Percentage Deviation of Dose Buildup Factors for a Point Isotropic Source, Obtained Using Taylor's and Berger's Formulas Versus Tabulated Buildup Factors, for Eight Energies (Trubey, 1966).

Medium	Mean Percentage Deviation			
	20 MFP Range		7 MFP Range	
	Berger*	Taylor	Berger**	Taylor
Water	4.0	3.6	1.2	3.7
Aluminum	2.5	2.8	0.7	2.5
Iron	2.1	2.5	0.5	2.5
Tin	1.3	1.9	0.2	1.7
Tungsten	1.7	1.6	0.3	1.2
Lead	2.3	0.8	0.7	0.5
Uranium	1.6	0.8	0.4	0.5
Ordinary concrete	3.2	2.9	2.0	4.0
Ferrophos. concrete	3.2	2.6	1.4	3.3
Magnetite concrete	2.9	4.2	0.9	4.8
Barytes concrete	2.6	3.4	0.6	3.7

*20-MFP parameters used.

**7-MFP parameters used.

(From ORNL-RSIC-10, "A Survey of Empirical Functions Used to Fit Gamma-Ray Buildup Factors," by D. K. Trubey dated February 1966, Oak Ridge National Laboratory.

Appendix B

Simplifying Assumptions

The choice of Taylor's form of the buildup factor in Appendix A was influenced by the need of dealing with extended sources of highly variable dimensions, characteristic of uranium-238 decay chain deposits when studied as a group. Such a general study is greatly simplified by a number of assumptions, presumed to apply for most soils containing U^{238} and/or daughters, but with express emphasis on uranium mill tailing piles.

Assumption 1. Infinite Planar Extent of Tailings

- a. Uranium mill tailings piles normally extend over tens of thousands - often hundreds of thousands - of square meters (Ford, Bacon and Davis, 1977).
- b. External exposures on the surface of tailings piles are usually characterized by "worst case" conditions - i.e., at the center of the pile surface, ignoring "edge effects."
- c. The major component of such exposures would be due to photons traveling through soil, mostly. If exposures were limited to these photons, a detector at the center of the pile surface, a short distance above the air-tailings interface, would not distinguish between a large, though finite, area and one of infinite extent.
- d. However, photons scattering through air can reach a given point from much greater distances than by traveling through

soil, and thus the exposure rate detected over tailings piles must include a "skyshine" component of photons from sources near the pile surface but distant from the detector (Beck, 1981). This component would increase as the pile surface area increases, a dependence that becomes more pronounced for decreasing depths of overburden.

- e. The assumption of infinitely wide areas (e.g., Beck, 1972) would not detract from the accuracy of calculations dealing with the exposure component in c), while conservatively maximizing the minor contribution of "skyshine,"*in d). For the purposes of simplifying calculation and comparison with the results of other investigators (Beck, 1972; Schiager, 1974) infinitely wide tailings piles were assumed for this study.

Assumption 2. Finite Depth of Tailings

The effect of different thicknesses of mill tailings on the exposure and dose rates is one of the objects of the present study.

Assumption 3. Smooth, Flat Interfaces

- a. Realistically, tailings-ground, overburden-tailings, air-tailings interfaces can be expected to be neither smooth nor flat.

* Author's note: "skyshine" contributions are not included in this study.

- b. Roughness at the air-tailings interface would "tend to increase the field close to the interface by a slight amount." (Beck, 1972)
- c. Thus, the assumption of smooth, flat interfaces leads to exposure rates, etc., being underestimated, slightly, for most surfaces. Severe roughness would presumably result in greater error.
- d. Smooth, flat interfaces are assumed in the present study, which greatly simplifies analysis. Since this assumption is routinely made in studies of this nature, comparison of results is also facilitated. Nevertheless, it represents a drawback of this and similar methods.

Assumption 4. Absence of Soil Moisture

- a. Increasing soil moisture from 0% to 25% by weight will not substantially affect gamma-ray transport (Beck, 1972).
- b. However, increases in soil moisture would always result in increases of in situ soil density, "which for the uniformly distributed sources reduces the source activity per gram and thus...fluxes, exposure rates, etc." (Beck, 1972)
- c. The present proposed method accommodates small, uniform, changes in soil density with extreme ease and, with consistent use of either "in situ" or "laboratory" soil densities, produces valid results.

- d. Thus, "absence of soil moisture" is not a strict requirement of the proposed method; it is merely a convenient choice, since the density of "dry packed tailings" studies in this case corresponds to the density of "moist packed earth" studied by other investigators (Schiager, 1974) thus simplifying comparison of results.

Assumption 5. No Radon Emanation

- a. Over 95% of the total photon energy emitted in the ^{238}U decay chain originates from ^{222}Rn and daughters.
- b. However, ^{222}Rn is a noble gas which can emanate into the soil or tailings air, diffusing through the soil and cover material, and eventually, into the atmosphere. Typically 20% of the ^{222}Rn is free to diffuse in this manner, thus effectively reducing the source of gamma rays within the tailings while simultaneously creating a source of gamma rays within the cover material.
- c. To facilitate comparison with results obtained by other researchers, who assumed "no radon emanation," the same simplifying assumption is made for the present method. This is roughly equivalent to assuming that cover material is impermeable to radon diffusion and may lead to over-estimating, by orders of magnitude, the effective shielding capabilities of cover, as discussed in Appendices J, L and M.

Assumption 6. Radioactive Equilibrium

For simplicity, all the members of the ^{238}U decay chain are assumed to be in radioactive equilibrium, notwithstanding the capability mentioned in 5c. Thus, source concentrations in pCi/g as used in this report refer to "pCi of ^{238}U per gram of soil," etc., which reflects standard practice.

Assumption 7. Uniform Distribution of Nuclides in Tailings

- a. A large volume of tailings may be expected to contain many local inhomogeneities.
- b. However, a detector is affected by gammas from many points in the pile, which reduces in some degree, the effect of local differences.
- c. For most sites, the assumption of uniform distribution has been found to be a valid approximation (Beck, 1972).

Assumptions 8,9. Uniform Distribution of Overburden Material

Replicating Assumptions 1 and 2, the overburden material is assumed to be of infinite planar extent but of some given, finite, thickness. The latter can be "zero" for the common case of "no overburden present."

Assumption 10. Identity of Buildup Factor Parameters for Tailings and Overburden

Tailings and overburden material are assumed to be identical insofar as buildup factor parameters are concerned.

In summation, a typical uranium-bearing soil or uranium mill tailings pile is represented as a flat slab of finite thickness but infinite in area, containing in uniform distribution and radioactive equilibrium, the nuclides of the uranium chain from either ^{238}U or $^{226}\text{Ra}^*$ to stable lead. The soil or tailings slab is covered with a similar slab of source-free overburden, in the more general case.

*The differences in the energies emitted in these two cases is minimal.

Appendix C

Exposure Rates and Flux Equations

The determination of exposure rates to photons from any radioactive source entails, basically, a conversion from photon flux. For photons of a specific energy E , the correspondence of exposure rate and flux may be expressed by

$$\dot{X}(E) = F_{\dot{X}} E \phi(E) \left[\frac{\mu_{en}(E)}{\rho} \right]_{\text{air}} \quad (1-C)$$

where $\dot{X}(E)$ = exposure rate from photons of energy E , in R/s

$F_{\dot{X}}$ = conversion constant

$$= 1.824401368 \times 10^{-8} \text{ g} \cdot \text{R/MeV}$$

E = gamma energy, in MeV

$\phi(E)$ = "flux" of gammas of energy E , in gammas/(cm²·s)

$\left[\frac{\mu_{en}(E)}{\rho} \right]_{\text{air}}$ = energy dependent mass energy absorption coefficient
for air, in cm²/g

An obviously necessary input to the above equation is calculation of the photon flux at the point of interest. For gamma rays of a specified energy, from extended sources, such calculation would consider primarily the geometric aspects of source distribution and overall source configuration, as affected by the spatial dependence of the buildup factor.

In the case under study, the extended source consists of uranium decay chain nuclides, at radioactive equilibrium, dispersed uniformly throughout an infinitely wide tailings slab of finite thickness covered with a source-free overburden slab. With these basic premises and Figure 1-C, general equations for the monoenergetic photon flux at any point "o" in the overburden, at a distance "d" from the overburden-tailings interface, are developed in the following pages.

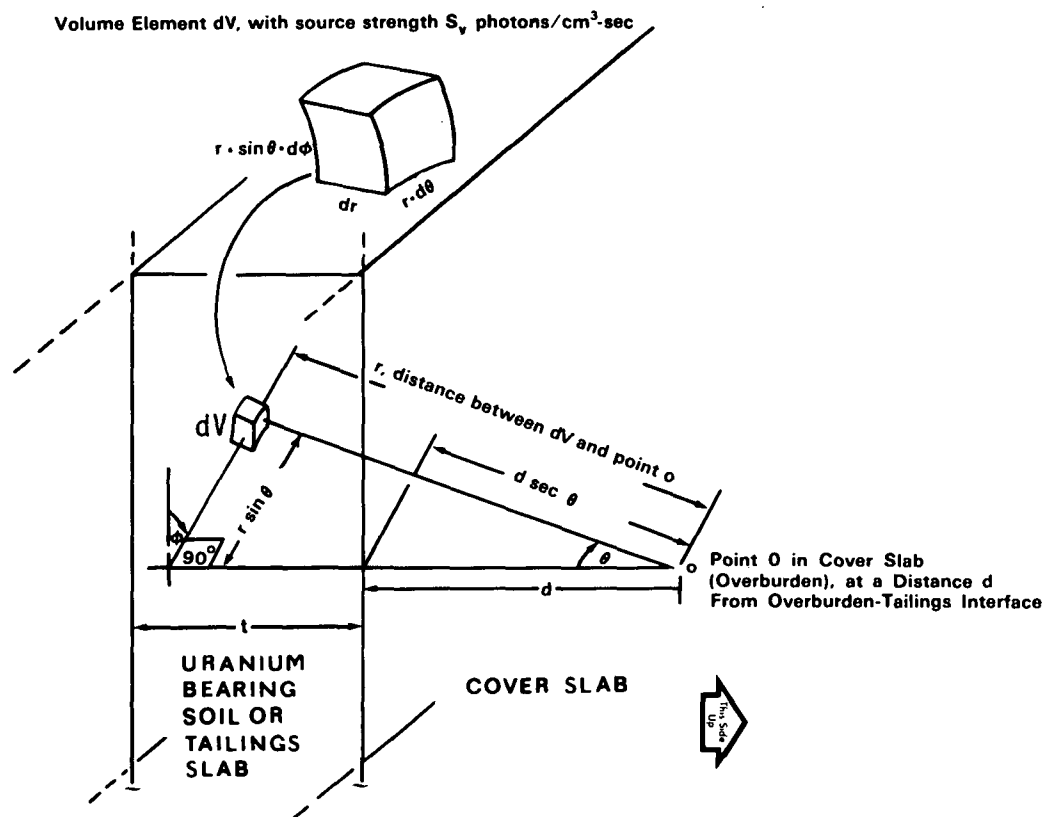


Figure 1-C. Geometry for flux calculations with a slab-distributed source (uranium-bearing soil or uranium mill tailings) covered with a source-free overburden slab.

Consider a generalized volume element dV within the tailings slab, in Figure 1, of specific source strength S_V , at a distance r from some unspecified point 0 in the overburden or cover material. Taking buildup into account, plus the generally assumed different attenuation capabilities of the two media, the flux contribution from dV at point 0 can be basically expressed (Morgan and Turner, 1967) as:

$$d\phi = \frac{S_V B e^{-\mu_t(r-d\sec\theta) - \mu_c d \sec\theta}}{4\pi r^2} dV \quad (2-C)$$

where ϕ = "flux", photons/cm².sec

S_V = source strength per unit volume, photons/cm³.sec

B = buildup factor, dimensionless

μ_t, μ_c = attenuation coefficients for uranium bearing soil (or tailings) and cover material, respectively, cm⁻¹

dV = volume element, cm³, equal to " $r^2 \sin\theta \, d\theta \, d\phi \, dr$ " (see Figure 1-C)

To obtain the total flux ϕ of photons of a given energy at 0, equation (2-C) must be integrated over the tailings and cover slabs dimensions. Such integration must include the buildup factor, as already discussed, and necessitates adapting the chosen buildup form to suit the geometric configuration. Referring to Equation (1-A), Assumption 10 and Figure 1-C, the spatial dependence of Taylor's Form of the buildup factor can be described,

* See Appendix B

for the present case, by Equation (3-C) below.

$$B_T(r, \theta) = Ae^{-\alpha_1 \mu t (r - d \sec \theta) - \alpha_1 \mu_c d \sec \theta} + [1-A]e^{-\alpha_2 \mu t (r - d \sec \theta) - \alpha_2 \mu_c d \sec \theta} \quad (3-C)$$

Equation (3-C) can now replace the generalized "B" in Equation (2-C) and the resultant expression integrated. Prior to doing so, however, the integrand can be simplified by multiplying Equation (3-C) by the exponential term in Equation (2-C)

$$B_T(r, \theta) \times e^{-\mu t (r - d \sec \theta) - \mu_c d \sec \theta} = Af_1(\theta) g_1(r) + (1-A)f_2(\theta)g_2(r) \quad (4-C)$$

$$\text{where } f_1(\theta) = e^{(\mu t - \mu_c)(1+\alpha_1)d \sec \theta}$$

$$g_1(r) = e^{-\mu t (1+\alpha_1)r}$$

$$\text{and } f_2(\theta) = e^{(\mu t - \mu_c)(1+\alpha_2)d \sec \theta}$$

$$g_2(r) = e^{-\mu t (1+\alpha_2)r}$$

With these transformations, the integration of Eqn. (2-C) can be indicated as

$$\phi = \int_V \frac{S_V [Af_1(\theta)g_1(r) + (1-A)f_2(\theta)g_2(r)]}{4\pi r^2} dV \quad (5-C)$$

$$\text{where } dV = r^2 \sin \theta d\theta d\phi dr$$

Therefore,

$$\phi = \frac{S_V}{4\pi} \int_0^{2\pi} d\phi \int_0^{\pi/2} \sin \theta d\theta \int_{d \sec \theta}^{(t+d) \sec \theta} [Af_1(\theta)g_1(r) + (1-A)f_2(\theta)g_2(r)] dr \quad (6-C)$$

The integration with respect to r produces the following two terms

$$\frac{A e^{-C_1 \sec \theta} (1 - e^{-T_1 \sec \theta})}{T_1/t} + \frac{(1-A) e^{-C_2 \sec \theta} (1 - e^{-T_2 \sec \theta})}{T_2/t} \quad (7-C)$$

$$\text{where } C_1 = \mu_{cd}(1+\alpha_1), \quad C_2 = \mu_{cd}(1+\alpha_2)$$

$$T_1 = \mu_{td}(1+\alpha_1), \quad T_2 = \mu_{td}(1+\alpha_2)$$

To integrate with respect to θ , the above is multiplied by $\sin \theta$ and the product expressed as the sum of four separate integrals

$$\begin{aligned} \frac{A}{T_1/t} & \left[\int_0^{\pi/2} e^{-C_1 \sec \theta} \sin \theta d\theta - \int_0^{\pi/2} e^{-(C_1+T_1) \sec \theta} \sin \theta d\theta \right] \\ & + \frac{(1-A)}{T_2/t} \left[\int_0^{\pi/2} e^{-C_2 \sec \theta} \sin \theta d\theta - \int_0^{\pi/2} e^{-(C_2+T_2) \sec \theta} \sin \theta d\theta \right] \end{aligned} \quad (8-C)$$

To perform the integrations, a substitution is required, with the corresponding changes in the limits of integration

$$y = \sec \theta$$

$$dy = \sec^2 \theta \sin \theta d\theta \quad (9-C)$$

$$= y^2 \sin \theta d\theta$$

$$\text{thus } \frac{dy}{y^2} = \sin \theta d\theta$$

As θ varies from 0 to $\pi/2$, $y = \sec \theta$ varies from 1 to ∞

Equation (8-C) can now be rewritten

$$\frac{A}{T_1/t} \left[\int_1^{\infty} \frac{e^{-C_1 y}}{y^2} dy - \int_1^{\infty} \frac{e^{-(C_1+T_1)y}}{y^2} dy \right] + \frac{(1-A)}{T_2/t} \left[\int_1^{\infty} \frac{e^{-C_2 y}}{y^2} dy - \int_1^{\infty} \frac{e^{-(C_2+T_2)y}}{y^2} dy \right] \quad (10-C)$$

The form of Equation (10-C) leads directly to an evaluation in terms of the familiar 2nd order exponential integral E_2 :

$$\frac{A}{T_1/t} \left[E_2(C_1) - E_2(C_1+T_1) \right] + \frac{(1-A)}{T_2/t} \left[E_2(C_2) - E_2(C_2+T_2) \right] \quad (11-C)$$

The last integration, with respect to ϕ , merely introduces a factor of 2π into the numerator of Equation (6-C) which now becomes

$$\phi = \frac{S_V}{2} \left\{ \frac{A}{T_1/t} \left[E_2(C_1) - E_2(C_1+T_1) \right] + \frac{(1-A)}{T_2/t} \left[E_2(C_2) - E_2(C_2+T_2) \right] \right\} \quad (12-C)$$

Replacing C_1 , C_2 , T_1 and T_2 with their equivalences, defined in Equation (7-C) permits rewriting Eqn. (12-C) in a more meaningful form.

$$\begin{aligned} \phi = & \frac{S_V A}{2\mu_t(1+\alpha_1)} \left\{ E_2[\mu_{cd}(1+\alpha_1)] - E_2[(\mu_{cd} + \mu_t t)(1+\alpha_1)] \right\} \\ & + \frac{S_V(1-A)}{2\mu_t(1+\alpha_2)} \left\{ E_2[\mu_{cd}(1+\alpha_2)] - E_2[(\mu_{cd} + \mu_t t)(1+\alpha_2)] \right\} \end{aligned} \quad (13-C)$$

The integration performed above was strictly geometric, involving only the physical dimensions of the tailings slab and cover; it was not affected procedurally by the energy-dependence of the buildup factor, attenuation, and source strength parameters. Nevertheless, the energy-dependence of these parameters cannot be neglected; it is obvious that they must all correspond to some definite energy E in any given particular case, or Equation (13-C) would be invalidated. More relevantly, this correspondence must extend to the resultant flux, now specifically limited to photons of one single energy. Thus, a more accurate rendition of Eqn. (13-C) would be as follows:

$$\begin{aligned} \phi(E) = & \frac{S_V(E)A(E)}{2\mu_t(E)[1+\alpha_1(E)]} \left\langle E_2 \left\{ \mu_{cd}(E)d[1+\alpha_1(E)] \right\} - E_2 \left\{ [\mu_{cd}(E)d + \mu_t(E)t][1+\alpha_1(E)] \right\} \right\rangle \\ & + \frac{S_V(E)[1-A(E)]}{2\mu_t(E)[1+\alpha_2(E)]} \left\langle E_2 \left\{ \mu_{cd}(E)d[1+\alpha_2(E)] \right\} - E_2 \left\{ [\mu_{cd}(E)d + \mu_t(E)t][1+\alpha_2(E)] \right\} \right\rangle \end{aligned} \quad (14-C)$$

where $\phi(E)$ = "flux" of photons of energy E, photons/cm².sec.

$S_V(E)$ = volumetric source strength, photons of energy E/cm³.sec.

$\mu_t(E)$ = attenuation coefficient of uranium-bearing soil or tailings material for energy E, cm⁻¹

$\mu_c(E)$ = attenuation coefficient of cover material for energy E, cm⁻¹

$A(E), \alpha_1(E), \left\{ \begin{array}{l} \text{Taylor's form buildup factor parameters for photons of} \\ \text{and } \alpha_2(E) \end{array} \right\} \text{ energy E, valid for both tailings and cover, dimensionless}$

t = thickness of tailings or uranium-bearing soil slab, cm

d = thickness of cover slab, cm

Note that the previously generalized distance "d" has been redefined, above, as "the thickness of the cover slab". This means that Equation (14-C) now results in the flux of photons of energy "E" at the top of the overburden or cover slab, at the air-cover interface, i.e. a "surface flux", at the soles of an observer's shoes, as it were. Treating "d" as a variable, the effect of increasing cover on the "surface flux" of a given energy can be determined. Setting "d" equal to "zero" produces the case of "bare" or "uncovered" tailings, with the maximum "surface flux" possible with a tailings slab of a specified thickness "t".

$$\begin{aligned} \phi(E) = & \frac{S_V(E)A(E)}{2\mu_t(E)[1+\alpha_1(E)]} \left\{ 1 - E^2 \left\{ \mu_t(E)t[1+\alpha_1(E)] \right\} \right\} \\ & + \frac{S_V(E)[1-A(E)]}{2\mu_t(E)[1+\alpha_2(E)]} \left\{ 1 - E^2 \left\{ \mu_t(E)t[1+\alpha_2(E)] \right\} \right\} \end{aligned} \quad (15-C)$$

Equation (15-C) also describes the effect of varying U.B.S. (uranium-bearing soil) or tailings slab thickness "t" on the "surface 'flux'" of photons of

energy "E", for the "bare U.B.S. or tailings" case. The conditions of maximum surface "flux" are obtained by postulating an infinite thickness, " $t=\infty$ ". Although infinitely thick tailings piles have not been reported to date, "fluxes" corresponding to such a "worst case" are approached asymptotically with "sufficiently large" but finite values of " t ".

$$\phi(E) = \frac{S_V(E)}{2\mu_t(E)} \left[\frac{A(E)}{1+\alpha_1(E)} + \frac{1-A(E)}{1+\alpha_2(E)} \right] \quad (16-C)$$

To isolate the effects of varying cover depth " d " on surface "fluxes", a constant thickness " t " must be maintained in Equation (14) while altering d . Setting " $t=\infty$ " again, as a convenient example, produces

$$\begin{aligned} \phi(E) = & \frac{S_V(E)A(E)}{2\mu_t(E)[1+\alpha_1(E)]} \left\langle E_2 \left\{ \mu_C(E)d[1+\alpha_1(E)] \right\} \right\rangle \\ & + \frac{S_V(E)[1-A(E)]}{2\mu_t(E)[1+\alpha_2(E)]} \left\langle E_2 \left\{ \mu_C(E)d[1+\alpha_2(E)] \right\} \right\rangle \end{aligned} \quad (17-C)$$

The energy-dependence of buildup, attenuation and source-strength parameters has been repeatedly noted in Equations (14-C) through (17-C) to stress the fact that their output is, in each case, a monoenergetic flux. By direct application of Equation (C-1) to such resultant single-energy flux(es) the corresponding exposure rate(s) can then be computed. However, the exposure rate attributable to photons of one specific energy would obviously not suffice to describe conditions at a uranium mill tailings pile, characterized by a complex spectrum of emission energies. The flux and then the exposure rate corresponding to each and every energy produced by the nuclide inventory of the pile would have to be calculated singly, followed by a process integrating all exposures. Note, however, that the integration cannot be performed analytically, since $S_V(E)$ is not a continuous function of energy; a numerical integration, best done with a computer, is required.

$$\dot{X}_{\Sigma E} = \sum_{i=1}^{\text{all } E} F_{\dot{X}} E_i \phi(E_i) \left[\frac{\mu_{en}(E_i)}{\rho} \right]_{\text{air}} \quad \text{where } \dot{X}_{\Sigma E} = \text{exposure rate due to photons of all energies, in R/s.}$$

This expression introduces a serious problem, namely that the buildup parameters $A(E)$, $\alpha_1(E)$ and $\alpha_2(E)$ of Taylor's form, upon which the analytical development is based, "are not available below 0.5 MeV" (Trubey, 1966). This means that up to 15% of the total photon energy emitted in a pile at radioactive equilibrium would be left unrepresented, unless some means to extend analysis below 0.5 MeV is found. One viable technique requires use of Berger's Form of the buildup factor,

$$B_B(E, \mu r) = 1 + C(E) \mu r e^{D(E) \mu r} \quad (18-C)$$

where $C(E)$, $D(E)$ = energy dependent fitting parameters, dimensionless

Applying Equation (18-C) to the conditions of Figure 1, Assumption 10, etc., produces the following expression for the spatial dependence of Berger's Form

$$B_B(r, \theta) = 1 + C [\mu_t(r - d \sec \theta) + \mu_c d \sec \theta] e^{D[\mu_t(r - d \sec \theta) + \mu_c d \sec \theta]} \quad (19-C)$$

Replacing the generalized "B" in Equation (2-C) with the above expression and carrying out the multiplication produces

$$d\phi = \frac{S_v}{4\pi} \sin \theta d\theta d\phi \left[e^{-f(r, \theta)} + C f(r, \theta) e^{(D-1)f(r, \theta)} \right] dr \quad (20-C)$$

where $f(r, \theta) = \mu_t r - (\mu_t - \mu_c) d \sec \theta$

To integrate the bracketed expression with respect to r , note that

$$\frac{df}{dr} = \mu_t, \text{ thus } dr = \frac{df}{\mu_t}, \quad (21-C)$$

which permits expressing the integrals as

$$\frac{1}{\mu_t} \int e^{-f} df + \frac{C}{\mu_t} \int f e^{(D-1)f} df \quad (22-C)$$

This produces the following two terms

$$\frac{1}{\mu_t} (-e^{-f}) + \frac{C}{\mu_t} \frac{e^{(D-1)f}}{(D-1)^2} \left[(D-1)f - 1 \right] + \text{constant} \quad (23-C)$$

With the limits of integration made explicit, the first term of (23-C) becomes

$$\frac{1}{\mu_t} \left[-e^{-\mu_t r + (\mu_t - \mu_c) d \sec \theta} \right]_{d \sec \theta}^{(d+t) \sec \theta} = \frac{1}{\mu_t} e^{-\mu_c d \sec \theta} \left(1 - e^{-\mu_t t \sec \theta} \right) \quad (24-C)$$

Continuing with this first term, the integration with respect to θ can be indicated as

$$\frac{1}{\mu_t} \left[\int_0^{\pi/2} e^{-\mu_c d \sec \theta} \sin \theta d\theta - \int_0^{\pi/2} e^{-(\mu_t t + \mu_c d) \sec \theta} \sin \theta d\theta \right] \quad (25-C)$$

With the substitution $y = \sec \theta$, (26-C)

$$dy = \sec^2 \theta \sin \theta d\theta$$

$$= y^2 \sin \theta d\theta$$

$$\text{thus } \frac{dy}{y^2} = \sin \theta d\theta$$

with the corresponding change of limits, (25-C) can be rewritten as

$$\frac{1}{\mu_t} \left[\int_1^\infty \frac{e^{-\mu_c dy}}{y^2} dy - \int_1^\infty \frac{e^{-(\mu_t t + \mu_c d)y}}{y^2} dy \right] \quad (27-C)$$

As with Equation (10-C), the above integration results in two 2nd order exponential integrals

$$\frac{1}{\mu_t} \left[E_2(\mu_c d) - E_2(\mu_t t + \mu_c d) \right] \quad (28-C)$$

Integrating this with respect to ϕ introduces a factor of 2π . Multiplying the product of 2π and (28-C) by the constant term of Equation (20-C) yields the first term of the integration of (20-C) with respect to r, θ, ϕ .

$$(\text{1st. Term}) = \frac{S_v}{2\mu_t} \left[E_2(\mu_c d) - E_2(\mu_t t + \mu_c d) \right] \quad (29-C)$$

Now the process of evaluating the second term of Equation (23-C) is undertaken:

$$\frac{C}{\mu_t} \left[\frac{e^{(D-1) \mu_t r - (\mu_t - \mu_c) d \sec \theta}}{(D-1)^2} \left\{ (D-1) \left[\mu_t r - (\mu_t - \mu_c) d \sec \theta \right] - 1 \right\} \right] \left[\begin{array}{l} (d+t) \sec \theta \\ d \sec \theta \end{array} \right] \quad (30-C)$$

Expression (30-C) results in a 4-term polynomial

$$\frac{C}{\mu_t (D-1)^2} \left[T_1(\theta) + T_2(\theta) + T_3(\theta) + T_4(\theta) \right] \quad (31-C)$$

$$\begin{aligned} \text{where } T_1(\theta) &= e^{(D-1)(\mu_t t + \mu_c d) \sec \theta} \\ T_2(\theta) &= e^{(D-1)(\mu_t t + \mu_c d) \sec \theta} (D-1)(\mu_t t + \mu_c d) \sec \theta \\ T_3(\theta) &= e^{(D-1)\mu_c d \sec \theta} (D-1)\mu_c d \sec \theta \\ T_4(\theta) &= e^{(D-1)\mu_c d \sec \theta} \end{aligned}$$

The integration with respect to θ is indicated below

$$\frac{C}{\mu_t (D-1)^2} \left[\int_0^{\pi/2} T_1(\theta) \sin \theta d\theta + \int_0^{\pi/2} T_2(\theta) \sin \theta d\theta + \int_0^{\pi/2} T_3(\theta) \sin \theta d\theta + \int_0^{\pi/2} T_4(\theta) \sin \theta d\theta \right]$$

For the terms including $T_1(\theta)$ and $T_3(\theta)$, the following substitution is useful

$$\begin{aligned} y &= \sec \theta & (32-C) \\ dy &= \sec \theta (\sin \theta \sec \theta) d\theta \\ \frac{dy}{y} &= \sin \theta \sec \theta d\theta \end{aligned}$$

For the terms including $T_2(\theta)$ and $T_4(\theta)$, the corresponding substitution is

$$\begin{aligned} y &= \sec \theta & (33-C) \\ dy &= \sec^2 \theta \sin \theta d\theta \\ \frac{dy}{y^2} &= \sin \theta d\theta \end{aligned}$$

These substitutions necessitate a change in limits of integration, from "0 to $\pi/2$ " to "1 to ∞ ". The integration with respect to θ now produces a polynomial in terms of 1st. and 2nd. order exponential integrals,

$$\frac{C}{\mu_t(D-1)^2} \times \left\{ \begin{array}{l} (D-1)(\mu_t t + \mu_c d) E_1 [-(D-1)(\mu_t t + \mu_c d)] \\ -E_2 [-(D-1)(\mu_t t + \mu_c d)] \\ -(D-1)\mu_c d E_1 [-(D-1)\mu_c d] \\ + E_2 [-(D-1)\mu_c d] \end{array} \right\} \quad (34-C)$$

The above expression can be simplified by making use of the following relationships

$$\begin{aligned} E_2(X) &= e^{-X} - X E_1(X) & (35-C) \\ \text{or} \quad E_1(X) &= \frac{-E_2(X) + e^{-X}}{X} \end{aligned}$$

With the transformations in (35-C) the first and third terms in brackets in become, respectively

$$E_2 \left[-(D-1)(\mu_t t + \mu_c d) \right] - e^{(D-1)(\mu_t t + \mu_c d)} \quad (36-C)$$

$$\text{and} \quad -E_2 \left[-(D-1)\mu_c d \right] + e^{(D-1)\mu_c d}$$

Cancelling like terms, this becomes

$$\frac{C}{\mu_t (D-1)^2} \left[e^{(D-1)\mu_c d} - e^{(D-1)(\mu_t t + \mu_c d)} \right] \quad (37-C)$$

$$\text{or} \quad \frac{C}{\mu_t (D-1)^2} e^{(D-1)\mu_c d} \left[1 - e^{(D-1)\mu_t t} \right]$$

Integrating with respect to ϕ , etc. results in the second term of the integration of Equation (20-C) with respect to r , θ , ϕ

$$\phi(\text{2nd Term}) = \frac{S_v C}{2\mu_t (D-1)^2} e^{(D-1)\mu_c d} \left[1 - e^{(D-1)\mu_t t} \right] \quad (38-C)$$

Adding the 1st term from Equation (29-C) and expressing the energy-dependence of relevant parameters produces

$$\phi(E) = \frac{S_v(E)}{2\mu_t(E)} \left\{ E_2[\mu_c(E)d] - E_2[\mu_t(E)t + \mu_c(E)d] \right. \\ \left. + \frac{C(E)}{[D(E)-1]^2} e^{[D(E)-1]\mu_c(E)d} \left\{ 1 - e^{[D(E)-1]\mu_t(E)t} \right\} \right\} \quad (39-C)$$

For the important case of an "infinitely thick" tailings slab ($t=\infty$) without cover material ($d=0$), Equation (39-C) reduces to

$$\phi(E) = \frac{S_v(E)}{2\mu_t(E)} \left\{ 1 + \frac{C(E)}{[D(E)-1]^2} \right\} \quad (40-C)$$

With the values of "surface flux " obtained through Equations (14-C) , (15-C),(16-C),(17-C) or (40-C), applied in Equation (1-C), the exposure rates at ground surface can be determined, for gamma radiation of a specific energy. However, much of the published data refers to exposure rates at a specific height (typically 1 meter) above ground surface. Accordingly, a modifying factor was sought, to relate "surface exposure rates" obtained from the above equations to the corresponding rates at one meter above ground, thus facilitating comparison with previous results.

This modifying factor can be expressed as a ratio of exposure rate at a height "h" above ground, including buildup and attenuation effects, to the corresponding exposure rate at ground level, for photons of a given energy E. The source of the emissions is assumed to be an infinitely thick slab with an air "cover" of thickness "h". The assumption of infinite thickness is meant to simplify analysis, based on yet another version of the buildup factor, the "linear" form,

$$B_L(E,\mu r) = 1 + \alpha(E)\mu(E)r \quad (41-C)$$

where $\alpha(E)$ = energy - dependent fitting parameter, dimensionless

Replacing μ_c and d in (2-C) with μ_{air} and h , respectively, plus including the above formula for B_L with the necessary specifications $\alpha_t(E)$ (for tailings) and $\alpha_{air}(E)$ results in an integrable expression. The details of the integration are given in Morgan and Turner (1967) and shall not be repeated here, with only the results being presented, below.

The flux of photons of energy E, at a height h above ground level, is

$$\phi = \frac{S_v}{2\mu_t} \left[(1 + \alpha_t) E_2(\mu_{air}h) + \alpha_{air}h E_1(\mu_{air}h) \right] \quad (42-C)$$

The second term within brackets is subject to the following relationship

$$\mu_{air}h E_1(\mu_{air}h) = e^{-\mu_{air}h} - E_2(\mu_{air}h)$$

where, for $h = 0$,

$$e^{-\mu_{air}h} \Big|_{h=0} = 1$$

$$\text{and } E_2(\mu_{air}h) \Big|_{h=0} = 1$$

Thus, for $h=0$, or "ground level case", (42-C) reduces to

$$\phi = \frac{S_v}{2\mu_t} (1 + \alpha_t) \quad (43-C)$$

The modifying factor is obtained by dividing (42-C) by (43-C),

$$F_M = E_2(\mu_{air}h) + \frac{\alpha_{air}\mu_{air}h E_1(\mu_{air}h)}{(1 + \alpha_t)} \quad (44-C)$$

The second term of (44-C) may be eliminated if buildup in one meter of air is neglected, i.e. the case of $B_L = 1$, unit buildup, implying that $\alpha_{air} = 0$ [see Equation (41-C)]. This reduces (44-C) to the following expression, with energy dependences indicated,

$$F_M(E) = E_2[\mu_{air}(E)h] \quad (45-C)$$

Although based on flux ratios, the modifying factor $F_M(E)$ is directly applicable to exposure rates, as an examination of Equation (1-C) can verify, due to mutually cancelling terms.

With this modification, the numerical integrations resulting in "total" exposure rates at ground level and at one meter above ground level can be represented by Equations (46-C) and (47-C), respectively.

$$\dot{X}_{\Sigma E_s} = \sum_{i=1}^n F_{\dot{X}E_i} \phi(E_i) \left[\frac{\mu_{en}(E_i)}{\rho} \right]_{\text{air}} \quad (46-C)$$

$$+ \sum_{j=1}^m F_{\dot{X}E_j} \phi(E_j) \left[\frac{\mu_{en}(E_j)}{\rho} \right]_{\text{air}}$$

and

$$\dot{X}_{\Sigma E_{1m}} = \sum_{i=1}^n F_{\dot{X}E_i} \phi(E_i) \left[\frac{\mu_{en}(E_i)}{\rho} \right]_{\text{air}} E_2 \left[\mu_{\text{air}}(E_i) 100\text{cm} \right] \quad (47-C)$$

$$+ \sum_{j=1}^m F_{\dot{X}E_j} \phi(E_j) \left[\frac{\mu_{en}(E_j)}{\rho} \right]_{\text{air}} E_2 \left[\mu_{\text{air}}(E_j) 100\text{cm} \right]$$

where $i = 1, 2, \dots, n$, indices of discrete energies below 0.5 MeV.

$j = 1, 2, \dots, m$, indices of discrete energies above 0.5 MeV.

The indices i and j in the above equations refer to discrete energies below and above 0.5 MeV, respectively, corresponding to the choice of buildup form: the first summation terms in both (46-C) and (47-C) indicate "the sums of exposure rates, at ground level and at 1 meter above the surface, due to gamma emissions of energies up to 0.5 MeV, calculated on the basis of Berger's buildup factor"; the second summation terms in both equations signify similar processes employing Taylor's form of the buildup factor, for energies greater than 0.5 MeV.

Appendix D

Decay Scheme and Energy Spectrum

The typical uranium bearing soil slab subject of this study is assumed to contain ^{238}U in radioactive equilibrium with all decay daughters through ^{210}Po , as shown in Figure 1-D. Several branching decays have been omitted, namely ^{218}At and ^{206}Tl (neither of which is a gamma emitter) and ^{210}Tl . None of the mentioned nuclides is produced in more than 0.02% of decays of the parent nuclide; the "main branch" nuclides ^{214}Pb , ^{210}Po and ^{214}Po , respectively, being assumed to correspond to 100% of the parent disintegrations, for simplicity. Consequently, the only branching included in the decay scheme is that of $^{234\text{m}}\text{Pa}$ -metastable (1.17 minutes) and ^{234}Pa (6.7 hours).

With the decay scheme of Fig. 1-D and the radionuclide decay data of Kocher (1977), a complete spectrum of gamma emission energies present in a uranium-bearing soil can be compiled. Postulating a "Base Case" of "1 pCi per cubic cm", and making use of Kocher's intensities, an energy-dependent "source term" $S_V(E)$ is found for each energy E , to implement Eqns. (14-C) through (17-C), (40-C) and finally (43-C) and (44-C). In agreement to the form of these last two equations, the $S_V(E)$ values are distributed between two tables. Table 1-D contains $S_V(E)$ terms for energies up to 0.5 MeV, for a total of $n=105$ values, while Table 2-D consists of the remaining $m=177$ values, for energies over 0.5 MeV, where "m" and "n" refer to indices in (43-C) and (44-C).

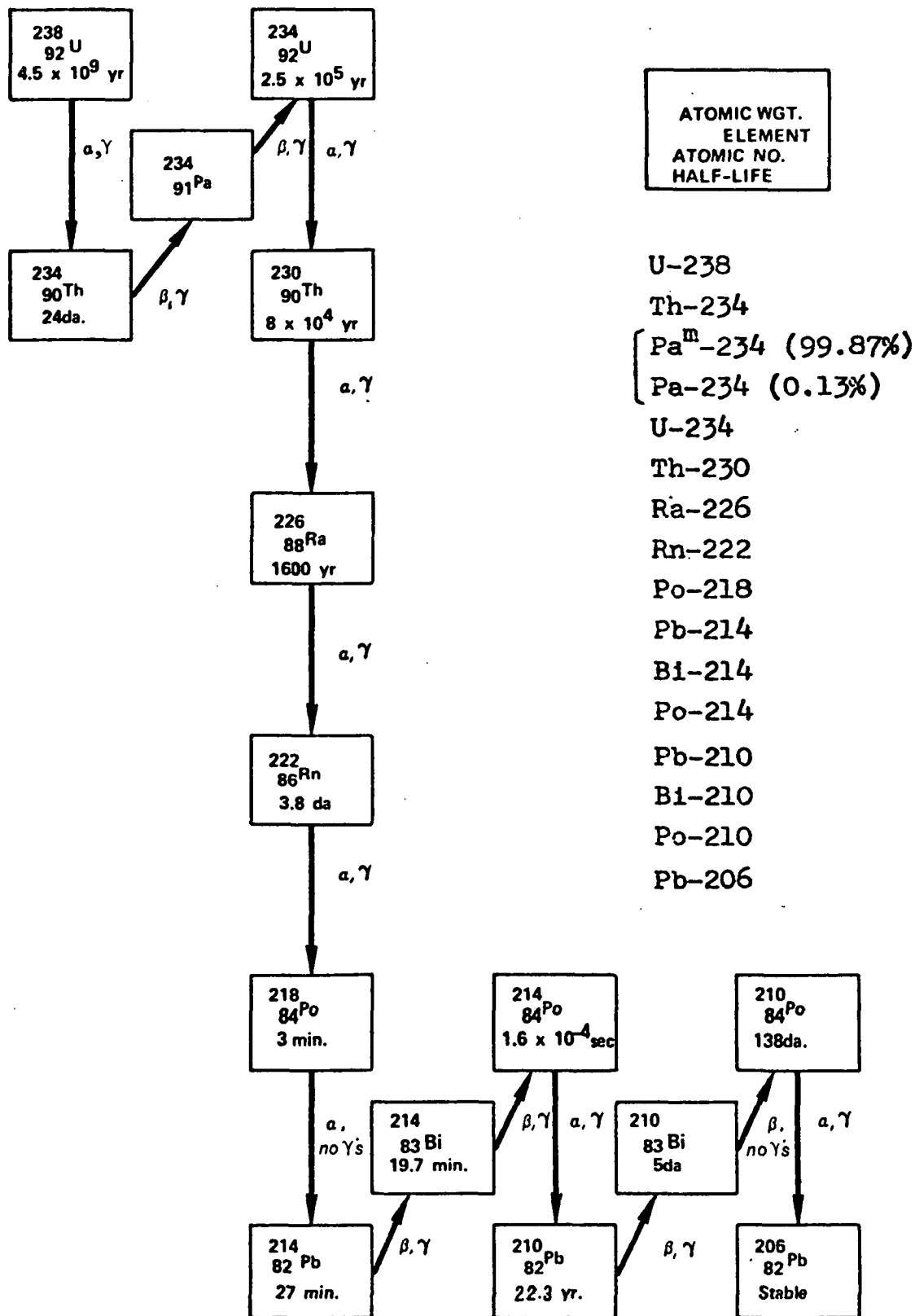


Figure 1-D. Uranium-238 Decay Series

Table 1-D Volumetric
Source Strength $S_V(E)$
for Energies $E \leq 0.5$ MeV
From Kocher (1977)

	Gamma Energy, in MeV, E	Intensity, or fraction of decays producing gammas of energy E, dimensionless	Volumetric Source Strength, in "gammas of energy E per cm ³ per sec" $S_V(E)$.	NUCLIDE
1	.13000E-01	.87000E-01	.32190E-07	²³⁸U
2	.49600E-01	.70000E-03	.25900E-04	
3	.13300E-01	.98000E-01	.36260E-07	²³⁴Th
4	.63282E-01	.39000E-01	.14430E-02	
5	.92367E-01	.25700E-01	.95090E-03	
6	.92792E-01	.30000E-01	.11100E-02	
7	.11281	.24900E-02	.92130E-04	
8	.76000E-01	.20000E-02	.74000E-04	
9	.13600E-01	.14920E-02	.54834E-04	²³⁴Pa
10	.43450E-01	.15600E-05	.57720E-07	
11	.63200E-01	.40300E-04	.14911E-05	
12	.69900E-01	.29900E-05	.11063E-06	
13	.80500E-01	.50700E-05	.18759E-06	
14	.94665E-01	.20150E-03	.74555E-05	
15	.98439E-01	.32630E-03	.12073E-04	
16	.99700E-01	.61100E-04	.22607E-05	
17	.10340	.15600E-05	.57720E-07	
18	.11100	.15210E-03	.56277E-05	
19	.12530	.14300E-04	.52910E-06	
20	.13128	.26000E-03	.96200E-05	
21	.13437	.27300E-05	.10101E-06	
22	.13770	.19500E-05	.72150E-07	
23	.14030	.12090E-04	.44733E-06	
24	.14410	.49400E-05	.18278E-06	
25	.15020	.26000E-05	.96200E-07	
26	.15270	.93459E-04	.34580E-05	
27	.15930	.94900E-05	.35113E-06	
28	.17080	.62400E-05	.23088E-06	
29	.17460	.24700E-05	.91390E-07	
30	.18600	.24700E-05	.91390E-07	
31	.19360	.70200E-05	.25974E-06	
32	.19970	.91000E-05	.33670E-06	
33	.20080	.14040E-04	.51948E-06	
34	.20290	.14300E-04	.52910E-06	
35	.22020	.29900E-05	.11063E-06	
36	.22687	.84500E-04	.31265E-05	
37	.22687	.49400E-04	.18278E-05	
38	.24540	.11700E-04	.43290E-06	
39	.24890	.40300E-04	.14911E-05	
40	.26710	.22100E-05	.81770E-07	
41	.27210	.15600E-04	.57720E-06	
42	.28610	.18200E-05	.67340E-07	
43	.28960	.14040E-05	.51948E-07	
44	.29370	.41600E-04	.15392E-05	
45	.31250	.37700E-05	.13949E-06	
46	.31630	.15600E-05	.57720E-07	
47	.32070	.15600E-05	.57720E-07	
48	.32830	.37700E-04	.13949E-05	
49	.32830	.37700E-04	.13949E-05	
50	.33030	.11440E-04	.42328E-06	
51	.35180	.74100E-05	.27417E-06	
52	.36960	.36400E-04	.13468E-05	

Table 1-D (Continued)

	Gamma Energy, in MeV, E	Intensity, or fraction of decays producing gammas of energy E, dimensionless	Volumetric Source Strength, in "gammas of energy E per cm ³ per sec" S _v (E).	NUCLIDE
53	.37220	.19500E-04	.72150E-06	²³⁴Pa (cont.)
54	.40980	.46800E-05	.17316E-06	
55	.42690	.50700E-05	.18759E-06	
56	.44690	.15600E-05	.57720E-07	
57	.45860	.19500E-04	.72150E-06	
58	.46180	.20800E-05	.76960E-07	
59	.46750	.49400E-05	.18278E-06	
60	.47210	.31200E-05	.11544E-06	
61	.47350	.23400E-05	.86580E-07	
62	.48000	.37700E-05	.13949E-06	
63	.48250	.37700E-05	.13949E-06	²³⁴Pa^m
64	.13600E-01	.43943E-02	.16259E-03	
65	.94465E-01	.11555E-02	.42753E-04	
66	.98439E-01	.18776E-02	.69470E-04	²³⁴U
67	.13000E-01	.10400	.38480E-02	
68	.53220E-01	.11800E-02	.43660E-04	
69	.12140	.40000E-03	.14800E-04	²³⁰Th
70	.12300E-01	.85000E-01	.31450E-02	
71	.67800E-01	.38000E-02	.14060E-03	
72	.17420	.70000E-03	.25900E-04	²²⁶Ra
73	.11700E-01	.81000E-02	.29970E-03	
74	.81070E-01	.18000E-02	.66600E-04	
75	.83780E-01	.29900E-02	.11063E-03	
76	.94900E-01	.13600E-02	.50320E-04	
77	.18599	.32800E-01	.12136E-02	²¹⁴Pb
78	.10800E-01	.13595	.50300E-02	
79	.53226E-01	.11000E-01	.40700E-03	
80	.74815E-01	.63300E-01	.23421E-02	
81	.77108E-01	.10700	.39590E-02	
82	.87300E-01	.47600E-01	.17612E-02	
83	.24191	.74700E-01	.27639E-02	
84	.25879	.55100E-02	.20387E-03	
85	.27453	.32000E-02	.11840E-03	
86	.29517	.19200	.71040E-02	
87	.35190	.37081	.13720E-01	
88	.48042	.33800E-02	.12506E-03	
89	.48708	.44000E-02	.16280E-03	
90	.42480	.50000E-03	.18500E-04	²¹⁴Bi
91	.11000E-01	.52000E-02	.19240E-03	
92	.76862E-01	.35800E-02	.13246E-03	
93	.79290E-01	.60000E-02	.22200E-03	
94	.89800E-01	.26900E-02	.99530E-04	
95	.27370	.18000E-02	.66600E-04	
96	.38700	.36000E-02	.13320E-03	
97	.38910	.41000E-02	.15170E-03	
98	.40574	.16700E-02	.61790E-04	
99	.42650	.11000E-02	.40700E-04	
100	.45477	.31800E-02	.11766E-03	
101	.46180	.21800E-02	.80660E-04	
102	.46969	.13300E-02	.49210E-04	
103	.47438	.11800E-02	.43660E-04	²¹⁰Pb
104	.10800E-01	.24300	.89910E-02	
105	.46500E-01	.40500E-01	.14985E-02	

Table 2-D Volumetric
Source Strength $S_v(E)$
for Energies $E > 0.5$ MeV
From Kocher (1977)

	Gamma Energy, in MeV, E	Intensity, or fraction of decays producing gammas of energy E, dimensionless	Volumetric Source Strength, in "gammas of energy E per cm ³ per sec" $S_v(E)$.	NUCLIDE
1	.50680	.18200E-04	.67340E-06	²³⁴ Pa
2	.51360	.15600E-04	.57720E-06	
3	.52060	.15600E-04	.57720E-06	
4	.52100	.15600E-04	.57720E-06	
5	.52900	.50700E-05	.18759E-06	
6	.53320	.26000E-05	.96200E-07	
7	.53710	.20800E-05	.76960E-07	
8	.55700	.32500E-05	.12025E-06	
9	.56650	.22100E-04	.81770E-06	
10	.56926	.13520E-03	.50024E-05	
11	.56926	.40300E-04	.14911E-05	
12	.57410	.26000E-04	.96200E-06	
13	.58410	.19500E-05	.72150E-07	
14	.59650	.78000E-05	.28860E-06	
15	.60290	.16900E-04	.62530E-06	
16	.61140	.10400E-04	.38480E-06	
17	.61620	.26000E-05	.96200E-07	
18	.62350	.13000E-05	.48100E-07	
19	.62750	.88400E-05	.32708E-06	
20	.63060	.53300E-05	.19721E-06	
21	.63450	.37700E-05	.13949E-06	
22	.63970	.27300E-05	.10101E-06	
23	.64320	.28600E-05	.10582E-06	
24	.64620	.28600E-05	.10582E-06	
25	.65320	.16900E-04	.62530E-06	
26	.65500	.79300E-05	.29341E-06	
27	.66060	.37700E-05	.13949E-06	
28	.66460	.19500E-04	.72150E-06	
29	.66670	.19500E-04	.72150E-06	
30	.66980	.19500E-04	.72150E-06	
31	.68330	.31200E-05	.11544E-06	
32	.68550	.35100E-05	.12987E-06	
33	.69250	.16900E-04	.62530E-06	
34	.69910	.59800E-04	.22126E-05	
35	.70600	.41600E-04	.15392E-05	
36	.71120	.20800E-05	.76960E-07	
37	.73300	.11050E-03	.40885E-05	
38	.73840	.10400E-04	.38480E-06	
39	.74281	.39000E-04	.14430E-05	
40	.74650	.11700E-04	.43290E-06	
41	.75480	.18200E-04	.67340E-06	
42	.76000	.20800E-05	.76960E-07	
43	.76636	.10400E-04	.38480E-06	
44	.76636	.26000E-05	.96200E-07	
45	.76870	.71500E-05	.26455E-06	
46	.77790	.26000E-05	.96200E-07	
47	.78080	.20800E-04	.76960E-06	
48	.78310	.63700E-05	.23569E-06	
49	.78627	.20800E-04	.76960E-06	
50	.79360	.19500E-04	.72150E-06	

Table 2-D (Continued)

	Gamma Energy, in MeV, E	Intensity, or fraction of decays producing gammas of energy E, dimensionless	Volumetric Source Strength, in "gammas of energy E per cm ³ per sec" S _v (E).	NUCLIDE
51	.79620	.44200E-04	.16354E-05	²³⁴Pa (Cont.)
52	.80450	.50700E-05	.18759E-06	
53	.80550	.42900E-04	.15873E-05	
54	.80810	.63700E-04	.23569E-05	
55	.81250	.63700E-05	.23569E-06	
56	.81940	.28600E-04	.10582E-05	
57	.82470	.46800E-04	.17316E-05	
58	.82630	.41600E-04	.15392E-05	
59	.83110	.72800E-04	.26936E-05	
60	.84190	.18200E-05	.67340E-07	
61	.84480	.76700E-05	.28379E-06	
62	.87290	.15600E-05	.57720E-07	
63	.87670	.35100E-04	.12987E-05	
64	.88051	.53300E-04	.19721E-05	
65	.88051	.84500E-04	.31265E-05	
66	.88324	.15600E-03	.57720E-05	
67	.89860	.52000E-04	.19240E-05	
68	.90480	.63700E-05	.23569E-06	
69	.92000	.50700E-05	.18759E-06	
70	.92460	.36400E-04	.13468E-05	
71	.92670	.14300E-03	.52910E-05	
72	.92670	.66300E-04	.24531E-05	
73	.94600	.26000E-03	.96200E-05	
74	.94900	.10140E-03	.37518E-05	
75	.97880	.18200E-04	.67340E-06	
76	.97880	.18200E-04	.67340E-06	
77	.98050	.28600E-04	.10582E-05	
78	.98050	.19500E-04	.72150E-06	
79	.98340	.31200E-04	.11544E-05	
80	1.0227	.46800E-05	.17316E-06	
81	1.0283	.10010E-04	.37037E-06	
82	1.0449	.63700E-05	.23569E-06	
83	1.0744	.22100E-05	.81770E-07	
84	1.0825	.98800E-05	.36556E-06	
95	1.1085	.37700E-05	.13949E-06	
86	1.1223	.63700E-05	.23569E-06	
87	1.1260	.10140E-04	.37518E-06	
88	1.1531	.29900E-05	.11063E-06	
89	1.1713	.32500E-05	.12025E-06	
90	1.2080	.37700E-05	.13949E-06	
91	1.2175	.49400E-05	.18278E-06	
92	1.2409	.27300E-05	.10101E-06	
93	1.2510	.37700E-05	.13949E-06	
94	1.2771	.16900E-05	.62530E-07	
95	1.2928	.89700E-05	.33189E-06	
96	1.3530	.22100E-04	.81770E-06	
97	1.3584	.26000E-05	.96200E-07	
98	1.3941	.50700E-04	.18759E-05	
99	1.3997	.27300E-05	.10101E-06	
100	1.4270	.27300E-05	.10101E-06	

Table 2-D (Continued)

	Gamma Energy, in MeV, E	Intensity, or fraction of decays producing gammas of energy E, dimensionless	Volumetric Source Strength, in "gammas of energy E per cm ³ per sec" S _v (E).	NUCLIDE
101	1.4461	.72800E-05	.26936E-06	²³⁴Pa (Cont.)
102	1.4526	.15600E-04	.57720E-06	
103	1.4600	.37700E-05	.13949E-06	
104	1.4937	.27300E-05	.10101E-06	
105	1.5160	.50700E-05	.18759E-06	
106	1.5801	.20800E-05	.76960E-07	
107	1.5854	.20800E-05	.76960E-07	
108	1.5938	.50700E-05	.18759E-06	
109	1.6280	.16900E-05	.62530E-07	
110	1.6382	.32500E-05	.12025E-06	
111	1.6560	.19500E-05	.72150E-07	
112	1.6685	.13780E-04	.50986E-06	
113	1.6863	.50700E-05	.18759E-06	
114	1.6940	.16900E-04	.62530E-06	
115	1.6998	.19500E-05	.72150E-07	
116	1.7560	.31200E-05	.11544E-06	
117	1.7722	.19500E-05	.72150E-07	
118	1.7969	.37700E-05	.13949E-06	
119	1.8911	.24700E-05	.91390E-07	
120	1.8975	.20800E-05	.76960E-07	
121	1.9050	.35100E-05	.12987E-06	
122	1.9265	.57200E-05	.21164E-06	
123	1.0061	.19240E-04	.71188E-06	
124	.76636	.20673E-02	.76490E-04	²³⁴Pa^m
125	1.0010	.58846E-02	.21773E-03	
126	.93050	.36952E-02	.13672E-03	
127	.51200	.80000E-03	.29600E-04	Rn-222
128	.53369	.19000E-02	.70300E-04	²¹⁴Pb
129	.58015	.36400E-02	.13468E-03	
130	.78591	.10900E-01	.40330E-03	
131	.83902	.59000E-02	.21830E-03	
132	.51100	.14700E-02	.54390E-04	²¹⁴Bi
133	.60932	.46180	.17087E-01	
134	.66545	.15600E-01	.57720E-03	
135	.70311	.47222E-02	.17472E-03	
136	.71986	.40300E-02	.14911E-03	
137	.75284	.13300E-02	.49210E-04	
138	.76836	.48800E-01	.18056E-02	
139	.78610	.31000E-02	.11470E-03	
140	.80617	.12300E-01	.45510E-03	
141	.82118	.15000E-02	.55500E-04	
142	.90425	.10500E-02	.38850E-04	
143	.93405	.31600E-01	.11692E-02	
144	.96408	.38300E-02	.14171E-03	
145	1.0520	.31500E-02	.11655E-03	
146	1.0700	.28500E-02	.10545E-03	
147	1.1203	.15000	.55500E-02	
148	1.1337	.25500E-02	.94350E-04	
149	1.1552	.16900E-02	.62530E-04	
150	1.2077	.46000E-02	.17020E-03	

Table 2-D(Continued)

	Gamma Energy, in MeV, E	Intensity, or fraction of decays producing gammas of energy E, dimensionless	Volumetric Source Strength, in "gammas of energy E per cm ³ per sec" S _v (E).	NUCLIDE
151	1.2381	.59200E-01	.21904E-02	²¹⁴Bi (Cont.)
152	1.2810	.14700E-01	.54390E-03	
153	1.3030	.12100E-02	.44770E-04	
154	1.3777	.40200E-01	.14874E-02	
155	1.3853	.78000E-02	.28960E-03	
156	1.4015	.13900E-01	.51430E-03	
157	1.4080	.24800E-01	.91760E-03	
158	1.5092	.21900E-01	.81030E-03	
159	1.5385	.41000E-02	.15170E-03	
160	1.5433	.35000E-02	.12950E-03	
161	1.5832	.72000E-02	.26440E-03	
162	1.5947	.26500E-02	.90050E-04	
163	1.5993	.33400E-02	.12358E-03	
164	1.6613	.11500E-01	.42550E-03	
165	1.6840	.23600E-02	.87320E-04	
166	1.7296	.30500E-01	.11280E-02	
167	1.7645	.15900	.56830E-02	
168	1.8384	.38300E-02	.14171E-03	
169	1.8474	.21200E-01	.78440E-03	
170	1.8732	.22600E-02	.83620E-04	
171	1.8963	.17700E-02	.65490E-04	
172	2.1185	.12100E-01	.44770E-03	
173	2.2041	.49900E-01	.18463E-02	
174	2.2934	.32400E-02	.11988E-03	
175	2.4477	.15500E-01	.57350E-03	
176	1.6543	.38700E-01	.14319E-02	Po-214
177	.79200	.10000E-03	.37000E-05	

Appendix E

Choice of Medium Representing Uranium Mill Tailings

The usefulness of equations based on Taylor's or Berger's buildup factor is closely connected to the availability of parameters corresponding to either form for a given transport medium. These parameters have been obtained for elements such as tin, lead, etc., for water and for homogeneous mixtures of well defined composition, such as the various types of concrete in Table 2-A but not for "soil" or "uranium mill tailings". This omission is due, in all probability, not only to the complexity of the projected task, but also to the envisioned lack of generality of the presumptive results (no two soils or tailings piles are more than vaguely similar in composition). Consequently, any relatively simple method based on the buildup factor concept must incorporate the parameters of one of the materials of Table 2-A, which entails a choice. The choice must be made realistically but conservatively, i.e., a material representing "tailings" should produce a greater, rather than smaller "buildup" of secondary radiation, regardless of any other characteristic.

The selection is facilitated by Equation (16-C) describing the "flux" of photons, emitted with some energy $E > 0.5$ MeV, at the surface of a bare tailings slab of infinite thickness, i.e., a "worst case" condition.

$$\phi(E) = \frac{S_V(E)}{2\mu_t(E)} \left[\frac{A(E)}{1+\alpha_1(E)} + \frac{1-A(E)}{1+\alpha_2(E)} \right]$$

Assuming the coefficient $\mu_t(E)$ for "tailings" to be already known as a function of energy, and bearing in mind that the values of $S_V(E)$ have been tabulated in Tables 1-D and 2-D, the flux $\phi(E)$ for a given energy is directly

proportional to the magnitude of the bracketed term in the above expression. This bracketed term is solely a function of the Taylor parameters A , α_1 , and α_2 which, in turn, depend exclusively on the choice of material, for a given energy E . Obviously, that transport medium which produces the largest values of the term in brackets would represent the most conservative choice.

The values of Taylor's parameters A , α_1 , and α_2 are given in Table 1-E for each of the 11 media previously listed in Table 2-A, and for energies ranging from 0.5 MeV to 3.0 MeV (this upper bound exceeding the highest gamma energy observed in the ^{238}U decay chain). Based on these values, the magnitude of the term $[A/(1+\alpha_1) + (1-A)/(1+\alpha_2)]$ has been plotted, for each material, over the indicated energy range, in Figure 1-E.

It is clear from this plot that either "water" or "ordinary concrete" would produce the highest values of buildup, necessitating additional criteria to effect a selection. In this regard, an important consideration is the need for extending analysis below the 0.5 MeV limit existing for Taylor's buildup factor. Since Berger's coefficients for 0.255 MeV exist for "water", but appear to be unavailable for "ordinary concrete" (Trubey, 1966), the choice of "water" parameters for energies above and below 0.5 MeV would be consistent and obvious.

The extent to which fluxes and exposure rates may be overestimated on the basis of the above selection cannot be precisely determined. By comparing the buildup in water to that in aluminum, Beck (1981) suggests that results obtained with the present selection may be high by 5 to 10%, at 1 meter, and even more at greater distances. However, the choice of water introduces compensating errors, alleviating, at least in part, the mentioned drawback, as discussed in Appendix G.

Table 1-E Buscaglione-Manzini* Coefficients
for Taylor Dose Buildup Factor Formula

Material	E_0 (MeV)	A	$-\alpha_1$	α_2
Water	0.5	100.845	0.12687	- 0.10925
	1	19.601	0.09037	- 0.02522
	2	12.612	0.05320	0.01932
	3	11.110	0.03550	0.03206
Aluminum	0.5	38.911	0.10015	- 0.06312
	1	28.782	0.06820	- 0.02973
	2	16.981	0.04588	0.00271
	3	10.583	0.04066	0.02514
Iron	0.5	31.379	0.06842	- 0.03742
	1	24.957	0.06086	- 0.02463
	2	17.622	0.04627	- 0.00526
	3	13.218	0.04431	- 0.00087
Tin	0.5	11.440	0.01800	0.03187
	1	11.426	0.04266	0.01606
	2	8.783	0.05349	0.01505
	3	5.400	0.07440	0.02080
Tungsten	0.5	2.655	0.01740	0.11340
	1	3.234	0.04754	0.13058
	2	3.504	0.06053	0.08862
	3	4.722	0.06468	0.01404
Lead	0.5	1.677	0.03084	0.30941
	1	2.984	0.03503	0.13486
	2	5.421	0.03482	0.04379
	3	5.580	0.05422	0.00611
Uranium	0.5	1.444	0.02459	0.35167
	1	2.081	0.03862	0.22639
	2	3.287	0.03997	0.08635
	3	4.883	0.04950	0.00981

Table 1-E (continued)

Material	E_0 (MeV)	A	$-\alpha_1$	α_2
Ordinary Concrete	0.5	38.225	0.14824	- 0.10579
	1	25.507	0.07230	- 0.01843
	2	18.089	0.04250	0.00849
	3	13.640	0.03200	0.02022
Ferrophosphorous Concrete	0.5	61.341	0.07292	- 0.05265
	1	46.087	0.05202	- 0.02845
	2	14.790	0.04720	0.00867
	3	10.399	0.04290	0.02211
Magnetite Concrete	0.5	75.471	0.07479	- 0.05534
	1	49.916	0.05195	- 0.02796
	2	14.260	0.04692	0.01531
	3	8.160	0.04700	0.04590
Barytes Concrete	0.5	33.026	0.06129	- 0.02883
	1	23.014	0.06255	- 0.02217
	2	9.350	0.05700	0.03850
	3	6.269	0.06064	0.04440

*From "A Survey of Empirical Functions Used to Fit Gamma-Ray Buildup Factors." By D.K. Trubey, ORNL-RSIC-10, Published February 1966.

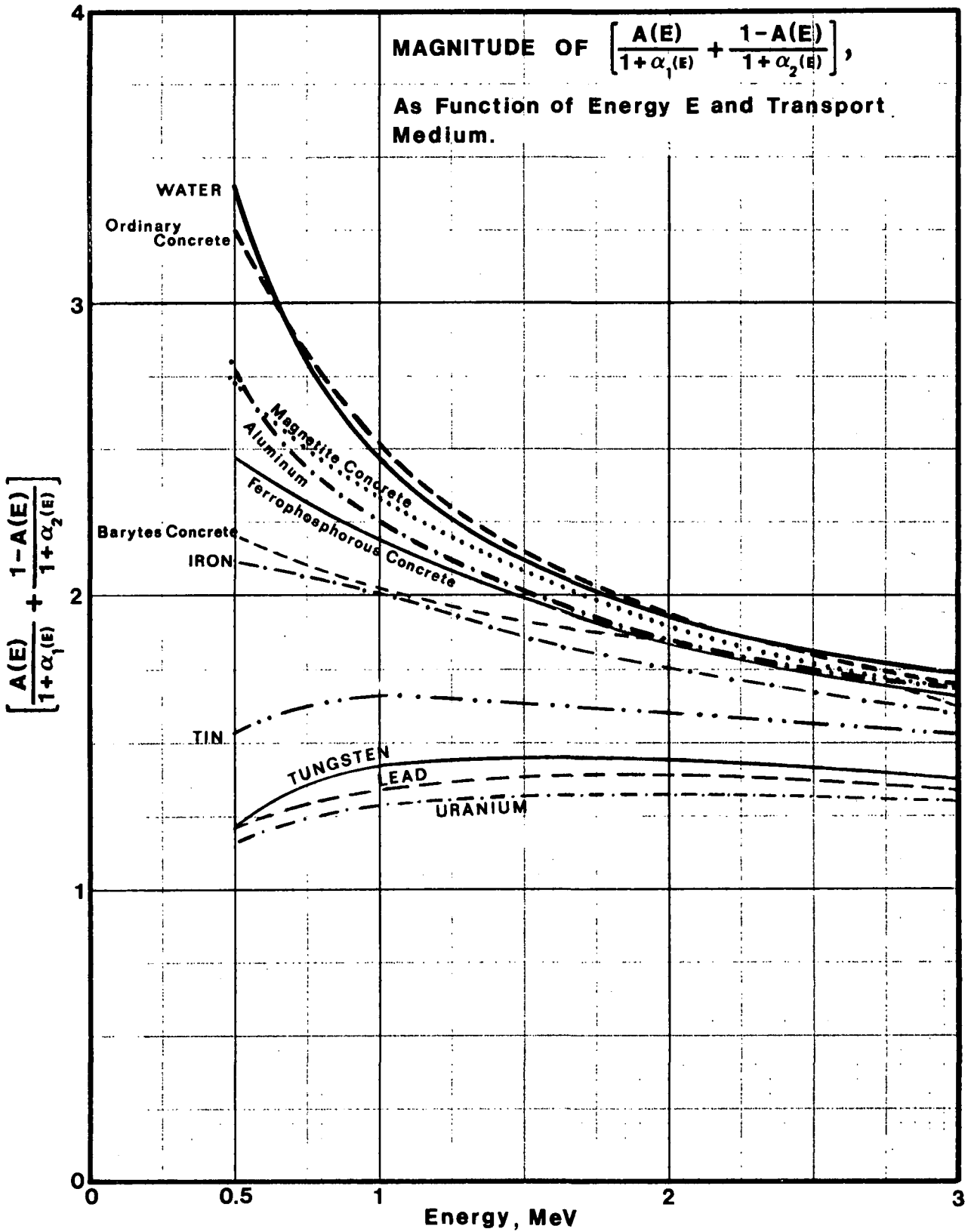


Figure 1-E Magnitude of $\left[\frac{A}{(1+\alpha_1)} + \frac{(1-A)}{(1+\alpha_2)} \right]$ as function of energy and choice of transport medium representing "uranium mill tailings"

Appendix F

Dose Buildup Coefficients for Taylor's and Berger's Formulas

The choice of Taylor's (and Berger's) "water parameters as conservative substitutes for the unavailable "U.B.S. or mill tailings" coefficients was based, primarily, on a visual inspection of Figure 1-E drawn using known values of A , α_1 , and α_2 at energies of 0.5, 1, 2, and 3 MeV (Table 1-E). These four values are obviously insufficient for meeting the requirements of Equations (43-C) and (44-C) and equations leading thereto - Tables 1-D and 2-D identify 282 different gamma energies from nuclides in the ^{238}U decay chain, ranging roughly from 0.01 to 2.45 MeV. Fortunately, both Taylor's and Berger's coefficients are smooth functions of energy, which enabled the present author to obtain the necessary curve-fitting expressions.

I. Taylor's Coefficients

For Taylor's coefficients, required for 177 gamma energies from 0.5 to 2.45 MeV (Table 2-D), the following equations apply:

$$\text{(Figure 1-F)} \quad A(E) = \exp\left(\frac{a}{b - E} + c\right) \quad (1-F)$$

$$\text{where } a = -0.560 \ 423 \ 309 \ 6$$

$$b = 0.266 \ 709 \ 011 \ 9$$

$$c = 2.211 \ 317 \ 385$$

$$\text{(Figure 2-F)} \quad \alpha_1(E) = a_1 + b_1 \ln E \quad (2-F)$$

where $a_1 = -0.090\ 035$

$b_1 = 0.053\ 141\ 671\ 84$

$$\text{(Figure 3-F)} \quad \alpha_2(E) = \frac{a_2}{b_2 + E} + c_2 E + d_2 \quad (3-F)$$

where $a_2 = -0.113\ 514\ 887\ 2$

$b_2 = 0.098\ 224\ 139\ 43$

$c_2 = -0.004\ 721\ 763\ 81$

$d_2 = 0.082\ 863\ 985\ 76$

Note that the energy range for which Taylor's coefficients are valid comprises 85% of the energy emitted in the ^{238}U decay chain, and that they are valid generally, i.e. without regard to the number of mean free paths involved (see Table 2-A, supra). Thus the brunt of calculations concerning the effects of varying U.B.S. or tailings slab thickness, cover material thickness, and relaxation lengths is aptly borne by these coefficients.

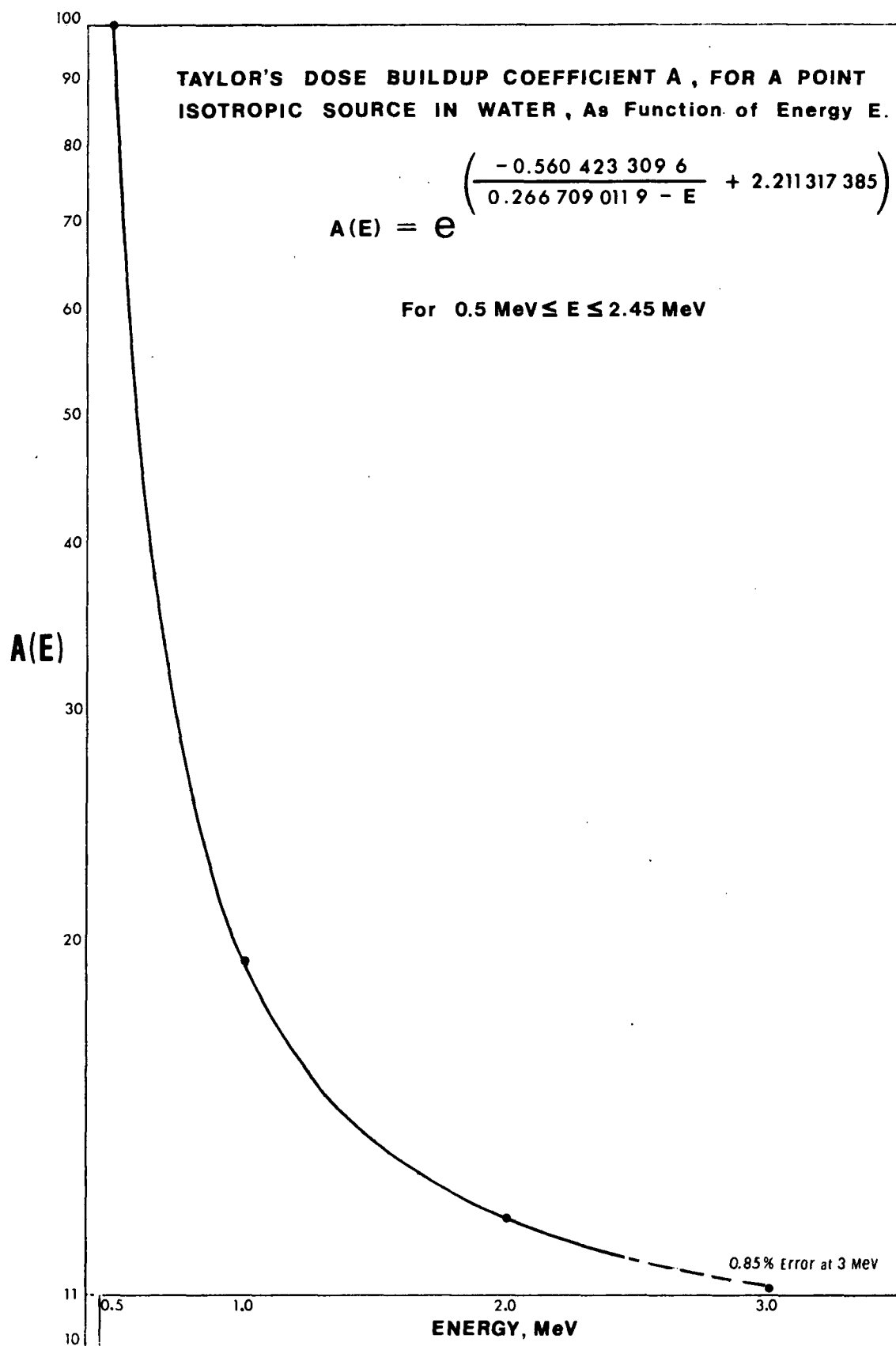


Figure 1-F. Taylor's Dose Buildup coefficient **A** , for a point isotropic source in water, as function of gamma energy E.

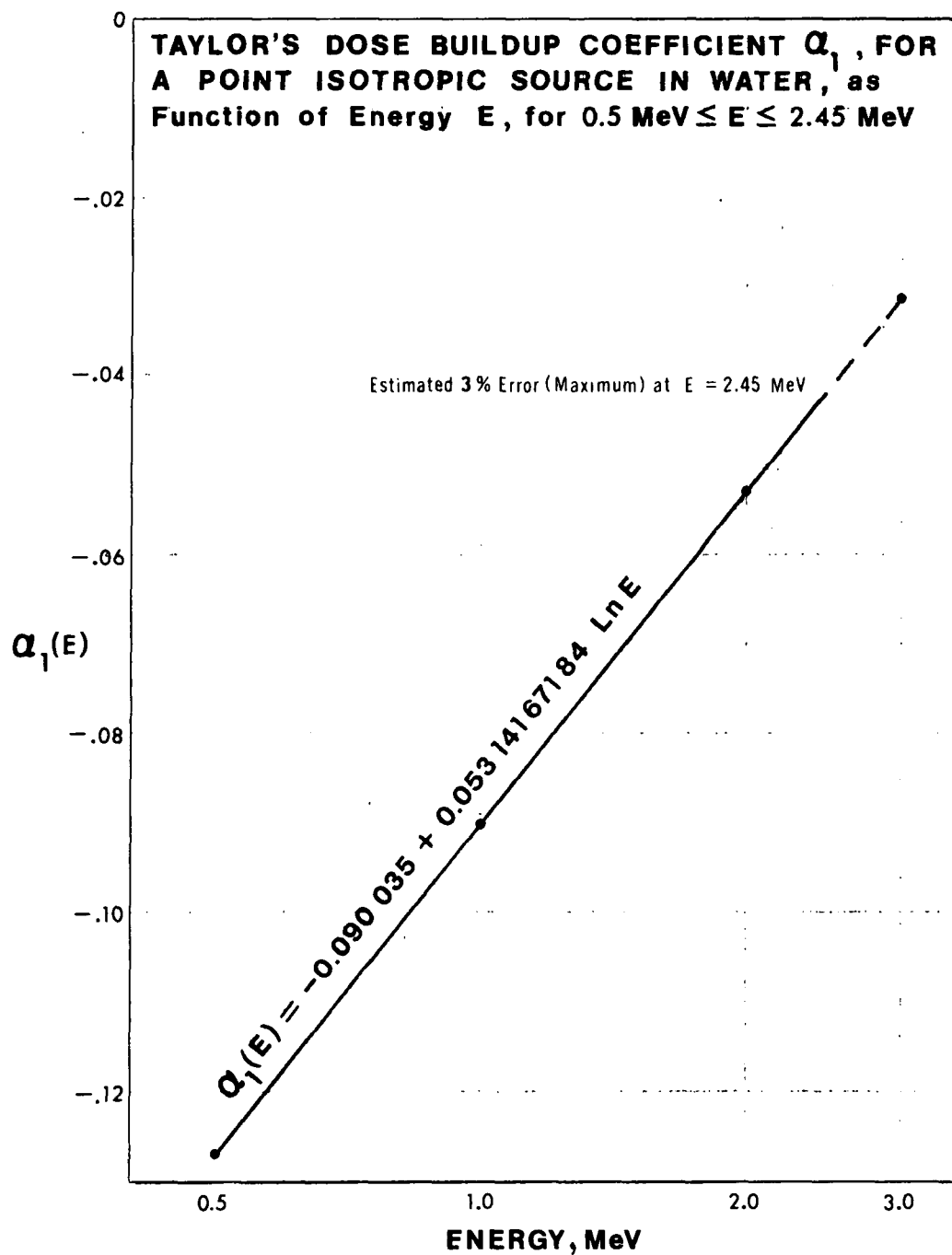


Figure 2-F. Taylor's Dose Buildup coefficient Q_1 , for a point isotropic source in water, as function of energy E.

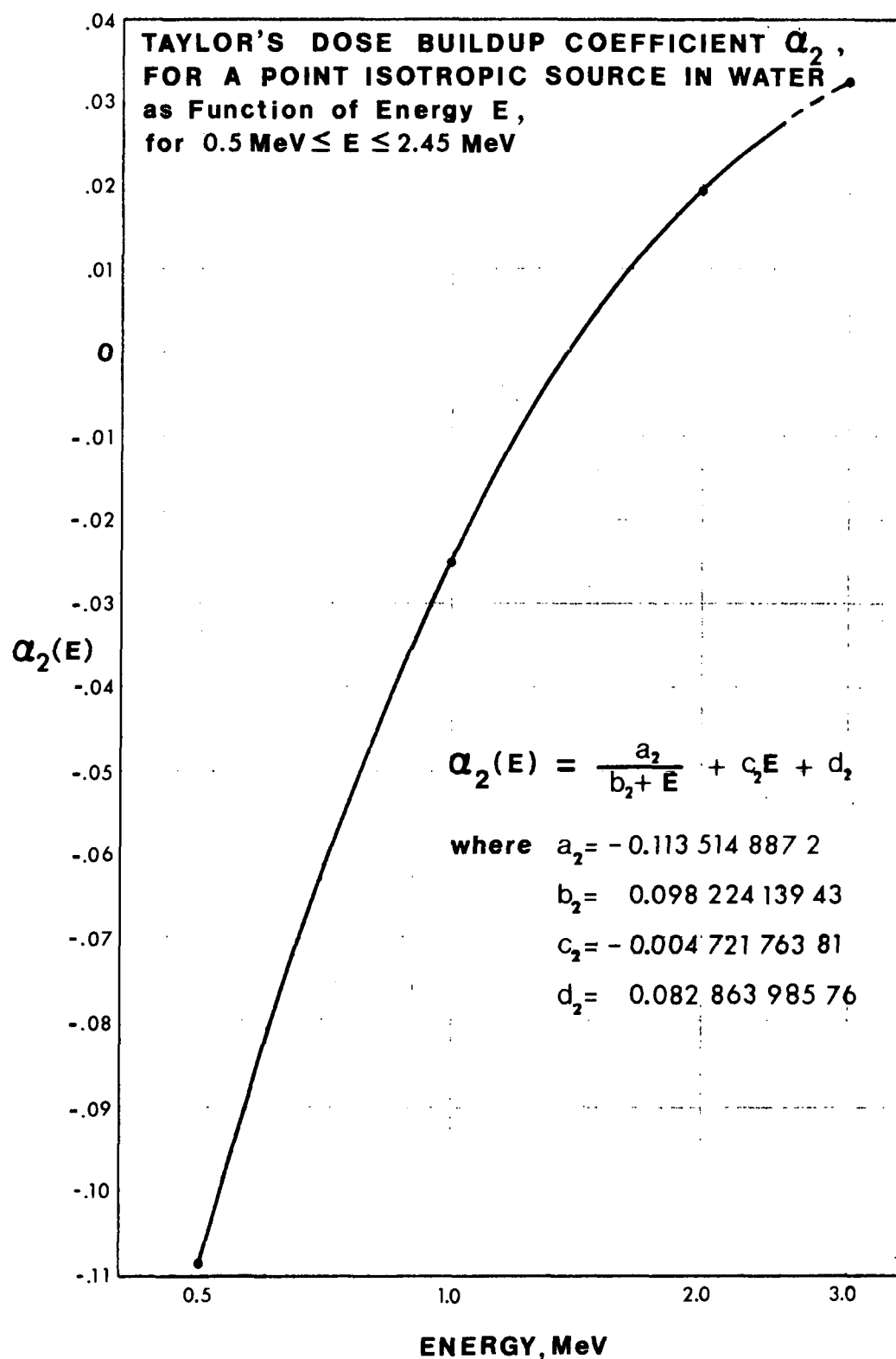


Figure 3-F. Taylor's Dose Buildup coefficient α_2 , for a point isotropic source in water, as function of energy E.

II. Berger's Coefficients

For Berger's factors, required for 105 gamma energies from 0.01 to 0.5 MeV (Table 1-D) a more limited application is appropriate. Note that Berger's parameters are, spatially, less generally valid than Taylor's, i.e. an element of uncertainty is introduced as a given number of MFP's is exceeded (see Table 2-A & supra). This is an undesirable effect in calculating relaxation lengths or any thickness-dependent quantity. Fortunately, Berger's factors need apply to only 15% of the total energy released by the ^{238}U decay chain, which suggests that simplified approaches would not result in gross overall error. Specifically, the best use of Berger's factors is thought to be one that bypasses - or ignores - the problems of discontinuity inherent to dealing with varying thicknesses of tailings, and limits their application to one simple case. This simple case is that of the bare tailings slab of "infinite" thickness, a "maximum flux" or "worst case" condition expressed by Equation (40-C) repeated below.

$$\phi(E) = \frac{S_v(E)}{2\mu_t(E)} \left\{ 1 + \frac{C(E)}{[D(E)-1]^2} \right\}$$

This equation may be viewed as producing a (somewhat) tentative corrective term to be added to the corresponding "worst case" fluxes (and exposures) obtained via Taylor's parameters and Equation (16-C), with other results adjusted accordingly when pertinent. Spatial dependence being absent from Equation (40-C), the energy dependence of Berger's factors may be dealt with in a "compound" manner, defining a "Berger's effective buildup factor for worst case conditions", or $B_{wc}(E)$.

$$B_{wc}(E) = 1 + \frac{C(E)}{[D(E)-1]^2} \quad (4-F)$$

Berger's Form parameters $C(E)$ and $D(E)$ have been calculated by A. B. Chilton for $\mu r \leq 7$, $\mu r \leq 10$, and $\mu r \leq 20$ (Trubey, 1966.). The choice of one set of parameters over another appears to be moot, since the slab under consideration is assumed to be of infinite areal extent, regardless of the manner in which the slab "infinite" thickness can be represented. Choosing the $C(E)$ and $D(E)$ parameters for the 20 MFP case may seem, at first regard, a slightly better option, since they apply over a greater range. To offset this presumed advantage, the corresponding parameters for the 7 MFP fit generally produce more conservative buildup values. This may be verified by comparing, in Figure 4-F, the buildup factors at various distances from a 0.255 MeV point source in an infinite water medium, obtained with Berger's formula using both 7 MFP and 20 MFP coefficients. Further analysis is suggested by these considerations.

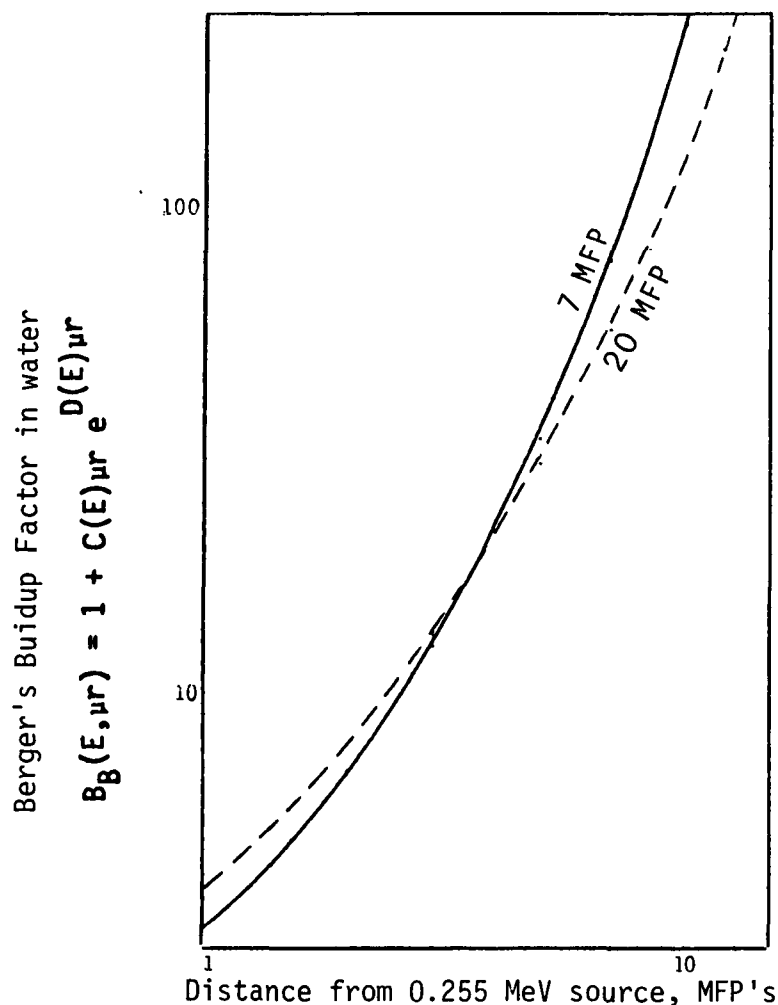


Figure 4-F. Buildup factors as functions of distance, in mean-free-paths, from a 0.255 MeV isotropic point source in an infinite water medium, calculated with Berger's buildup formula using C and D buildup coefficients based on 20 MFP and 7 curve fits. The latter result in higher buildup for distances over 4 MFP's.

For distances up to 4 MFP's from the 0.255 MeV point source, buildup factors obtained with C and D coefficients based on the 20 MFP fit are slightly higher than the corresponding buildup based on 7 MFP fit coefficients. This observation achieves significance when the buildup term $[1+C/(D-1)^2]$, for the bare, infinitely thick source slab case (see Table 1), is evaluated with both sets of C and D parameters: the 20-MFP-fit values for C and D result in a buildup term that is also higher (by 8% or 9%) than the value produced by the 7-MFP-fit coefficients, implying that buildup from sources within a short distance from a receptor will override all buildup effects from more distant sources. This "distance of observable effect" must be, indeed, rather short, since the 7-MFP-fit buildup factor at 10 MFP's from the 0.255 MeV source exceeds the 20-MFP-fit buildup factor by 87% (see Figure 4-F), and by roughly 400% at 20 MFP's, while the above comparison of buildup terms for infinite source slabs obviously negates such enormous differences. Consequently, the $B_{wc}(E)$ term in Equation (4-F) may be gainfully evaluated with C(E) and D(E) coefficients applicable to distances of less than 10 MFP's, with 7-MFP-fit parameters being a natural choice. This is an important factor considering that the 20 MFP fit at 0.255 MeV ("dose buildup", point source in water) produces a maximum error of 30%, whereas that for a 7 MFP fit is only 10% (Trubey, 1966). Since the parameters C(E) and D(E) are not available for energies below 0.255 MeV, some judicious extrapolation is required to cover the remainder of the gamma energy range, in which light the choice of 7 MFP coefficients appears judicious by offering less possibility of serious error.

The values acquired by $B_{wc}(E)$ as function of energy, based on Berger's parameters C(E) and D(E), for the 7 MFP fit, are given in Table 1-F.

Table 1-F. Values of B_{WC} , C^* and D^* for Energies 0.255 MeV to 1.0 MeV

Energy E (MeV)	Dimensionless parameters		
	C(E)	D(E)	$B_{WC}(E) = 1 + \frac{C(E)}{[D(E)-1]^2}$
0.255	1.7506	0.2609	4.2046
0.5	1.3245	0.2078	3.1105
1.0	1.0622	0.1052	2.3266

* Coefficients C and D from Trubey (1966)

The corresponding curve-fitting equation for B_{WC} as function of energy follows:

$$\text{(Figure 4-F)} \quad B_{WC}(E) = 1.0 + \exp\left(\frac{a_3}{\ln E - b_3} + c_3\right) \quad (5-F)$$

$$\text{where } a_3 = 204.525 \ 558 \ 5$$

$$b_3 = 17.131 \ 305 \ 11$$

$$c_3 = 12.221 \ 355 \ 02$$

Although the values used in the curve fit ranged from 0.255 MeV to 1.0 MeV, inclusive, the range of Equation (5-F) applicable to the purposes of this study is determined as $0.185 \text{ MeV} \leq E \leq 0.5 \text{ MeV}$. The upper bound is prescribed by the availability of Taylor's coefficients (preferred to Berger's) for energies $E \geq 0.5 \text{ MeV}$. The setting of the lower bound at a value below 0.255 MeV is based on necessity, and requires additional explanation.

Generally, some extrapolation of a curve fitting equation may be regarded as valid, to the extent that it does not conflict with accepted facts. Such a conflict occurs at the lowest energies of the ^{238}U chain decay spectrum. To be specific, at $E = 0.01 \text{ MeV}$, Equation (5-F) produces $B_{WC} = 17.6$. This is clearly a fallacy, since at this energy the mass energy-absorption coefficient μ_{en}/ρ approaches the value of the mass-attenuation coefficient μ/ρ , suggesting that

$B_{wc}(0.01 \text{ MeV}) \approx 1.0$. Consequently, some correction is required if Equation (5-F) is to apply to energies below 0.255 MeV. The correction should produce a net effective buildup factor meeting mainly the following constraints:

1. At $E = 0.01 \text{ MeV}$, the net effective buildup factor should have a value of 1.0
2. For the range $0.255 \text{ MeV} \leq E \leq 0.5 \text{ MeV}$, the values obtained through Equation (5-F) should remain unaltered.
3. The resultant curve should lack discontinuities. Thus the maximum buildup cannot occur at 0.255 MeV ($d^2 B_{wc} / dE^2$ is negative at $E = 0.255 \text{ MeV}$)
4. For lack of better information concerning soil cross-sections, the maximum buildup is assumed to appear at $E \approx 0.12 \text{ MeV}$, roughly mid-range of $0.01 \text{ MeV} \leq E \leq 0.255 \text{ MeV}$.

An energy-dependent correction term $C_T(E)$, when subtracted from the corresponding values of $B_{wc}(E)$, produces an "extrapolated" net effective buildup factor $B_{xwc}(E)$ in agreement with the set constraints (Figure -F).

$$B_{xwc}(E) = B_{wc}(E) - C_T(E) \quad (6-F)$$

$$\text{where } C_T(E) = \exp \left(\frac{d_3}{\ln E + f_3} + g_3 \ln + h_3 \right) \quad (7-F)$$

$$\text{and } d_3 = 1.757 \ 679 \ 538$$

$$f_3 = 1.682 \ 331 \ 986$$

$$g_3 = -0.281 \ 565 \ 645$$

$$h_3 = 2.116 \ 732 \ 933$$

The range of applicability of Equations (6-F) and (7-F) comprises energies $0.01 \text{ MeV} \leq E \leq 0.185 \text{ MeV}$, thus complementing the range set for Equation (5-F) of $0.185 \text{ MeV} \leq E \leq 0.5 \text{ MeV}$. The setting of $E = 0.185 \text{ MeV}$ as boundary between the two ranges is based on the observation that $C_T(E)$ becomes negligibly small as E increases to 0.185 MeV, but infinitely large when $E = \exp(-f_3)$ is exceeded.

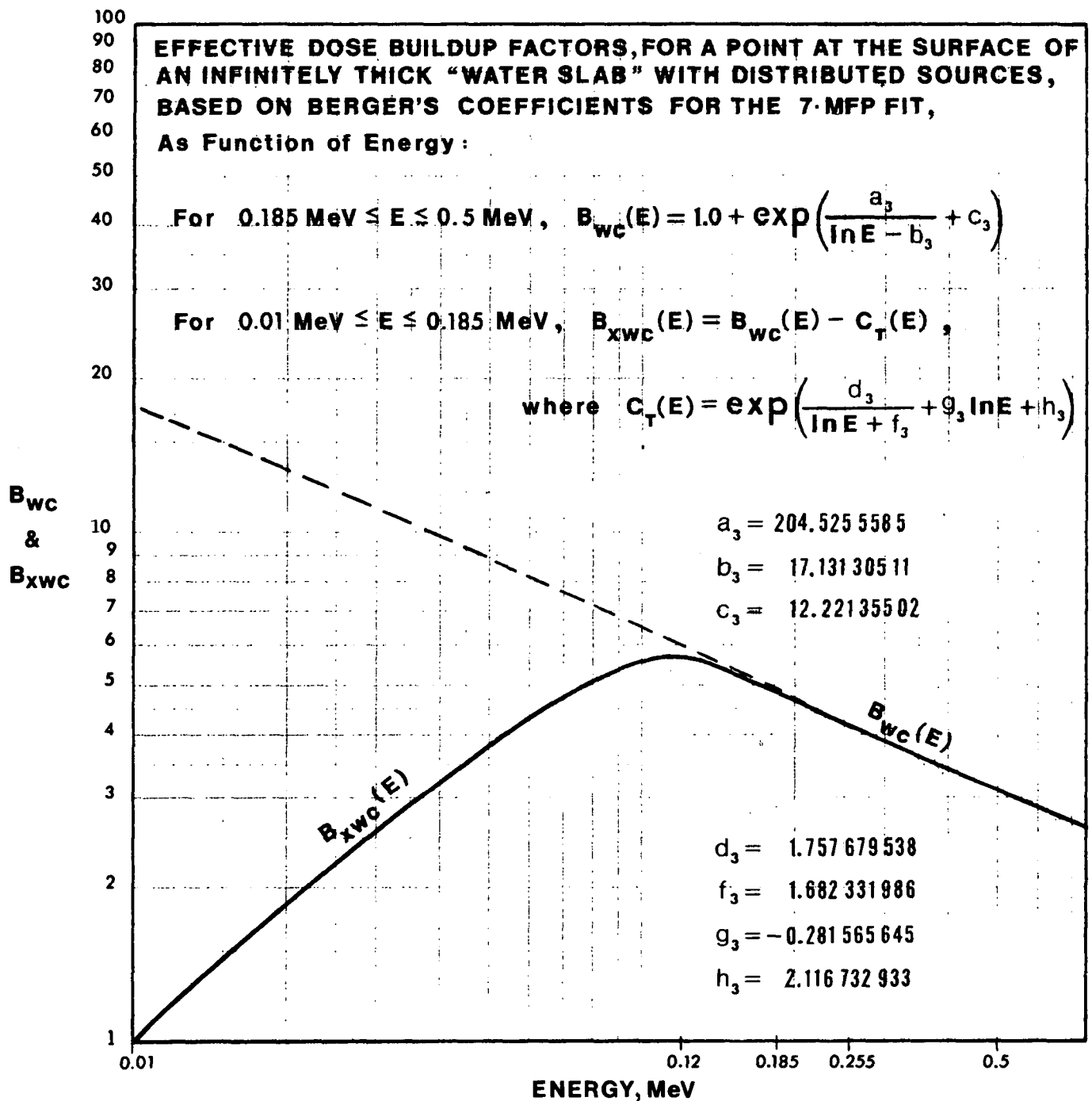


Figure 5-F. Effective Buildup Factors $B_{wc}(E)$ and $B_{xwc}(E)$ for a point at the surface of an infinitely thick slab with distributed sources, based on Berger's dose buildup coefficients for water (0-7 MFP fit), as function of energy.

Appendix G

Ancillary Curve - Fitting Equations

In addition to Taylor's and Berger's coefficients, the equations introduced in preceding sections include other energy-dependent parameters, namely

$\mu_t(E)$ = energy-dependent attenuation coefficient of tailings, cm^{-1}

$\mu_c(E)$ = energy-dependent attenuation coefficient of cover material, cm^{-1}

$\mu_{\text{air}}(E)$ = energy-dependent attenuation coefficient of air, cm^{-1}

$\left[\frac{\mu_{\text{en}}(E)}{\rho} \right]_{\text{air}}$ = energy-dependent mass-energy absorption coefficient of air, cm^2/g

In conjunction with several geometric parameters, most of those mentioned above serve as input to the argument of yet another function,

$E_2(\text{argument})$ = Second order exponential integral

where argument = $f[\alpha_1(E), \alpha_2(E), \mu_t(E), \mu_c(E), \mu_{\text{air}}(E), d \text{ and/or } t]$

All these quantities have been extensively tabulated in several publications (e.g. Radiological Health Handbook), in which form they can be used directly in any computer program possessing the necessary interpolating subroutines. Nevertheless, since a simpler process was envisioned in developing the present method, it was thought best to express them as explicit functions of energy, or of the generalized argument in the case of the exponential integral.

Attenuation coefficients for "tailings" or "soil" (cover material) are not available, which necessitates approximating these functions of energy on the

basis of coefficients obtained for other materials. The approach is suggested by Figure 1-G, in which mass-attenuation coefficients μ/ρ are plotted as functions of energy for various materials. These were chosen according to their abundance in the earth crust and represent, in broad terms, the main components of a generalized "soil". Quoting Hammond (1966), "oxygen accounts for about 47% of the crust by weight, while silicon comprises about 28%, and aluminum about 8%. These elements, plus iron, calcium, sodium, potassium, and magnesium, account for about 99% of the earth's crust." Other materials were added for diverse reasons. Carbon and water were included by at least one researcher (Beck, 1972) among typical soil components. Since both water and concrete were equally relevant in choosing parameters for Taylor's buildup formula, the latter material was added for comparison purposes. Silica (SiO) is the major component of tailings, with all the elements mentioned above, plus uranium, being present as complex silicates (G.E.I.S. Uranium Milling, 1979).

One important observation can be made from Figure 1-G, that for energies $0.25 \text{ MeV} \leq E \leq 3.0 \text{ MeV}$, the μ/ρ coefficients of the various materials lie within a narrow band of values, with a maximum difference of about 15% (between H₂O and Fe, at $E = 0.8, 1.0$, and 1.5 MeV). This suggests, for these energies, a generalized mass-attenuation coefficient approximately independent of material, and depending solely on energy.

$$\left[\frac{\mu(E)}{\rho} \right]_m \approx \left[\frac{\mu(E)}{\rho} \right]_G \quad \begin{array}{l} \text{where } m = \text{H}_2\text{O, Fe, Al etc.} \\ G = \text{generalized "soil"} \end{array} \quad (1-G)$$

This generalization allows choosing the mass-attenuation coefficient of water to represent the "generalized μ/ρ " in (1-G), without introducing gross error, while retaining consistency with the choice of medium in selecting Taylor's

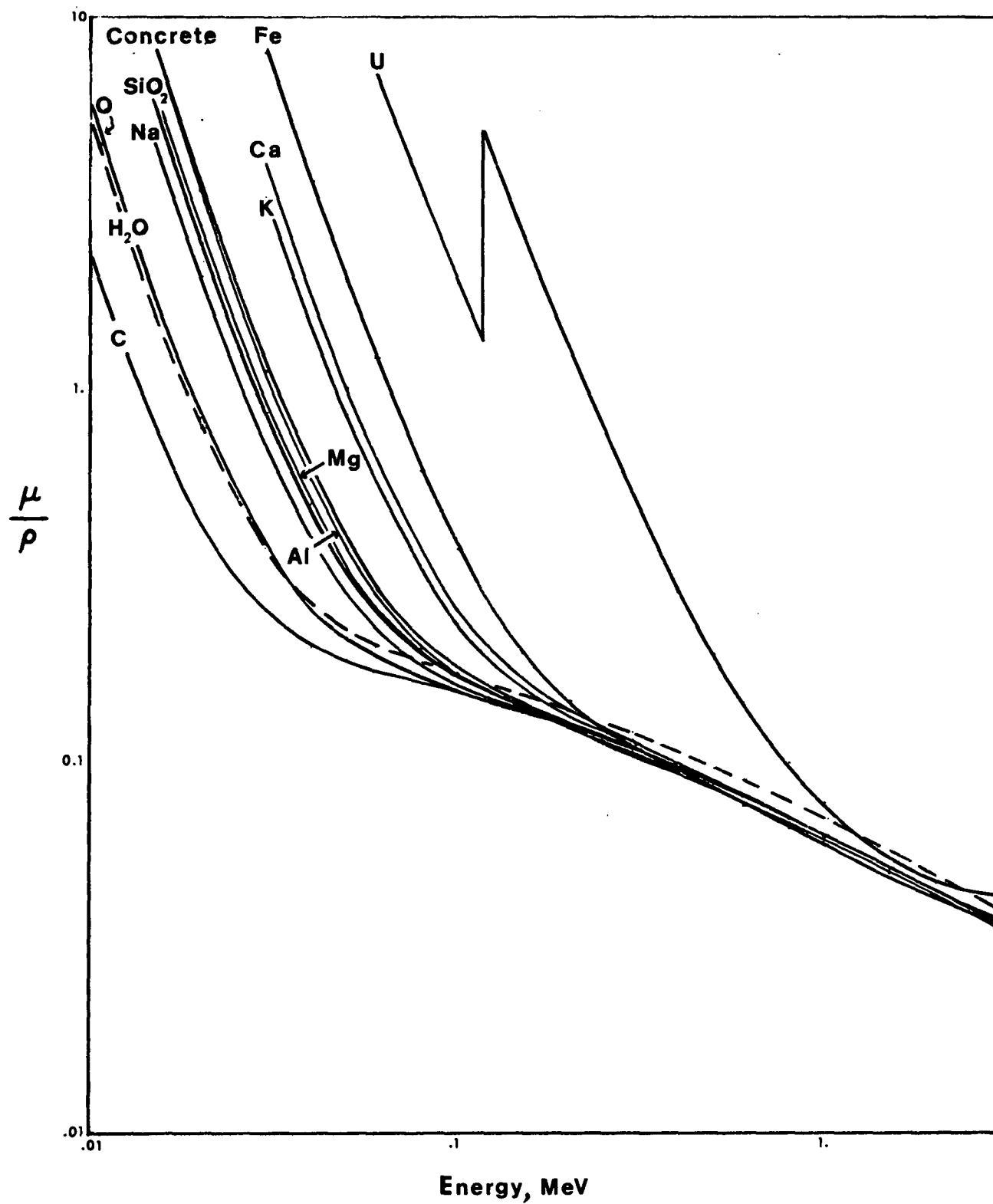


Figure 1-G. Mass attenuation coefficients for various materials.

and Berger's buildup parameters. Henceforth, by definition,

$$\left[\frac{\mu(E)}{\rho} \right]_G \equiv \left[\frac{\mu(E)}{\rho} \right]_{H_2O} \quad (2-G)$$

Consequently, the linear attenuation coefficient $\mu(E)_m$ of any of the soil materials in Figure 1-G, and thus that of soil itself, can be approximated by multiplying the mass-attenuation coefficient of water, at the energy E, by the density ρ_m of the given material.

$$\mu(E)_m \approx \left[\frac{\mu(E)}{\rho} \right]_{H_2O} \times \rho_m \quad (3-G)$$

Since the density of "tailings" is expected to be roughly that of "soil" (cover material), it follows that

$$\mu_t(E) \approx \mu_c(E) \approx \left[\frac{\mu(E)}{\rho} \right]_{H_2O} \times 1.6 \text{ g/cm}^3 \quad (4-G)$$

where "1.6 g/cm " is the density of both "tailings" and "moist packed soil", as per Schiager, 1974.

The selection of the mass-attenuation coefficient of water to represent the "generalized mass-attenuation coefficient" in (1-G) was influenced by the choice of Taylor's and Berger's buildup coefficients for "water" in lieu of the unavailable "soil" parameters, envisioned as a conservative alternative that would increase, rather than reduce, the calculated values of "flux". The wish for consistency discouraged other choices, although Equations (16-C) and (40-C) indicate that a lower coefficient, such as that of C in Figure 1-G, would further increase calculated "flux", leading to an extremely conservative model.

In that context, $(\mu/\rho)_{H_2O}$ is very conservative for $E < 0.1 \text{ MeV}$ but, at

higher energies, it exceeds the coefficients of most soil materials generally by some 10%, that of Al rather uniformly by 13%, and that of Fe by up to 15% (Figure 1-G). Correspondingly, the fluxes and exposure rates at these higher energies would be unquestionably lower than those for true soil, were it not for the compensatory effect of the conservatively chosen buildup factor (Appendix E).

This effect is illustrated by a rough comparison of fluxes and exposure rates calculated by using water to represent soil versus those obtained by using aluminum "which is a fairly good approximation for soil" (Beck, 1981). Referring to Equation (16-C), the effect of using the H_2O buildup factor rather than that of Al is that of increasing flux and exposure rate, at any given energy, by a factor " $[B]_{H_2O} / [B]_{Al}$ ", equal to the ratio of the corresponding bracketed "buildup terms" in Figure 1-E (indicated by "[B]" in present notation). On the other hand, the use of the H_2O mass-attenuation coefficient $(\mu/\rho)_{H_2O}$ instead of $(\mu/\rho)_{Al}$ in Equation (4-G) increases μ_t by the ratio " $(\mu/\rho)_{H_2O} / (\mu/\rho)_{Al}$ ", which amounts to reducing flux in (16-C) by a factor " $(\mu/\rho)_{Al} / (\mu/\rho)_{H_2O}$ ". Listing both increase and reduction factors in Table 1-G for the energy intervals used by Beck (1972) indicates that their net effect, or product, is one of increasing low energy fluxes and reducing high energy fluxes by up to 9%, respectively, assuming unit intensity for each energy interval. Considering the actual tabulated intensities (also from Beck, 1972) and average energies for each interval indicates an overall flux overestimation of 0.5% and a total exposure rate underestimation of 4%, always assuming that Al is the exact analog of soil. A discussion in Appendix I suggests some liabilities of this assumption. In the interim, the above calculations serve to point out that the choice of H_2O to represent soil will not result in gross error.

Table 1-G. Effects on Flux and Exposure Rates of Using Water Buildup Factor and Mass Attenuation Coefficient Instead of the Corresponding Parameters for Aluminum

① Energy Interval (MeV)	② Average Energy (MeV)	③ Intensity (gammas per disintgrtn)	④ Reduction Factor: $\left[\frac{(\mu/\rho)_{Al}}{(\mu/\rho)_{H_2O}} \right]$	⑤ Increase Factor (Buildup "Term" Ratios): $[B]_{H_2O}/[B]_{Al}$	⑥ Exposure Rate and Flux Ratios per Unit Intsty. (⑤ x ④)
.05- .15	.1	.139	1.0	1.0 *	1.0
.15- .25	.2	.104	.8905	1.223 *	1.089
.25- .35	.3	.196	.8739	1.223 *	1.069
.35- .45	.4	.361	.8745	1.223 *	1.07
.45- .55	.5	.022	.8719	1.223	1.066
.55- .65	.6	.436	.8705	1.2	1.045
.65- .75	.7	.027	.8704	1.165	1.014
.75- .85	.8	.084	.8702	1.136	.989
.85- .95	.9	.032	.8686	1.112	.966
.95-1.05	1.0	.014	.8670	1.098	.952
1.05-1.35	1.2	.252	.8680	1.067	.926
1.35-1.65	1.5	.137	.8696	1.052	.915
1.65-1.95	1.8	.218	.8725	1.047	.914
1.95-2.55	2.25	.081	.8788	1.042	.916
2.55	2.55	.002	.8840	1.035	.915

Notes:

* From Figure 1-E, the ratio of the "bracketted" buildup "term" of water to that of aluminum is 1.223 at 0.5 Mev, and likely to increase for energies $E < 0.5$ MeV. Thus, a minimum ratio of 1.223 was assumed to be valid for energies $0.15 \text{ MeV} \leq E \leq 0.5 \text{ MeV}$.

①,③ From Beck (1972)

② Midpoint of energy interval

④ From Equations (15-C),(16-C),etc. and Equations (1-G) through (4-G): for $E > 0.1$ MeV, $(\mu/\rho)_{H_2O} > (\mu/\rho)_{Al}$, thus using $(\mu/\rho)_{H_2O}$ in (4-G) will produce somewhat higher values of $\mu_t(E)$ which, in turn, will reduce flux calculated through Equations (16-C), etc. by the indicated ratio.

⑤ From Figure 1-E: $[B] = \left[\frac{A}{1+\alpha_1} + \frac{1-A}{1+\alpha_2} \right]$, i.e. "bracketted buildup 'term'".

⑥ Net effect of reduction and increase factors; product of ④ x ⑤ .

$$\text{Overall effect on flux} = \frac{\sum [③ \times ⑥]}{\sum [③ \times 1.0]} = 1.005, \text{ i.e. a } 0.5\% \text{ increase}$$

$$\text{Effect on total exposure rate} = \frac{\sum [③ \times ⑥ \times ②]}{\sum [③ \times 1.0 \times ②]} = 0.96, \text{ a } 4\% \text{ decrease}$$

No similar complications attach to $\mu_{\text{air}}(E)$, which is simply

$$\mu_{\text{air}}(E) = \left[\frac{\mu(E)}{\rho} \right]_{\text{air}} \times 0.001293 \text{ g/cm}^3 \quad (5-G)$$

where "0.001293 g/cm³" is the density of dry air at 760 mm Hg and 0°C.

Values obtained from the Radiological Health Handbook (1970) were used in fitting curves to the mass attenuation coefficients for water and air, and to the mass energy-absorption coefficient for air, as functions of energy:

Mass Attenuation coefficient of Water $\left[\frac{\mu(E)}{\rho} \right]_{\text{H}_2\text{O}}$, as function of energy
(Figure 2-G) :

$$\text{for } .01 \text{ MeV} \leq E \leq .08 \text{ MeV}, (\mu/\rho)_{\text{H}_2\text{O}} = F_4(E) + G_4(E) \quad (6-G)$$

$$\text{for } .08 \text{ MeV} \leq E \leq 3.0 \text{ MeV}, (\mu/\rho)_{\text{H}_2\text{O}} = G_4(E) \quad (7-G)$$

$$\text{where } F_4(E) = \exp \frac{a_4}{\ln E + b_4} + c_4 \ln E + d_4$$

$$G_4(E) = \exp \frac{f_4}{\ln E + g_4} + h_4$$

and	$a_4 = 0.571\ 008\ 922\ 1$	$f_4 = 53.135\ 288\ 31$
	$b_4 = 2.485\ 192\ 485$	$g_4 = -10.621\ 802\ 09$
	$c_4 = -3.082\ 595\ 417$	$h_4 = 2.353\ 164\ 25$
	$d_4 = -12.345\ 692\ 43$	

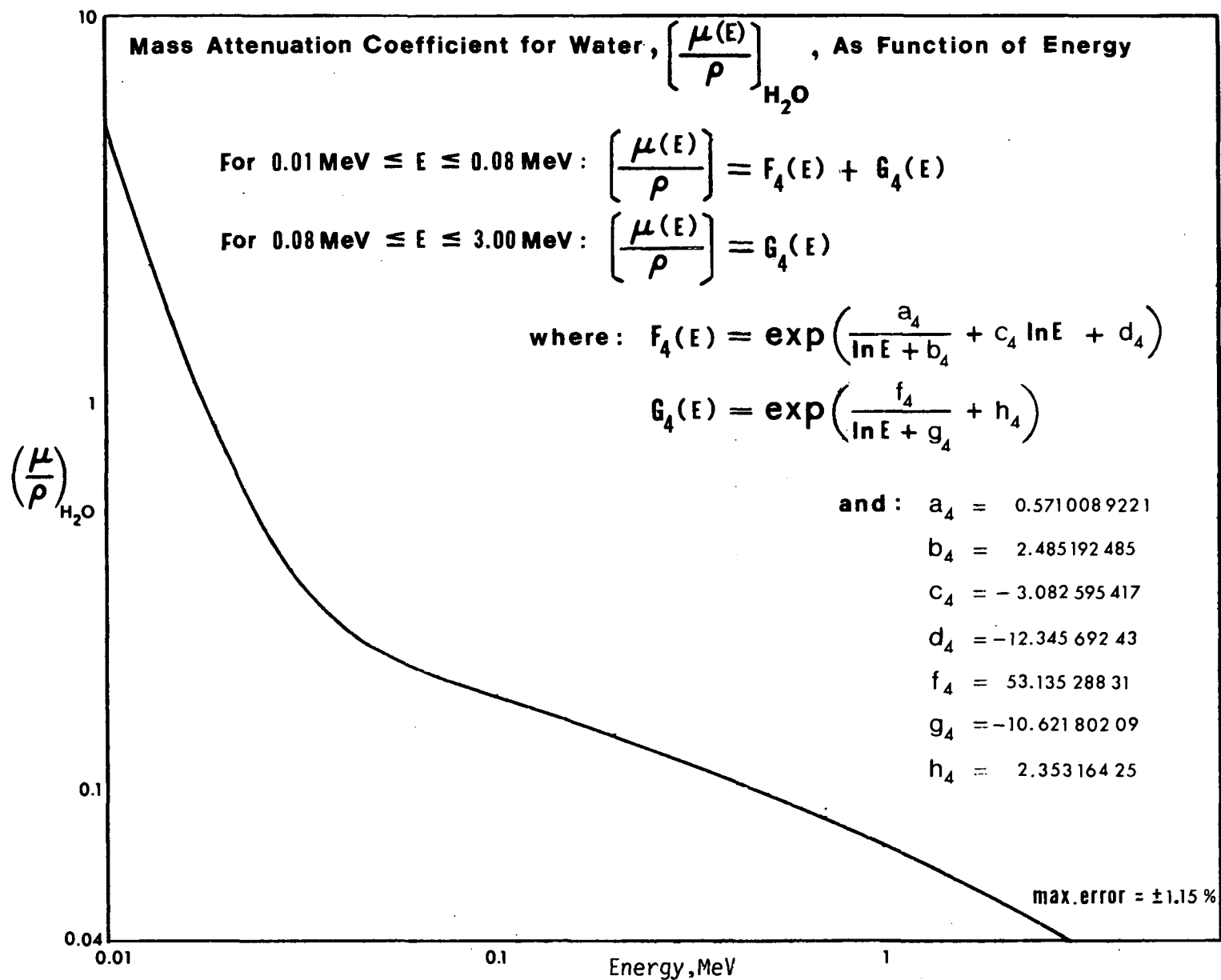


Figure 2-G. Mass attenuation coefficient for water, as function of energy

Mass Attenuation Coefficient of air $\left[\frac{\mu(E)}{\rho} \right]_{\text{air}}$, as function of energy (Figure 3-G):

$$\text{for } .01 \text{ MeV} \leq E \leq .015 \text{ MeV}, \left(\frac{\mu}{\rho} \right)_{\text{air}} = F_5(E) = \exp (a_5 \ln E + b_5) \quad (8-G)$$

$$\text{where } a_5 = -2.883 \ 555 \ 097$$

$$b_5 = -11.671 \ 826 \ 05$$

$$\text{for } .015 \text{ MeV} \leq E \leq .6 \text{ MeV}, \left(\frac{\mu}{\rho} \right)_{\text{air}} = F_5(E) + G_5(E) \quad (9-G)$$

$$\text{where } G_5(E) = \exp \left(\frac{c_5}{\ln E + d_5} + f_5 \ln E + g_5 \right)$$

$$\text{and } c_5 = -1.028 \ 577 \ 166$$

$$d_5 = 4.464 \ 072 \ 73$$

$$f_5 = -0.451 \ 578 \ 597$$

$$g_5 = -2.482 \ 816 \ 293$$

$$\text{for } .6 \text{ MeV} \leq E \leq 3.0 \text{ MeV}, \left(\frac{\mu}{\rho} \right)_{\text{air}} = G_5(E) + H_5(E) \quad (10-G)$$

$$\text{where } H_5(E) = \frac{h_5}{\ln E + k_5} + l_5$$

$$\text{and } h_5 = 3.409 \ 847 \ 524 \times 10^{-2}$$

$$k_5 = 2.730 \ 717 \ 269$$

$$l_5 = -1.536 \ 800 \ 255 \times 10^{-2}$$

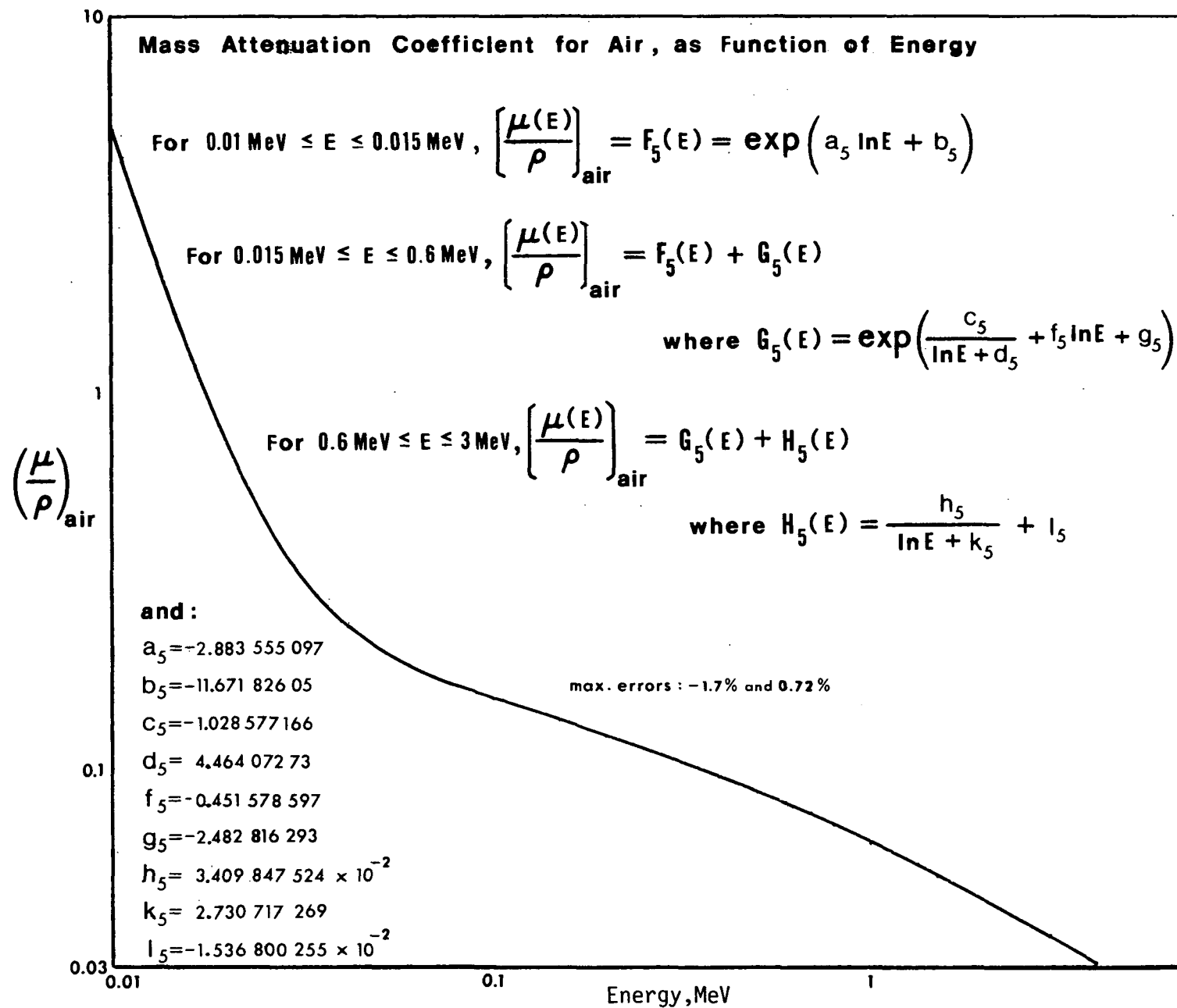


Figure 3-G. Mass attenuation coefficient for air, as function of energy

Mass Energy-Absorption Coefficient of Air $\left[\frac{\mu_{en}(E)}{\rho} \right]_{air}$, as function of energy
(Figure 4-G):

$$\text{for } .01 \text{ MeV} \leq E \leq .02 \text{ MeV}, \left(\frac{\mu_{en}}{\rho} \right)_{air} = F_6(E) = \exp(a_6 \ln E + b_6) \quad (11-G)$$

$$\text{where } a_6 = -3.157 \ 083 \ 5$$

$$b_6 = -13.0$$

$$\text{for } .02 \text{ MeV} \leq E \leq .5 \text{ MeV}, \left(\frac{\mu_{en}}{\rho} \right)_{air} = F_6(E) + G_6(E) \quad (12-G)$$

$$\text{where } G_6(E) = \exp \left(\frac{c_6}{\ln E + d_6} + f_6 \ln E + g_6 \right)$$

$$\text{and } c_6 = -1.812 \ 611 \ 059$$

$$d_6 = 3.938 \ 990 \ 767$$

$$f_6 = -0.103 \ 883 \ 0383$$

$$g_6 = -3.030 \ 852 \ 910$$

$$\text{for } .5 \text{ MeV} \leq E \leq 2.45 \text{ MeV},$$

$$\left(\frac{\mu_{en}}{\rho} \right)_{air} = \exp \left(\frac{h_6}{\ln E + k_6} + l_6 \ln E + m_6 \right) \quad (13-G)$$

$$\text{and } h_6 = 1781.994 \ 330$$

$$k_6 = -24.226 \ 319 \ 540$$

$$l_6 = 2.866 \ 717 \ 707$$

$$m_6 = 69.980 \ 580 \ 070$$

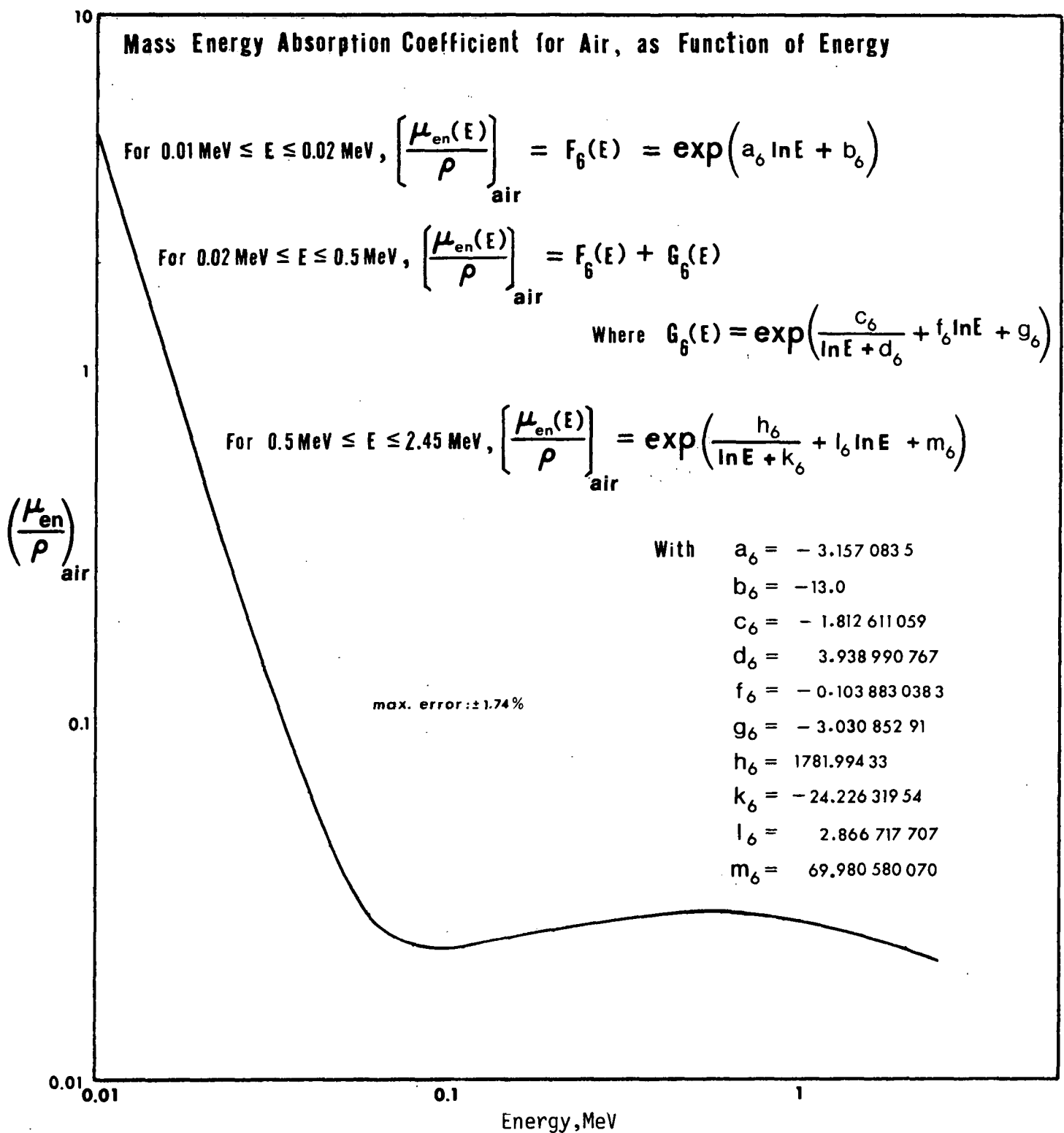


Figure 4-G. Mass energy-absorption coefficient for air, as function of energy.

The values used in curve-fitting the 2nd order exponential integral as function of the argument were taken from the Handbook of Mathematical Functions AMS 55, National Bureau of Standards (1964).

E₂, 2nd Order Exponential Integral, as function of the argument x (Figure 5-G):

for $0 \leq x \leq 0.5$,

$$E_2(x) = \exp\left(\frac{a_7}{x + b_7} + c_7\right) + x \ln x \quad (14-G)$$

where $a_7 = 0.666\ 274\ 740\ 5$

$b_7 = -1.200\ 944\ 510$

$c_7 = 0.554\ 709\ 010\ 2$

for $0.5 \leq x \leq 100.0$

$$\text{and } E_2(x) = \frac{1.0 + \exp\left(\frac{d_7}{\ln x + f_7} + g_7 \ln x + h_7\right)}{(2 + x)e^x} \quad (15-G)$$

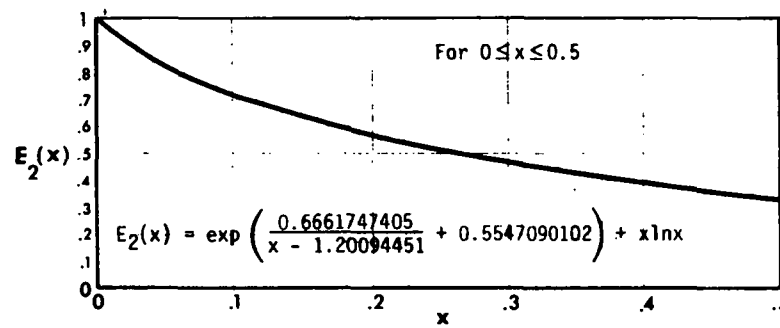
where $d_7 = -282.378\ 704\ 2$

$f_7 = 10.976\ 502\ 83$

$g_7 = -3.179\ 407\ 102$

$h_7 = 24.195\ 713\ 71$

The maximum error observed in this curve-fit was approximately 0.5%.



For $0 \geq x \geq 0.5$

$$E_2(x) = \exp\left(\frac{0.6661747405}{x - 1.20094451} + 0.5547090102\right) + x \cdot \ln x$$

For $x \geq 0.5$

$$E_2(x) = \frac{1 + \exp\left(\frac{-282.3787042}{\ln x + 10.97650283} - 3.179407102 \cdot \ln x + 24.19571371\right)}{(2 + x) e^x}$$

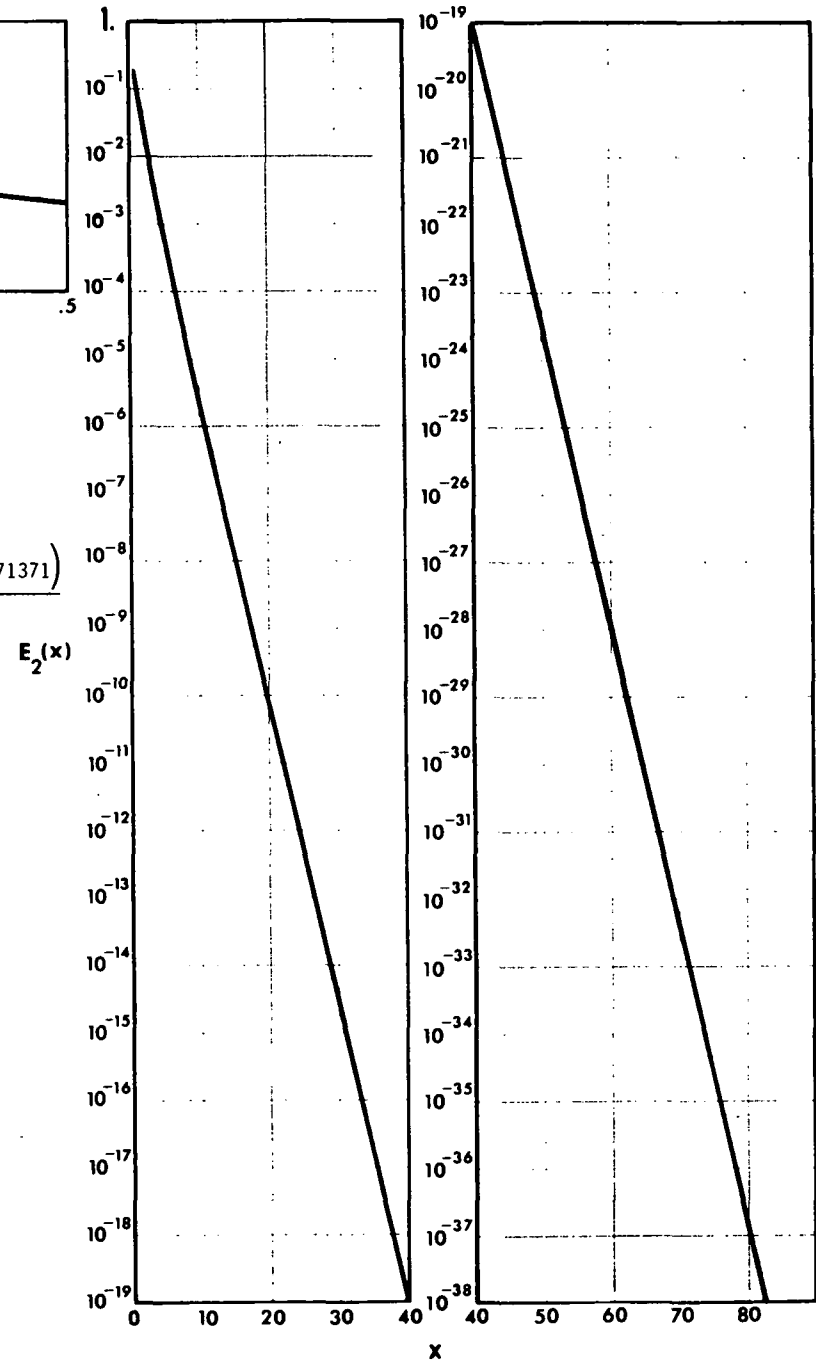


Figure 5-G. Graphical representation of the Second Order Exponential Integral E_2 , as a function of the generalized argument x , obtained on the basis of values from the Handbook of Mathematical Functions AMS 55, Natl. Bureau of Standards (1964). The curve-fitting expressions, by the present author, approximate these values with a maximum observed error of about 0.5% ($\frac{1}{2}\%$).

Appendix H

Computer Implementation

One of the main objectives of the present report is to implement a method for determining exposure rates over uranium bearing soils that not only would be fairly reliable and well founded, but also be reasonably simple to apply. An extreme case involving the use of a programmable desk calculator has been envisioned. This would require partitioning the energy spectrum into several ranges, in accordance with the range limits set for the various curve-fitting equations. The minimum number of ranges would thus be roughly a half-dozen, with a maximum depending on the values of the argument for the second order exponential integral E , Equations (14-G) and (15-G). The pertinent equations would then be applied to each of the energies within a given range, exposures summed, and the calculator reprogrammed for the next range.

Treating 282 gamma energies by the process described above is likely to be tedious and time consuming. An alternate approach was followed by the present author, involving the use of a computer. However, to test ease of application, software development was abrogated in favor of implementation through the ISIS program on a CDC 6400 computer. ISIS (1975) is an interactive statistical package permitting the creation and manipulation of data files through simple commands following the conventions of FORTRAN EXTENDED. New files may be generated from previously created files and stored by the computer. Naturally, no user commands are "stored" beyond the time at which a new file has been created, i.e., no permanent new software is maintained by ISIS.

A basic example of the operational scheme is provided by Figure 1-H, depicting the process whereby effects of varying thicknesses of the uranium bearing soil slab on exposure rates are determined. As initial input, the two files "BELOHAF" and "OVERHAF"* were created by using the ISIS "utility" TYPDAT (TYPE DATA), each containing energies E_i and the corresponding source terms $S_V(E_i)$ for $E < 0.5$ MeV and $E > 0.5$ MeV, from Tables 1-D and 2-D, respectively, and stored in memory. Subsequently, two other files, "BERGERS" and "TAYLORS", were generated through "utility" TRADAT (TRANSform DATA), listing buildup coefficients, attenuation parameters, etc. for each of the 105 and 177 energies in files "BELOHAF" and "OVERHAF", respectively. These two new files were also stored.** Since the buildup coefficient in file "BERGERS" includes an extrapolation of unverified validity for $E < 0.255$ MeV, and Berger's coefficients are range dependent, no further use was made of this file in the present case (see Table 2-A, Equations (6-F), (7-F) and accompanying discussions). File "TAYLORS", however, was transformed repeatedly with TRADAT, using specific values of "t" (uranium bearing soil slab thickness) to create successive files "XPOS1", "XPOS2", etc., containing "fluxes" and exposure rates for each energy E_i in each of the given cases $t = 1$ cm, $t = 2$ cm, etc. Again, the various "XPOS..." files were stored. Average exposure rates were obtained with ISIS utility MULDES (MULTivariate DESCRIPTION) applied to each "XPOS..." file, and multiplied by "177" to determine the total exposure rate $\dot{X}(t)$ for each specified t.

* ISIS data file names are restricted to seven alphabetic characters.

** "Storing" a file implies "making a file permanent", without curtailing the user's facility for altering copies of this permanent file in the process of generating new files.

Note that the several $\dot{X}(t)$ values are given in terms of R/sec per pCi/cm³ necessitating an increase by a factor of 3.6×10 to be expressed in $\mu\text{R/h}$ per pCi/cm³, and multiplication by 1.6 g/cm³ (soil density) to produce values in $\mu\text{R/hr}$ per pCi/g.

Four separate calculations were carried out using this and similar schemes. A brief summary of Tables and equations relevant to each calculation is given below.

Calculation 1) Maximum exposure rates at the ground surface.

This calculation was performed assuming a uranium-bearing soil slab of infinite thickness without overburden, employing the files and equations referenced below.

For $E < 0.5$ MeV:

Table 1-D (File "BELOHAF"), 105 energies and source terms,
Equations (5-F), (6-F), (7-F) for "Berger's effective buildup factor for 'worst case conditions'",
Equations (3-G), (6-G), (7-G) for the linear attenuation coefficient of soil,
Equations (11-G), (12-G) for the mass energy absorption coefficient of air,
Equation (40-C) for "flux",
Equation (1-C) for exposure rate (File "LODOSEM" with 105 energies and exposure rates).

For $E > 0.5$ MeV:

Table 2-D (File "OVERHAF"), 177 energies and source terms,
Equations (1-F), (2-F), (3-F) for Taylor's buildup coefficients,

Equations (3-G), (7-G) for the linear attenuation coefficient of soil,
Equation (13-G) for the mass energy absorption coefficient of air,
Equation (16-C) for "flux",
Equation (1-C) for exposure rate (File "HIDOSEM" with 177 energies and exposure rates).

Equation (46-C) for summation of exposure rates both for $E < 0.5$ MeV and $E > 0.5$ MeV.

Calculation 2) Maximum exposure rates at one meter above ground surface.

This calculation reduces the exposure rates due to each of the 282 energies in 1) corresponding to the effects of air attenuation.

For $E < 0.5$ MeV:

File "LODOSEM", with 105 energies and exposure rates,
Equations (5-G), (8-G), (9-G) for linear attenuation coefficient of air,
Equations (14-G), (15-G) for 2nd order exponential integral values, modifying factor,
Equation (47-C) for summation of exposure rates (1st term).

For $E > 0.5$ MeV:

File "HIDOSEM", with 177 energies and exposure rates,
Equations (5-G), (9-G), (10-G) for linear attenuation coefficient of air,
Equations (14-G), (15-G) for 2nd order exponential integral values, modifying factor,
Equation (47-C) for summation of exposure rates (2nd term)

Equation (47-C) for summation of exposure rates (1st and 2nd term)

Calculation 3) Dependence of exposure rate on thickness of uranium bearing soil slab.

This calculation determines the effect of varying the thickness "t" of a uranium bearing soil slab without cover material on exposure rates due to gamma energies higher than 0.5 MeV (85% of total energy emitted).

Table 2-D (File "OVERHAF"), 177 energies and source terms,
Equations (1-F), (2-F), (3-F) for Taylor's buildup coefficients,
Equations (3-G), (7-G) for the linear attenuation coefficient of soil.
Equations (14-G), (15-G) with a specific value of t, for 2nd order exponential values,
Equation (15-C) for flux,
Equation (1-C) for exposure rate
Equation (46-C), 2nd term, for summation of monoenergetic exposure rates resultant from a slab of thickness "t".

The process is then repeated for the next chosen value of t, etc.

Calculation 4) Dependence of exposure rate on depth of cover slab.

This calculation determines the effect of varying the depth "d" of overburden material covering an infinitely thick uranium bearing soil slab on exposure rates due to energies greater than 0.5 MeV.

The tables and equations of 3) are used in 4) with the sole exception of Equation (15-C) for "flux", here replaced by Equation (17-C), "d" becoming the new input variable.

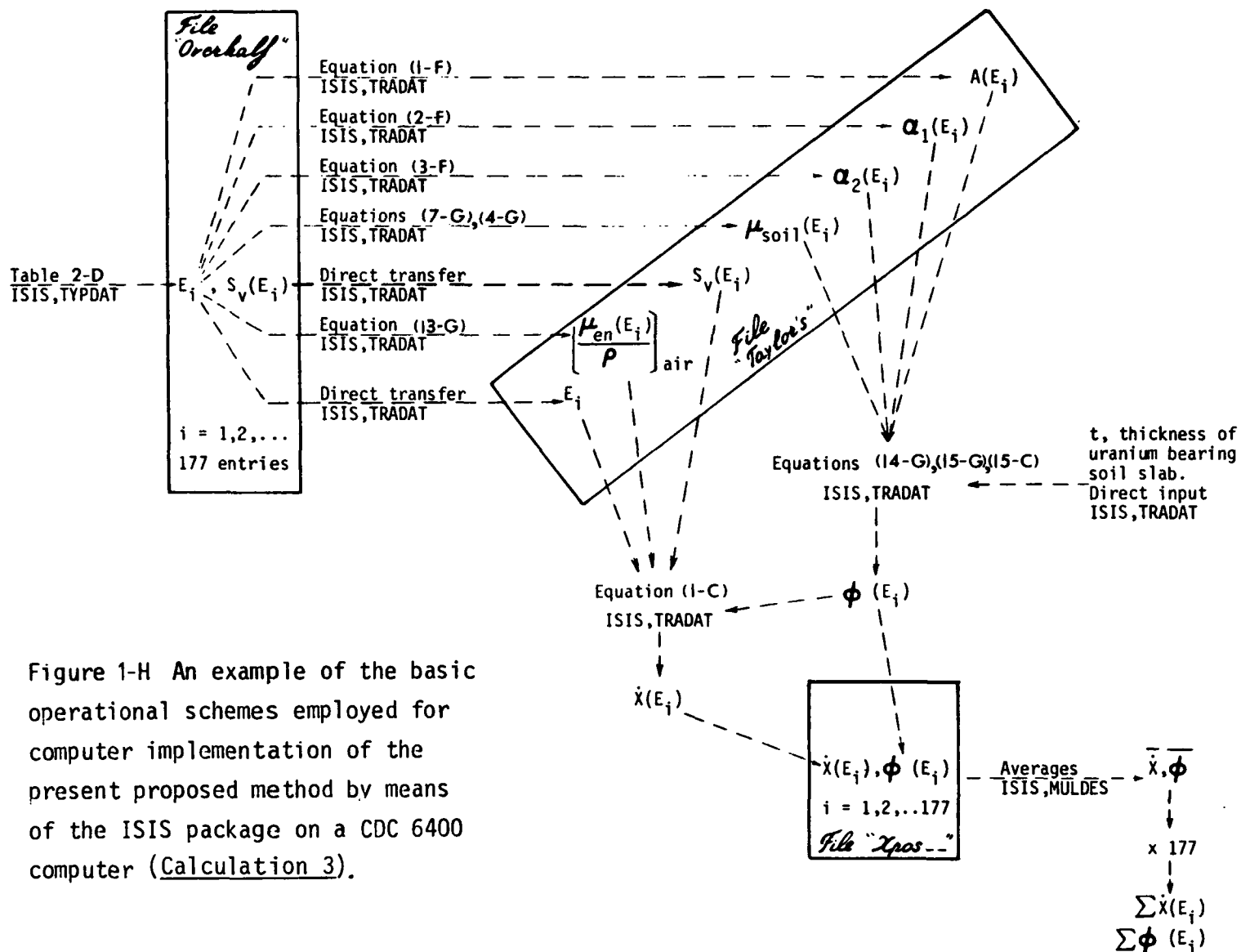


Figure 1-H An example of the basic operational schemes employed for computer implementation of the present proposed method by means of the ISIS package on a CDC 6400 computer (Calculation 3).

APPENDIX I

Sample Calculations for a Monoenergetic Case

Application of Basic Computational Scheme to ^{40}K uniformly distributed in soil with infinite half-space geometry:

$$\begin{array}{lcl}
 \text{Basis: } 1 \text{ pCi/cm}^3 & & E = 1.464 \text{ MeV} \\
 1 \text{ pCi/cm}^3 = > \frac{3.7 \times 10^{-2} \text{ decays}}{\text{cm}^3 \cdot \text{second}} & \left. \vphantom{\begin{array}{l} 1 \text{ pCi/cm}^3 \\ \text{Intensity} \end{array}} \right\} & S_V(E) = 3.959 \times 10^{-3} \frac{\gamma' s}{\text{cm}^3 \cdot \text{s}} \\
 \text{Intensity} = 10.7\% = > \frac{.107 \gamma' s}{\text{Decay}} & &
 \end{array}$$

TAYLOR'S BUILDUP FACTOR COEFFICIENTS FOR $E = 1.464 \text{ MeV}$

From Equation (1-F) $A = 14.576 \ 250 \ 06$

From Equation (2-F) $\alpha_1 = -0.069 \ 778 \ 860 \ 58$

From Equation (3-F) $\alpha_2 = 0.003 \ 288 \ 967 \ 120$

SOIL ATTENUATION COEFFICIENT FOR $E = 1.464 \text{ MeV}$

From Equation (7-G) $(\mu/\rho)_{\text{H}_2\text{O}} = 0.058 \ 688 \ 605 \ 16 \text{ cm}^2/\text{g}$

From Equation (4-G) $\mu_{\text{soil}} = 0.093 \ 901 \ 768 \ 26 \text{ cm}^{-1}$

GROUND SURFACE FLUX FOR $E = 1.464 \text{ MeV}$

From Equation (16-C) $\phi = 4.506 \ 843 \ 598 \times 10^{-2} \frac{\gamma' s}{\text{cm}^2 \cdot \text{s}}$

AIR MASS - ENERGY ABSORPTION COEFFICIENT FOR $E = 1.464 \text{ MeV}$

From Equation (13-G) $(\mu_{\text{en}}/\rho)_{\text{air}} = 2.576 \ 712 \ 795 \times 10^{-2} \text{ cm}^2/\text{g}$

EXPOSURE RATE PER pCi/g AT GROUND SURFACE FOR E = 1.464 MeV

From Equation (1-C) $\dot{X}_S = 3.101\ 701\ 261 \times 10^{-11}$ R/S per pCi/cm³

Conversion $\dot{X}_S = 1.786\ 579\ 926 \times 10^{-1}$ μ R/h per pCi/g

AIR ATTENUATION COEFFICIENTS FOR E = 1.464 MeV

From Equations (9-G),(10-G) $(\mu/\rho)_{air} = 5.244\ 559\ 536 \times 10^{-2}$ cm²/g

From Equation (5-G) $\mu_{air} = 6.781\ 215\ 480 \times 10^{-5}$ cm⁻¹

ARGUMENT FOR 2nd ORDER EXPONENTIAL INTEGRAL

$$\mu_{air} \times 100\text{ cm} = 6.781\ 215\ 480 \times 10^{-3}$$

VALUE OF 2nd ORDER EXPONENTIAL INTEGRAL = Modifying Factor for \dot{X}_{1m}

From Equation (14-G) $E_2[\mu_{air} \times 100\text{ cm}] = 0.962\ 992\ 296\ 8$

Exposure Rate at 1 meter Above Ground Level For E = 1.464 MeV

$$\dot{X}_{1m} = 1.786\ 579\ 926 \times 10^{-1} \mu\text{R/h per pCi/g} \times E_2[\mu_{air} \times 100\text{ cm}]$$

$$= 1.720\ 462\ 706 \times 10^{-1} \mu\text{R/h per pCi/g}$$

$$= 0.172 \mu\text{R/h per pCi/g}$$

Beck (1972) result: $\dot{X}_{1m} = 0.179 \mu\text{R/h per pCi/g}$

Replacing the buildup factor coefficients and mass-attenuation parameters for water [Equations (1-F) through (3-F) and (7-G)] with those for aluminum results in $\dot{X}_{1m} = 0.189 \mu\text{R/h per pCi/g}$

The curve-fitting equations for the relevant aluminum coefficients appear in Figure 1-I, including that for the buildup parameters in compound form [see bracketted "buildup term" in Equation (16-C)].

$$(\mu/\rho)_{Al} = 0.0613 \exp(-0.504855762 \ln E)$$

at $E = 1.464$ MeV, $(\mu/\rho)_{Al} = 0.0505692 \text{ cm}^2/\text{g}$

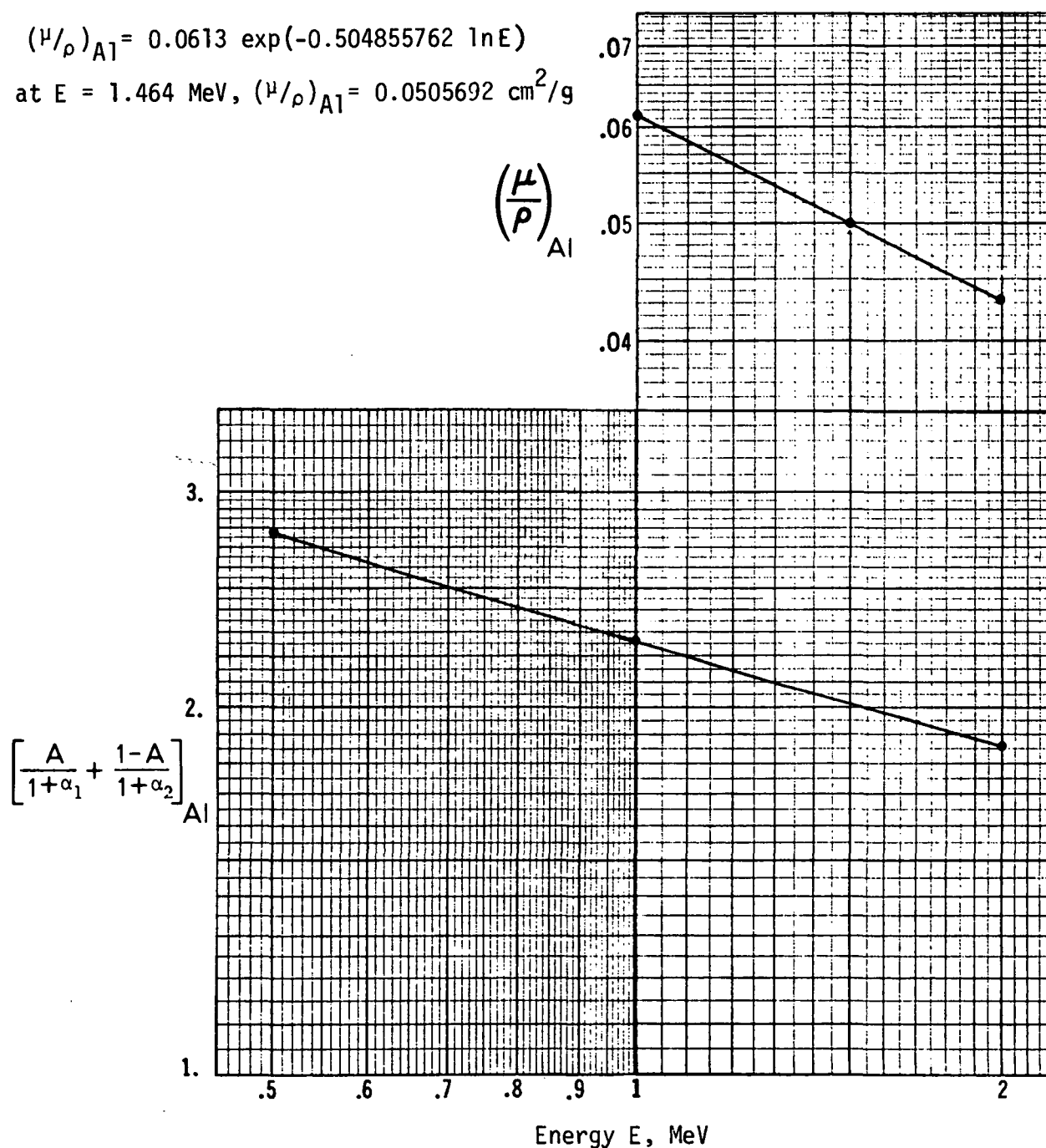


Figure 1-I. Mass-attenuation coefficient and buildup "term" for aluminum, for the energy range $1.0 \text{ MeV} \leq E \leq 2.0 \text{ MeV}$ and $0.5 \text{ MeV} \leq E \leq 2.0 \text{ MeV}$, respectively, and corresponding curve-fitting equations.

$$\left[\frac{A}{1+\alpha_1} + \frac{1-A}{1+\alpha_2} \right]_{Al} = 0.01084064452 \exp \left[\frac{98.69809348}{18.49056767 + \ln E} \right]$$

at $E = 1.464$ MeV, $\left[\frac{A}{1+\alpha_1} + \frac{1-A}{1+\alpha_2} \right]_{Al} = 2.02483558$

The exposure rate calculated using aluminum mass-attenuation and buildup factor coefficients is clearly more conservative - roughly 10 % greater- than the result based on the corresponding water parameters, at 1.464 MeV. However, the latter result shows better agreement with the value published by Beck in 1972. This suggests that aluminum is not necessarily a better analog for "soil" than water, in applications of the present method.

$$(\mu/\rho)_{Al} = 0.0613 \exp(-0.504855762 \ln E)$$

at $E = 1.464$ MeV, $(\mu/\rho)_{Al} = 0.0505692 \text{ cm}^2/\text{g}$

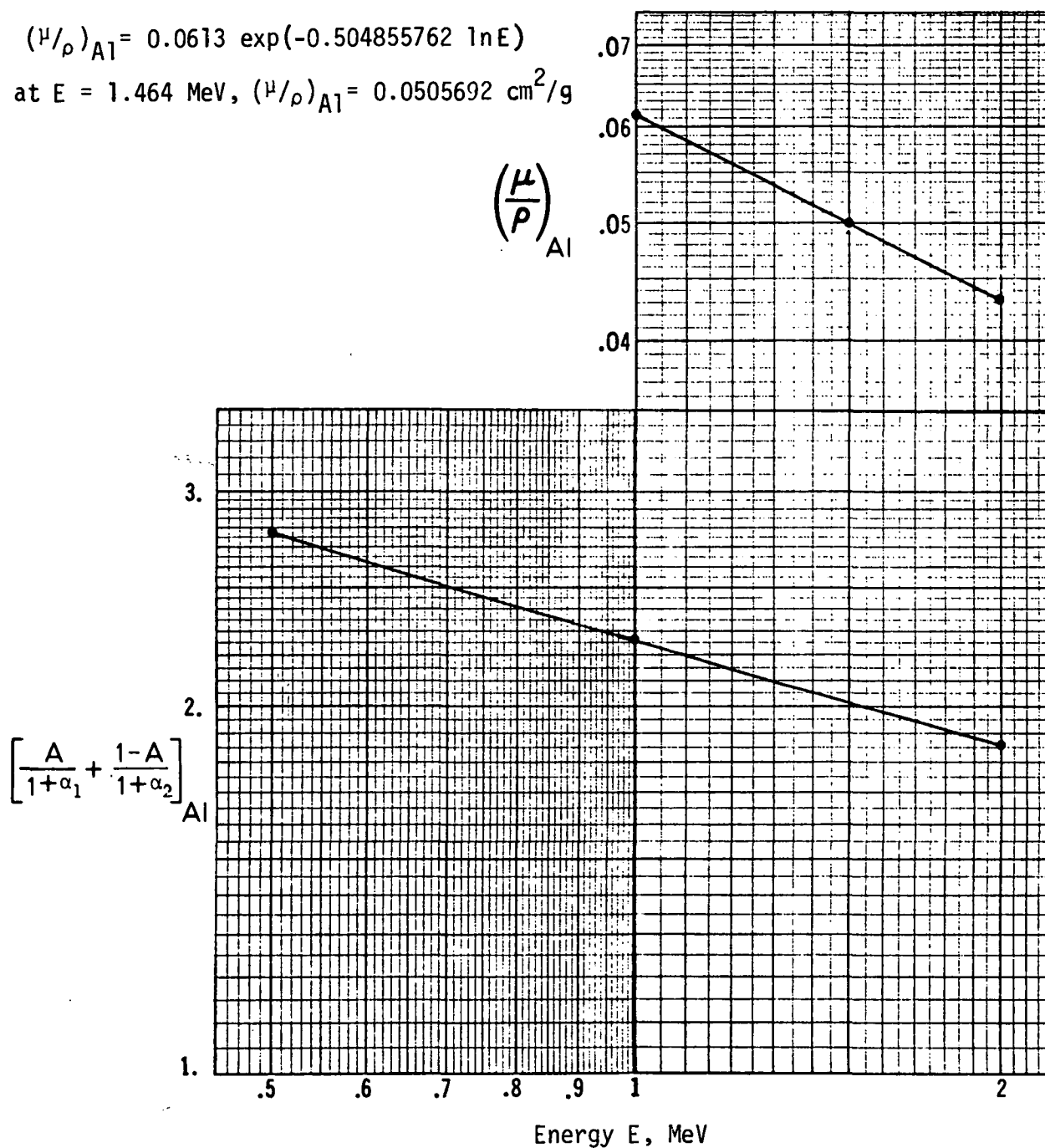


Figure 1-I. Mass-attenuation coefficient and buildup "term" for aluminum, for the energy range $1.0 \text{ MeV} \leq E \leq 2.0 \text{ MeV}$ and $0.5 \text{ MeV} \leq E \leq 2.0 \text{ MeV}$, respectively, and corresponding curve-fitting equations.

$$\left[\frac{A}{1+\alpha_1} + \frac{1-A}{1+\alpha_2} \right]_{Al} = 0.01084064452 \exp \left[\frac{98.69809348}{18.49056767 + \ln E} \right]$$

at $E = 1.464$ MeV, $\left[\frac{A}{1+\alpha_1} + \frac{1-A}{1+\alpha_2} \right]_{Al} = 2.02483558$

The exposure rate calculated using aluminum mass-attenuation and buildup factor coefficients is clearly more conservative - roughly 10 % greater- than the result based on the corresponding water parameters, at 1.464 MeV. However, the latter result shows better agreement with the value published by Beck in 1972. This suggests that aluminum is not necessarily a better analog for "soil" than water, in applications of the present method.

Appendix J

Comments on Curve-Fitting Exposure Rate Models

None of the Equations (25), (26), (28) and (30) has been obtained, independently, from theoretical considerations, but from curve-fitting techniques ultimately devolving to an iterative process for determining coefficients of optimum fit. Fortuitously, these coefficients were found to be simple powers of the natural logarithm base "e", leading to convenient, concise expressions with a misleading resemblance to analytically derived functions. Nevertheless, the interrelationship of these "pseudo-analytical" expressions may be shown to be consistent with the theoretical bases of the present work.

The obvious contribution of Equations (26) and (28) to the model of Equation (30) may be reviewed in summarizing (30) as the product of two ratios, each of them expressed as an independent function of a single variable, either uranium-bearing soil slab thickness "t" or depth of overburden "d". Since both variables are totally independent of each other, the model represents each ratio to be independently valid, a validity that extends to their product.

Although the effects of uranium-bearing soil slabs of varying thickness, in Equation (28), are conceptually independent from the consequences of varying depth of overburden, in Equation (26), the two equations embody similarities of form that indicate an interconnection. This interconnection may be supported on analytical grounds. Comparisons of Equations (15-C), (16-C) and (17-C), implemented by Equation (1-C) and the treatment of Appendix K ultimately yield, for the special cases $t = d$, the formal relationship

$$\frac{\dot{X}(t)}{\dot{X}(\infty)} = 1 - \frac{\dot{X}(d)}{\dot{X}(0)}, \text{ for values } t = d \quad (1-J)$$

$\dot{X}(\infty) = \dot{X}(0)$ as defined for Tables 2 and 3.

The applicability of Equation (1-J) is restricted by the requirements that the uranium-bearing soil and overburden have the same attenuation coefficient and that the same building factor be applicable to both materials. These conditions are fulfilled through Assumption (10) and Equation (4-G) in the present study, and lead to results supporting the validity of (1-J), as comparison of Tables 2 and 3 may verify.

The relationship in Equation (1-J) suggests that any expression describing accurately the behavior of $\dot{X}(d)/\dot{X}(0)$ could be used to generate a reliable model of $\dot{X}(t)/\dot{X}(\infty)$, and vice versa, with little more than a change of independent variable. Such procedure was applied to Equation (26) to generate Equation (28).

In addition to being analytically useful, Equation (1-J) provides a valuable criteria of accuracy in "curve-fitting", by implying that any model successfully replicating the values of Table 3 must also, when transformed by (1-J), closely reproduce the value of Table 2 to be considered valid. This amounts to requiring that one-curve fitting equation satisfy two sets of tabulated values, independently calculated. This criterion is met by Equation (26), and therefore by Equation (28) as well, enhancing the credibility of

these equations* plus, by implication, that of (30).

The origins of Equations (30) and (28) may be traced beyond Equation (26), which has sources of its own. These are to be found in Equations (24) and (25), the former being primarily a definition of "depth-dependent relaxation length" $L(d)$ and necessary introduction to the latter, which applies this concept to summarize the results of Table 3 as a curve-fitting equation.

The logarithmic form of the resultant expression for $L(d)$, in (25), was suggested directly by Figure 2, a continuous graph based on Table 3 values of "relaxation length".

The accuracy of Equations (30), (28) and (26) may be seen to depend on an accurate fit of $L(d)$, such as, presumably, that of Equation (25). In that regard, the graph in Figure 2 invites tempting simplifications of the form $L(d) = a + b \ln(d/d_0)$ which must be discarded as undesirable. The various

*Author's note. It does not necessarily follow that any curve-fitting equation reproducing the values of one of the Tables 2, 3 will lead to a successful model for the other. Applying the observation that powers of "e" appeared to be particularly useful in obtaining such equations, the present author tested an alternative fit $\dot{\chi}(t)/\dot{\chi}(\infty) = \tanh [e^{-(e-1)}(t/t_0)e^{-2}]$ to the values of Table 2, with a maximum error at any point of 1.6%. Unfortunately, the corresponding expression $\dot{\chi}(d)/\dot{\chi}(0) = 1 - \tanh [e^{-(e-1)}(d/d_0)e^{-2}]$ obtained by applying (1-J), yielded errors of up to 30%, at $d = 100$ cm.

shortcomings of this formulation may be examined quantitatively by comparing Equation (25) with an example of the simpler form, also by the present author,

$$L(d) = 5 + 1.23 \ln(d/d_0) , \text{ in cm} \quad (2-J)$$

The simplified formulation implies negative values of $L(d)$ for small values of d , which makes it conceptually unattractive. It also increases curve-fitting error in the range $1 \text{ cm} \leq d \leq 100 \text{ cm}$, as compared to the results of (25). This increase is inherent in the simpler formulation, corresponding to a semi-logarithmic 2-point fit. By contrast, Equation (25) requires a 3-point fit.

Of greater significance are the consequences of the simplified formulation for the region $d > 100 \text{ cm}$. It was pointed out, elsewhere in this report, that computer round off precluded obtaining reliable results for t or d greater than 100 cm. Whereas for $\dot{X}(t)/\dot{X}(\infty)$ this is largely inconsequential, such handicap in determining $\dot{X}(d)/\dot{X}(0)$ for $d > 100 \text{ cm}$ is of greater importance. Consequently, the need for accuracy in curve-fitting equations for $L(d)$ and $\dot{X}(d)/\dot{X}(0)$ in the region $d \leq 100 \text{ cm}$ increases proportionately to the degree of generality such expressions may be required to have; specifically for applying them to the region $d > 100 \text{ cm}$.

Any simple equation of the form $L(d) = a + b \ln(d/d_0)$ providing a reasonable fit to the values in Table 3 may be expected to underestimate both $L(d)$ and $\dot{X}(d)/\dot{X}(0)$ for $d > 100 \text{ cm}$. This is due to the fact that the rate of increase of $L(d)$ with respect to $\ln(d/d_0)$ in the above expression is a constant, "b", whereas the graph in Figure 2 shows a slowly but steadily increasing slope.

The consequences of the simpler formulation may be tested by comparing $L(d)$ and $\dot{X}(d)/\dot{X}(0)$ resultant from Equations (25) and (26) with the corresponding values produced by (2-J). The latter generates values which are consistently and progressively lower than those produced by (25) and (26) as d increases past $d = 100$ cm. This indicates that (25) and (26) are more conservative in gaging the effectiveness of the cover slab in reducing exposures, i.e., they are less apt to overestimate the exposure-reducing capabilities of overburden, for $d > 100$ cm.

Having defended the advantages of the proposed models against tempting but short-sighted approximations, it becomes necessary to address the more fundamental problem of a "depth dependent relaxation length", $L(d)$. Without this concept, Equation (25) and, by implication, Equations (26) and (30), lack foundation.

The analytical bases of the present technique may be advanced in support of this concept. On the other hand, the more traditional notion of a relaxation constant appears to be supported by empirical data, in treating which, however, the depth-dependent behavior of the slowly-varying function $L(d)$ may be all too easily neglected. Note, for instance, that Equation (25) predicts a change in L of some 10 mm between depths of 1 foot and 2 feet, of another 5 mm between 2 feet and 3 feet, etc. Such differences may be easily attributed to other factors, or ignored altogether in developing simpler models for which a "safety margin" would be eminently desirable.

A constant, depth-independent L may provide a substantial "safety factor", if used judiciously, through underestimation of the exposure-reducing capabilities

of overburden. Such judicious use entails setting limits on the thickness of the cover slab for which a given constant L may be used. Exceeding these limits will produce the opposite effect, i.e., the exposure rates will be underestimated.

With the aid of Equation (25), specific limits may be determined for each given L . In the author's experience, proposed values of L vary between 10 and 14 cm. Replacing the depth-dependent $L(d)$ in (25) with a generalized constant L representing these values, and solving for d produces

$$d_L = \exp[Le^{-1/4}]/2e^3 - 1/e \quad (3-J)$$

where L = generalized constant relaxation length

= 10, 11, 12, 13, 14 cm

d_L = limit depth, in cm, which must not be exceeded if
a constant L is used in Equations (26), (30)

The results are summarized below.

Table 1-J. Thickness of the Overburden Slab Which Must Not Be Exceeded
With the Use of a Constant L

Constant L (cm)	Depth limit d_L which must not be exceeded if equation $\dot{X}(d)/\dot{X}(0) = \exp(-d/L)$ is to produce conservative results i.e., overestimation of $\dot{X}(d)/\dot{X}(0)$, thus a "safety factor".
10	59.7 cm or approximately 2 feet
11	130 cm or approximately 4 feet
12	285 cm or approximately 9 feet
13	620 cm or approximately 20 feet
14	1350 cm or approximately 44 feet

Appendix K

Interrelationship of Exposure Ratios

The relationship of $\dot{X}(t)/\dot{X}(\infty)$ in Equation (28) to $\dot{X}(d)/\dot{X}(o)$ in Equation (26) is based on the following analysis:

The exposure rate to gammas of energy E from sources distributed throughout a uranium-bearing slab of thickness t may be determined by combining Equations (15-C) and (1-C),

$$\dot{X}(E,t) = G(E) \left\{ A_1(E)[1-E_2(t,E,\alpha_{1E})] + A_2(E)[1-E_2(t,E,\alpha_{2E})] \right\} \quad (1-K)$$

$$\text{where } G(E) = F \dot{X} E \left[\frac{\mu_{en}(E)}{\rho} \right]_{\text{air}}$$

$$A_1(E) = \frac{Sv(E) A(E)}{2\mu(E)[1+\alpha_1(E)]}$$

$$A_2(E) = \frac{Sv(E)[1-A(E)]}{2\mu(E)[1+\alpha_2(E)]}$$

$$E_2(t,E,\alpha_{1E}) = E_2 \left\{ \mu(E)t[1+\alpha_1(E)] \right\}$$

$$E_2(t,E,\alpha_{2E}) = E_2 \left\{ \mu(E)t[1+\alpha_2(E)] \right\}$$

$$\text{and } \mu = \mu_t = \mu_c$$

The expression (1-K) may be rewritten, for convenience, as

$$\dot{X}(E,t) = G(E)[A_1(E) + A_2(E)] - G(E)[A_1(E)E_2(t,E,\alpha_{1E}) + A_2(E)E_2(t,E,\alpha_{2E})] \quad (2-K)$$

For the special case $t=\infty$, this becomes

$$\dot{X}(E,\infty) = G(E)[A_1(E) + A_2(E)] \quad (3-K)$$

Dividing (2-K) by (3-K) results in the following ratio

$$\frac{\dot{X}(E,t)}{\dot{X}(E,\infty)} = 1 - \frac{A_1(E)E_2(t,E,\alpha_{1E}) + A_2(E)E_2(t,E,\alpha_{2E})}{A_1(E) + A_2(E)} \quad (4-K)$$

A similar process, applied to Equations (17-C), (1-C), produces

$$\frac{\dot{X}(E,d)}{\dot{X}(E,0)} = \frac{A_1(E)E_2(d,E,\alpha_1E) + A_2(E)E_2(d,E,\alpha_2E)}{A_1(E) + A_2(E)} \quad (5-K)$$

$$\text{where } E_2(d,E,\alpha_1E) = E_2 \left\{ \mu(E)d[1+\alpha_1(E)] \right\}$$

$$E_2(e,E,\alpha_2E) = E_2 \left\{ \mu(E)d[1+\alpha_2(E)] \right\}$$

A comparison of (5-K) and 4-K) indicates that, for the special cases of $t = d$,

$$\frac{\dot{X}(E,t)}{\dot{X}(E,\infty)} = 1 - \frac{\dot{X}(E,d)}{\dot{X}(E,0)} \quad (6-K)$$

In keeping to the simplified notation used throughout the report, each of the ratios of Equation (6-K) is expressed in terms of either of two geometric variables, t or d , while omitting any mention of the second geometric parameter, which is held constant. A more complete rendition of the dependence of exposure rate on energy and geometric variables would be

$\dot{X}(E,t,d)$ = exposure rate due to gammas of energy E ,
from a uranium-bearing slab of thickness t ,
covered with overburden to a depth d .

On that basis, the components of (6-K) could be rewritten as follows

$$\begin{aligned} \text{a)} \quad & \dot{X}(E,t) \equiv \dot{X}(E,t,0) \left\{ \begin{array}{l} \text{i.e. cover thickness } d = 0, \\ \text{b)} \quad \dot{X}(E,\infty) \equiv \dot{X}(E,\infty,0) \end{array} \right\} \text{ in both cases} \\ \text{and} \quad & \\ \text{c)} \quad & \dot{X}(E,d) \equiv \dot{X}(E,\infty,d) \left\{ \begin{array}{l} \text{i.e. thickness of uranium-bearing} \\ \text{d)} \quad \dot{X}(E,0) \equiv \dot{X}(E,\infty,0) \end{array} \right\} \text{ slab } t = \infty, \text{ in both cases} \end{aligned} \quad (7-K)$$

A comparison of above identities b) and d) serves to emphasize the fact that the denominators in Equation (6-K) are equal. This permits rewriting (6-K) in the following manner,

$$\dot{X}(E,t) = \dot{X}(E,\infty,0) - \dot{X}(E,d) \quad (8-K)$$

Consequently, a summation of exposure rates over all energies E_i may be indicated as

$$\sum_{i=1}^N \dot{X}(E_i, t) = \sum_{i=1}^N \dot{X}(E_i, \infty, 0) - \sum_{i=1}^N \dot{X}(E_i, d) \quad (9-K)$$

$N = \# \text{ of } \gamma \text{ lines}$

Dividing both sides of (9-K) by the total exposure rate due to gammas of all energies from tailing slab infinitely thick with no cover, $\sum_{i=1}^N \dot{X}(E_i, \infty, 0)$, results in

$$\frac{\sum_{i=1}^N \dot{X}(E_i, t)}{\sum_{i=1}^N \dot{X}(E_i, \infty, 0)} = 1 - \frac{\sum_{i=1}^N \dot{X}(E_i, d)}{\sum_{i=1}^N \dot{X}(E_i, \infty, 0)} \quad (10-K)$$

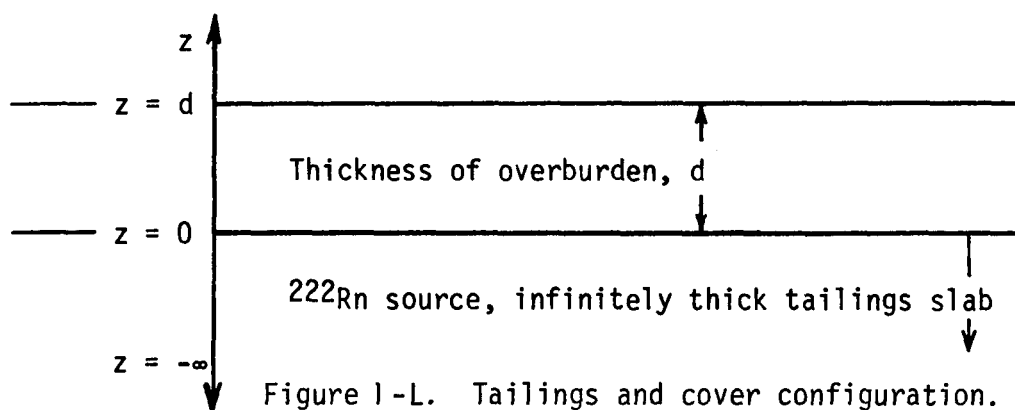
The above expression is exactly equivalent to that of Equation (6-K) which, in simplified notation, is

$$\frac{\dot{X}(t)}{\dot{X}(\infty)} = 1 - \frac{\dot{X}(d)}{\dot{X}(0)}$$

Appendix L

Radon Distribution Through Overburden

Diffusion theory and Fick's law were used to model the ^{222}Rn concentration in an infinitely thick tailings pile covered with a finite thickness d of overburden, both of infinite areal extent, as shown in Figure 1-L.



The fraction of ^{222}Rn which emanates from the source material in the tailings represents a flux which is proportional to the concentration gradient, as per Fick's law

$$J(z) = -D \frac{dC(z)}{dz} \quad (1-L)$$

where $J(z)$ = depth-dependent radon flux, in $\text{pCi}/\text{cm}^2.\text{s}$

$C(z)$ = depth-dependent "free" radon concentration, in pCi/cm^3

D = diffusion coefficient of "free" radon in soil, in cm^2/s

Applying Fick's law to the general diffusion equation produces, at steady state,

$$\frac{d^2C}{dz^2} - \alpha^2 C + S = 0 \quad (2-L)$$

$$\text{where } \alpha^2 = \frac{\lambda_{\text{Rn}}}{D}$$

$$\text{and } S = \frac{C_{\text{Ra}} \lambda_{\text{Rn}} E}{D}$$

$$\text{and } S = \frac{C_{Ra} \lambda_{Rn} E}{D}$$

with λ_{Rn} = ^{222}Rn decay constant, in s^{-1}

C_{Ra} = ^{226}Ra concentrations in tailings, in pCi/g

E = emanating power of ^{222}Rn in tailings, dimensionless

The general solutions of (2-L) for the concentration of ^{222}Rn as function of depth, $C(z)$, are

$$C_t(z) = Ae^{\alpha z} + Be^{-\alpha z} + \frac{S}{\alpha^2}, \text{ for } z \leq 0 \text{ (tailings)} \quad (3-L)$$

$$\text{and } C_c(z) = Ee^{\alpha z} + Fe^{-\alpha z}, \text{ for } z \geq 0 \text{ (cover)} \quad (4-L)$$

Four boundary conditions are required to determine the values of A , B , E and F . They are

B.C.1 $J_t(-\infty) = 0$ At $-\infty$, the concentration of free radon is assumed to be at an absolute maximum, thus $dC(-\infty)/dz = 0$ and $J_t(-\infty) = 0$.

B.C.2 $C_t(0) = C_c(0)$
 B.C.3 $J_t(0) = J_c(0)$ } Both the free radon concentration and flux are continuous at the tailings-cover interface.

B.C.4 $C_c(d) = 0$ The free radon concentration at the cover-atmosphere interface is assumed to be very small, i.e., approaching "zero". In reality, Fick's law does not apply to such interface.

Solving for A , B , E , F :

From B.C.1: $J_t(-\infty) = 0$

$$\text{or } -D \left. \frac{dC_t(z)}{dz} \right|_{z=-\infty} = -D(\alpha A e^{\alpha z} - \alpha B e^{-\alpha z}) \Big|_{z=-\infty} = 0$$

this means that $B = 0$, otherwise J would be infinitely large
thus, $C_t(z) = Ae^{\alpha z} + \frac{S}{\alpha^2}$ for $z \leq 0$ (5-L)

From B.C.4: $C_c(d) = 0$

$$\text{or } Ee^{\alpha d} + Fe^{-\alpha d} = 0$$

$$\text{so, } E = -Fe^{-2\alpha d}$$

$$\text{and } C_c(z) = Fe^{-\alpha d} [e^{\alpha d} - \alpha z - e^{-(\alpha d - \alpha z)}] \text{ for } z \geq 0 \quad (6-L)$$

From B.C.3: $J_t(0) = J_c(0)$

Equating the derivatives of (5-L) and (6-L) at $z = 0$ produces

$$A = -Fe^{-\alpha d}(e^{\alpha d} + e^{-\alpha d})$$

$$\text{thus } C_t(z) = \frac{S}{\alpha^2} - Fe^{-\alpha d}(e^{\alpha d} + e^{-\alpha d}) e^{\alpha z} \text{ for } z \leq 0 \quad (7-L)$$

From B.C.2: $C_t(0) = C_c(0)$

Equating (6-L) and (7-L) at $z = 0$ results in

$$\frac{S}{\alpha^2} - Fe^{-\alpha d}(e^{\alpha d} + e^{-\alpha d}) = Fe^{-\alpha d}(e^{\alpha d} - e^{-\alpha d})$$

$$\text{or } F = \frac{S}{2\alpha^2} \quad (8-L)$$

Inserting (8-L) into (7-L) produces an equation describing the free radon concentration as function of depth in the tailings, i.e., for $z \leq 0$

$$C_t(z) = \frac{S}{\alpha^2} [1 - e^{\alpha(z-d)} \cosh(\alpha d)] \text{ for } z \leq 0 \text{ (tailings)} \quad (9-L)$$

$$\text{and } S = \frac{C_{Ra} \lambda_{Rn} E}{D}$$

with λ_{Rn} = ^{222}Rn decay constant, in s^{-1}

C_{Ra} = ^{226}Ra concentrations in tailings, in pCi/g

E = emanating power of ^{222}Rn in tailings, dimensionless

The general solutions of (2-L) for the concentration of ^{222}Rn as function of depth, $C(z)$, are

$$C_t(z) = Ae^{\alpha z} + Be^{-\alpha z} + \frac{S}{\alpha^2}, \text{ for } z \leq 0 \text{ (tailings)} \quad (3-L)$$

$$\text{and } C_c(z) = Ee^{\alpha z} + Fe^{-\alpha z}, \text{ for } z \geq 0 \text{ (cover)} \quad (4-L)$$

Four boundary conditions are required to determine the values of A, B, E and F. They are

B.C.1 $J_t(-\infty) = 0$ At $-\infty$, the concentration of free radon is assumed to be at an absolute maximum, thus $dC(-\infty)/dz = 0$ and $J_t(-\infty) = 0$.

B.C.2 $C_t(0) = C_c(0)$
 B.C.3 $J_t(0) = J_c(0)$ } Both the free radon concentration and flux are continuous at the tailings-cover interface.

B.C.4 $C_c(d) = 0$ The free radon concentration at the cover-atmosphere interface is assumed to be very small, i.e., approaching "zero". In reality, Fick's law does not apply to such interface.

Solving for A, B, E, F:

From B.C.1: $J_t(-\infty) = 0$

$$\text{or } -D \frac{dC_t(z)}{dz} \Big|_{z=-\infty} = -D(\alpha A e^{\alpha z} - \alpha B e^{-\alpha z}) \Big|_{z=-\infty} = 0$$

this means that $B = 0$, otherwise J would be infinitely large

$$\text{thus, } C_t(z) = Ae^{\alpha z} + \frac{S}{\alpha^2} \text{ for } z \leq 0 \quad (5-L)$$

$$\text{From B.C.4: } C_c(d) = 0$$

$$\text{or } Ee^{\alpha d} + Fe^{-\alpha d} = 0$$

$$\text{so, } E = -Fe^{-2\alpha d}$$

$$\text{and } C_c(z) = Fe^{-\alpha d} [e^{\alpha d - \alpha z} - e^{-(\alpha d - \alpha z)}] \text{ for } z \geq 0 \quad (6-L)$$

$$\text{From B.C.3: } J_t(0) = J_c(0)$$

Equating the derivatives of (5-L) and (6-L) at $z = 0$ produces

$$A = -Fe^{-\alpha d}(e^{\alpha d} + e^{-\alpha d})$$

$$\text{thus } C_t(z) = \frac{S}{\alpha^2} - Fe^{-\alpha d}(e^{\alpha d} + e^{-\alpha d}) e^{\alpha z} \text{ for } z \leq 0 \quad (7-L)$$

$$\text{From B.C.2: } C_t(0) = C_c(0)$$

Equating (6-L) and (7-L) at $z = 0$ results in

$$\frac{S}{\alpha^2} - Fe^{-\alpha d}(e^{\alpha d} + e^{-\alpha d}) = Fe^{-\alpha d}(e^{\alpha d} - e^{-\alpha d})$$

$$\text{or } F = \frac{S}{2\alpha^2} \quad (8-L)$$

Inserting (8-L) into (7-L) produces an equation describing the free radon concentration as function of depth in the tailings, i.e., for $z \leq 0$

$$C_t(z) = \frac{S}{\alpha^2} [1 - e^{\alpha(z-d)} \cosh(\alpha d)] \text{ for } z \leq 0 \text{ (tailings)} \quad (9-L)$$

Appendix M

Effects of Radon Diffusion on Exposure Rates

The effects of radon diffusion through cover material on exposure rates was estimated by numerical integration techniques, employing the models developed in the study and the radon concentration formulas from Appendix L. The method assumes the typical "infinitely thick" tailings slab covered with overburden of depth d to be equivalent to a large number of infinitely thick slabs, occupying simultaneously the same space but with varying radon concentrations and depths of cover. The fundamental concept is partially illustrated in Figure 1-M, for the specific case $d = 100$ cm and $D = 0.02$ cm²/s, and further amplified by the following description.

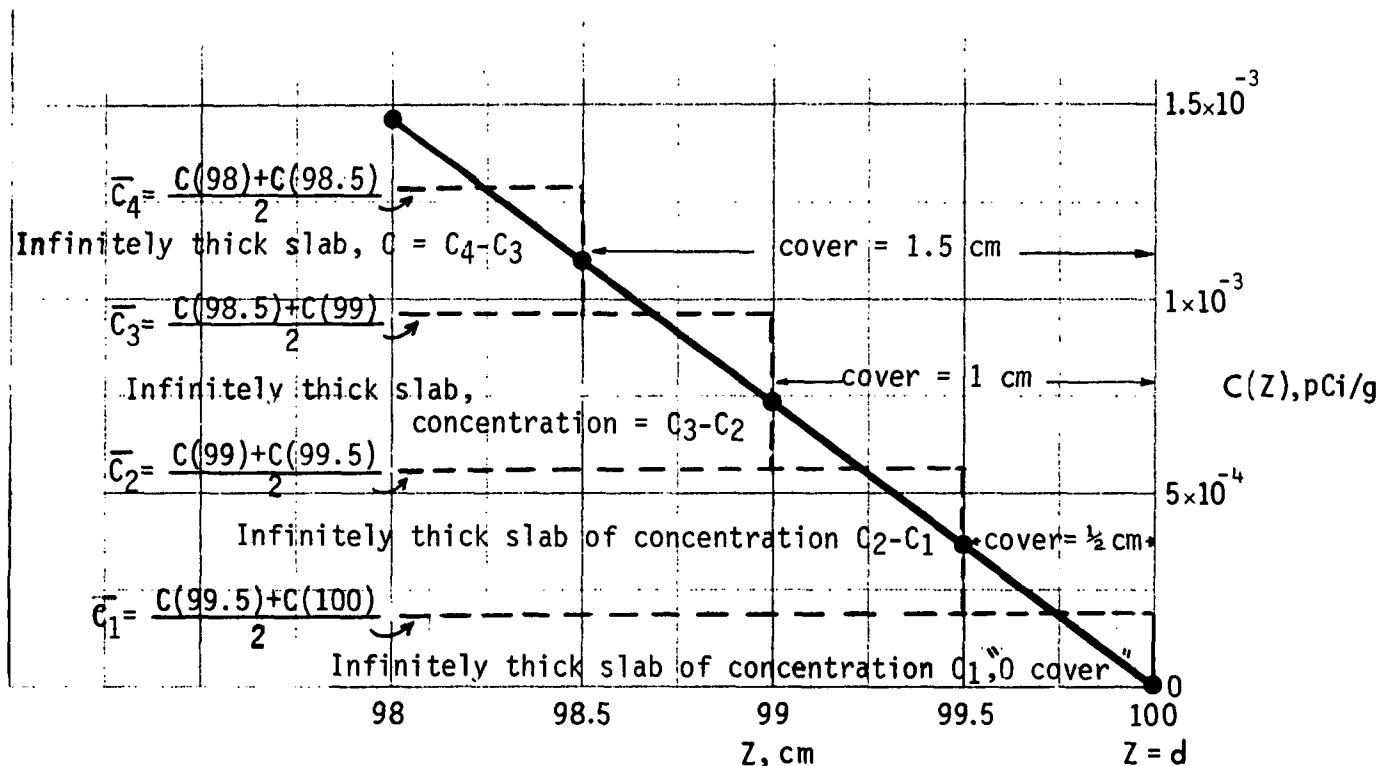


Figure 1 - M. Schematic representation of numerical integration method, applied to the top two cm of a cover of thickness $d = 100$ cm, on top of an infinitely thick tailings slab, with a radon diffusion coefficient of $D = 0.02$ cm²/s, for $E = 0.2$

Having decided on a specific set of values E , d , D , the distribution of radon $C(z)$ in the cover and tailings is determined by Equations (11-L) and (14-L), at regular intervals Δz . The average concentration between two successive points is then calculated by

$$\bar{C}_n = \frac{C_{d-n\Delta z} + C_{d-(n-1)\Delta z}}{2}$$

where $n = 1, 2, 3, \dots$

and $C_{d-n\Delta z}$ = concentration $C(z)$ at location $z = d - n\Delta z$

As n increases, \bar{C}_n increases also, by an amount $\Delta\bar{C}_m = \bar{C}_n - \bar{C}_{n-1}$ (see Figure 1-M), the increment becoming effective at a distance $z_m = d - (n-1)\Delta z$

Setting $m = n$, and adopting the convention that $\bar{C}_0 = 0$, the above may be restated as $\Delta\bar{C}_m$ not being present for all $z > z_m$, appearing as a step function at $z = z_m$, and continuing to exist for all $z < z_m$. This is tantamount to assuming the existence of an infinitely thick slab of concentration $\Delta\bar{C}_m$, with a source-free cover of depth $d - z_m = (n-1)\Delta z$. Such configuration is ideally suited for the calculation of exposure rates through application of Equation (30) to the various slabs of incremental concentration $\Delta\bar{C}_m$ and depth of cover $(n-1)\Delta z$. Adding the increments $\Delta\dot{X}$ resultant from each of these calculations produces the total exposure rate due to an infinitely thick tailings slab with cover d and diffusion coefficient D .

Repeating this procedure for various d and D values leads to the exposure rates depicted in Figure 2-M, all for $E = 0.2$.

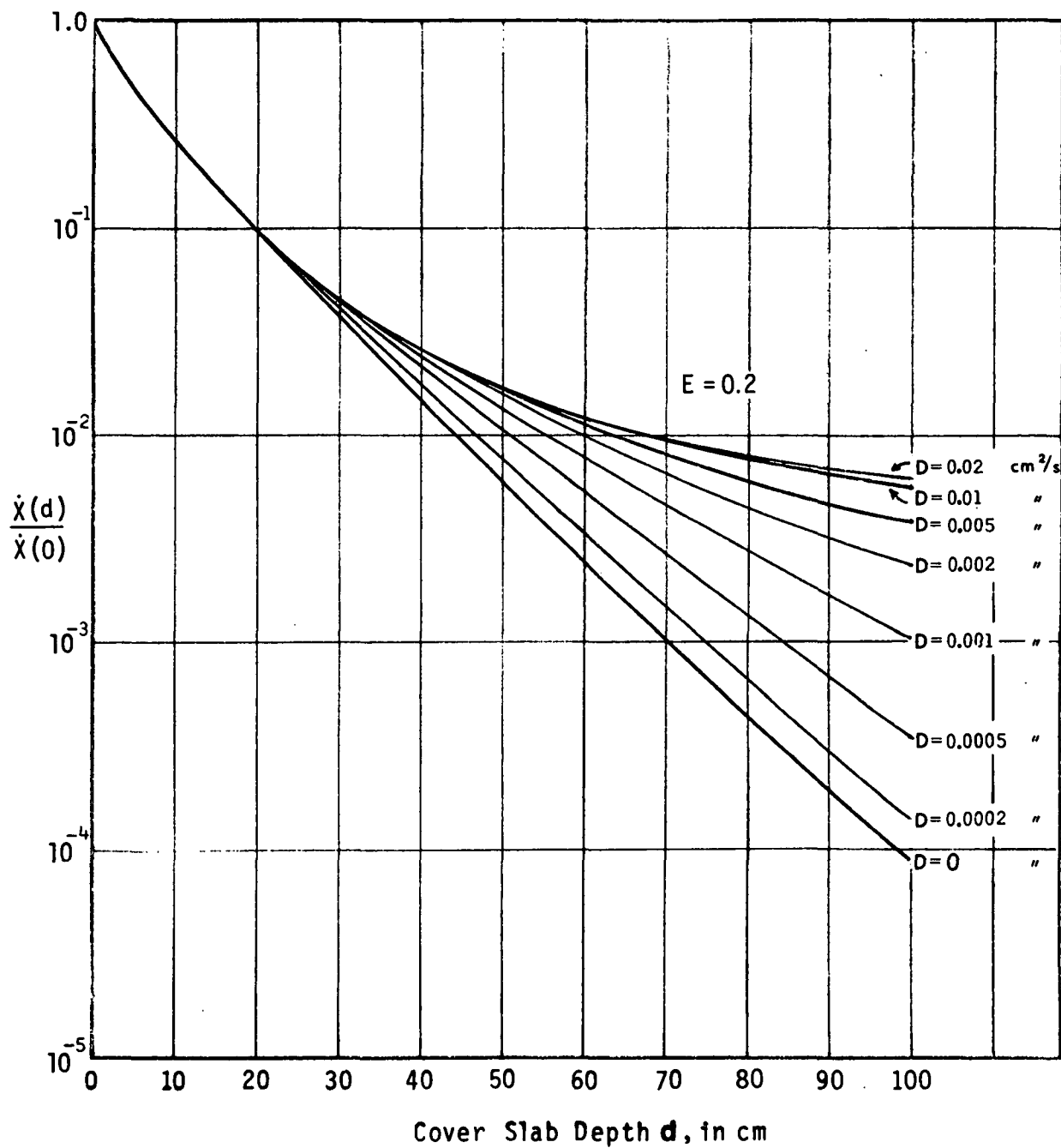


Figure 2-M. Relative decrease in exposure rates, with respect to maximum exposure rate possible, as function of increasing thickness d of the overburden slab, for emanating power $E = 20\%$ and different value of radon diffusion coefficient in soil, D , in the range $0.02 \text{ cm}^2/\text{s} \geq D \geq 0.0002 \text{ cm}^2/\text{s}$.

TECHNICAL REPORT DATA <i>(Please read Instructions on the reverse before completing)</i>		
1. REPORT NO. EPA-520/6-82-014	2.	3. RECIPIENT'S ACCESSION NO.
4. TITLE AND SUBTITLE A Basic Technique and Models for Determining Exposure Rates Over Uranium-Bearing Soils	5. REPORT DATE August 1982	6. PERFORMING ORGANIZATION CODE
	8. PERFORMING ORGANIZATION REPORT NO.	
7. AUTHOR(S) George V. Oksza-Chocimowski	10. PROGRAM ELEMENT NO.	
9. PERFORMING ORGANIZATION NAME AND ADDRESS U.S. Environmental Protection Agency Office of Radiation Programs, Las Vegas Facility P.O. Box 18416 Las Vegas, Nevada 89114	11. CONTRACT/GRANT NO.	
	13. TYPE OF REPORT AND PERIOD COVERED Technical Note	
12. SPONSORING AGENCY NAME AND ADDRESS Same as above	14. SPONSORING AGENCY CODE	
15. SUPPLEMENTARY NOTES		
16. ABSTRACT The application of simple computer-implemented analytical procedures to predict exposure rates over uranium-bearing soil deposits is demonstrated in this report. The method is based, conceptually, on the energy-dependent point-source buildup factor and, operationally, on two consecutive integrations. The dependence of photon fluxes on spatial variables is simplified by an analytical integration over the physical dimensions of the deposit, represented as a slab bearing homogeneously distributed nuclides of the uranium-238 decay chain, at equilibrium, and covered with a source-free overburden slab; both slabs being of variable thickness but of infinite areal extent. Elementary computer techniques are then employed to integrate numerically the exposure rates corresponding to the specific energies of uranium-238 decay chain, for chosen thicknesses of the overburden and uranium-bearing slabs. The numerical integration requires the use of buildup factors, attenuation and absorption coefficients expressed as continuous functions of energy by curve-fitting equations included in the report. As direct application of the method, maximum exposure rates over uranium-bearing soils are calculated, and the dependence of exposure rates on the thickness of the uranium-bearing slab and depth of overburden is reduced to a simple model. These results, valid for uranium mill tailings piles, are compared to those of other authors, and applied to determine changes in exposure rates due to radon gas emanation from source materials.		
17. KEY WORDS AND DOCUMENT ANALYSIS		
a. DESCRIPTORS	b. IDENTIFIERS/OPEN ENDED TERMS	c. COSATI Field/Group
Radioactive Wastes	Uranium Mill Tailings	1807
Uranium Ore Deposits	Uranium-238 Decay Chain	0807
Gamma Irradiation/X Ray Irradiation	Exposure Rates	1808
Radiation Shielding	Overburden	1806
Radon	Radon Gas Exhalation	0702
Mathematical Models	Buildup/Curve-fitting models.	1201
18. DISTRIBUTION STATEMENT Release Unlimited	19. SECURITY CLASS (This Report) Unclassified	21. NO. OF PAGES 159
	20. SECURITY CLASS (This page) Unclassified	22. PRICE